Report 2505

POTENTIAL FLOW ABOUT SERIES 58 BODIES IN GENERAL TRANSLATIONAL AND ROTATIONAL MOTION

NAVAL SHIP RESEARCH AND DEVELOPMENT CENTER
WASHINGTON, D.C. 20007

POTENTIAL FLOW ABOUT SERIES 58 BODIES IN GENERAL TRANSLATIONAL AND ROTATIONAL MOTION

HYDROMECHANICS LABORATORY
RESEARCH AND DEVELOPMENT REPORT

June 1967

Report 2505

The Naval Ship Research and Development Center is a U.S. Navy center for laboratory effort directed at achieving improved sea and air vehicles. It was formed in March 1967 by merging the David Taylor Model Basin at Carderock, Maryland and the Marine Engineering Laboratory at Annapolis, Maryland.

Naval Ship Research and Development Center
Washington, D. C. 20007

POTENTIAL FLOW ABOUT SERIES 58 BODIES IN GENERAL TRANSLATIONAL AND ROTATIONAL MOTION

by

L. Landweber and Matilde Macagno
Iowa Institute of Hydraulic Research
State University of Iowa
Iowa City, Iowa

Contract N600(167)55727)x)

June 1967

Report 2505

TABLE OF CONTENTS

LIST OF FIGURES

LIST OF TABLES

Page

Page

NOTATION

C_D	Drag coefficient
C_p	Pressure coefficient
D	Drag
d	Maximum diameter of a body of revolution
$E(k)$, $J(k)$, $K(k)$	Complete elliptic integrals
h_i	Linearizing factors of curvilinear coordinates
K	Curvature
k	Parameter of elliptical functions
k_e	Parameter of elliptical functions for an ellipsoid
k_1	Added-mass coefficient in longitudinal motion
k_2	Added-mass coefficient in transverse motion
ℓ	Length of body
m	Dimensionless abscissa corresponding to maximum ordinate
$\bar{n}$	Unit vector along outward normal to surface
p	Pressure on body
R_0	Radius of curvature at nose of body
R_1	Radius of curvature at tail of body
r_0	Dimensionless radius at nose of body
r_1	Dimensionless radius at tail of body
s, n, θ	System of parallel orthogonal coordinates
t	Time
U	Velocity vector of origin of coordinates attached to the body
U_1, U_2, U_3	Components of $\bar{U}$ for axisymmetric body

U_4, U_5, U_6	Components of velocity at surface of body
u, v, w	Velocity components at a point of fluid
u_{1s}	Factor of tangential velocity component along body for axial flow
$u_{2\theta}, u_{2s}$	Factors of tangential velocity component along body for transverse flow
$u_{R\theta}, u_{Rs}$	Factors of velocity when body is rotating about the z-axis
V	Volume of body
$\bar{v}$	Velocity vector at a point of the fluid
x, y, z	Rectangular Cartesian coordinates
α	Angle of attack
γ	Arctan (dr/dx)
ϵ	Error in computing velocity U_{1s}
ξ, η, ζ	Coordinates of a point on surface of body
ρ	Mass density of fluid
φ	Prismatic coefficient
ϕ_i	Velocity potential corresponding to unit value of U_i
ψ	Stream function
$\bar{\omega}$	Angular velocity vector
λ	Length/diameter ratio
μ, ζ, θ	Ellipsoidal coordinates
Φ	Total velocity potential

ABSTRACT

The potential-flow pressure and velocity distributions for a family of bodies of revolution, Series 58, were computed for various modes of motion. The results of these computations are presented, and their application of the determination of the flow field and minimum-pressure coefficients for arbitrary motion of the bodies are discussed.

The calculations were performed with the original UNIVAC installation at the David Taylor Model Basin and were checked with IBM 650 and 7070 installations at the State University of Iowa.

INTRODUCTION

As part of a systematic study of the hydrodynamic properties of a particular family of bodies of revolution, Series 58,[1] the potential-flow pressure distributions for the members of this family, for general translational and rotational motion, have been computed. The purpose of this report is to present the results of these computations and to discuss their application to the determination of the flow field and minimum-pressure coefficients for arbitrary motion of the body. These results have already been applied to the evaluation of the added masses for this family.[2]

The procedure employed to compute the velocity distribution on the body surface is essentially that described in Reference 3. The calculations were performed with the original UNIVAC installation at the David Taylor Model Basin and were partly checked by using a more accurate program,[3] with IBM 650 and 7070 installations at the State University of Iowa.

STATEMENT OF PROBLEM

Let us suppose that the x-axis coincides with that of the body of revolution, that the body extends along its axis from $x = -1$ to $x = +1$, and that the x, y, z axes, which are fixed in the body, form a rectangular, right-handed coordinate system; see Figure 1.

The equation of the body surface is expressible in the form

$$y = r(x) \cos \theta, \qquad z = r(x) \sin \theta$$

where $r(x)$ is a prescribed function. Arc length s along a meridian section of the body will be measured clockwise from the point $x = -1$; put

---

[1]References are listed on page 116.

$$\sin \gamma = \frac{dr}{ds} \quad , \quad \cos \gamma = \frac{dx}{ds} \quad ; \quad \tan \gamma = \frac{dr}{dx} \qquad [1]$$

It will be further supposed that the origin of coordinates has velocity components U_1, U_2, U_3 which may be functions of time and that the body is rotating with an angular velocity of components U_4, U_5, U_6 with respect to the x, y, and z axes. It will be assumed that the fluid is incompressible and inviscid, that it is at rest at infinity, and that the flow is irrotational.

Under the foregoing assumptions there exist velocity potentials $\phi_i(x, y, z)$ associated with each velocity component U_i, $i = 1, 2, \ldots 6$, such that the velocity potential for an arbitrary state of motion of the body is

$$\Phi(x, y, z, t) = \sum_{i=1}^{6} U_i \phi_i \qquad [2]$$

and the velocity vector $\overline{v}$ of the flow at a point of the fluid is

$$\overline{v} = \text{grad } \Phi = \sum_{i=1}^{6} U_i \text{ grad } \phi_i \qquad [3]$$

The six functions ϕ_i occurring in Equations [2] and [3] can be expressed in terms of three independent functions, $u_{1s}(x)$, $u_{2\theta}(x)$, $u_{R\theta}(x)$, $-1 \leq x \leq 1$, according to the following formulas:

$$\phi_1(x) = x + \int u_{1s} \sec \gamma \, dx \qquad [4]$$

$$\phi_2(x) = r(x)\,(1 - u_{2\theta}) \cos \theta \qquad [5]$$

$$\phi_3(x) = r(x)\,(1 - u_{2\theta}) \sin \theta \qquad [6]$$

$$\phi_4(x) = 0 \qquad [7]$$

$$\phi_5(x) = r\, u_{R\theta} \sin \theta \qquad [8]$$

$$\phi_6(x) = -\, r\, u_{R\theta} \cos \theta \qquad [9]$$

These equations give values of ϕ_i on the surface of the body. Here the quantity u_{1s} represents the velocity at the surface of the body, positive in the sense of increasing s, when it is immersed in a uniform stream of unit velocity in the negative x-direction; $u_{2\theta}$ represents the velocity at the surface, on the meridian $\theta = \pi/2$, in the direction of increasing θ, when it is immersed in a uniform stream of unit velocity in the negative y-direction; and $u_{R\theta}$ is the velocity at the surface, on the meridian $\theta = \pi/2$, when the body is rotating with unit angular velocity about the z-axis. The velocity components at any point of the surface, when the body is moving with translational and rotational components U_1, U_2 ... U_6, obtained from Equation [3], are

$$U_s = \frac{\partial \Phi}{\partial s} = U_1 (u_{1s} + \cos \gamma) + (U_2 \cos \theta + U_3 \sin \theta)(\sin \gamma + u_{2s}) - (U_5 \sin \theta - U_6 \cos \theta) u_{Rs} \quad [10]$$

$$U_n = \frac{\partial \Phi}{\partial n} = - U_1 \sin \gamma + (U_2 \cos \theta + U_3 \sin \theta) \cos \gamma - (x \cos \gamma + r \sin \gamma)(U_5 \sin \theta - U_6 \cos \theta) \quad [11]$$

$$U_\theta = \frac{1}{r} \frac{\partial \Phi}{\partial \theta} = (U_2 \sin \theta - U_3 \cos \theta)(u_{2\theta} - 1) + (U_5 \cos \theta + U_6 \sin \theta) u_{R\theta} \quad [12]$$

where

$$\left.\begin{aligned} u_{2s} &= - u_{2\theta} \sin \gamma - r \frac{du_{2\theta}}{dx} \cos \gamma \\ u_{Rs} &= - u_{R\theta} \sin \gamma - r \frac{du_{R\theta}}{dx} \cos \gamma \end{aligned}\right\} \quad [13]$$

Here the quantity u_{2s} is the velocity on the meridian $\theta = 0$ in the direction of increasing s when the body is immersed in a uniform stream of unit velocity in the negative y-direction, and u_{Rs} is the velocity on the same meridian and in the same direction when the body is rotating with unit angular velocity about the z-axis.

The velocity potentials at a point (x, y, z) of the fluid can be obtained from the surface distributions, Equations [4] to [9], by means of Green's formula[4]

$$4\pi \phi_i (x, y, z) = \iint \left[- \frac{1}{R} \frac{\partial \phi_i}{\partial n} + \phi_i \frac{\partial}{\partial n} \left(\frac{1}{R} \right) \right] dS \quad [14]$$

where

$$R^2 = (x - \xi)^2 + (y - \eta)^2 + (z - \zeta)^2$$

Here ξ, η, ζ denote the coordinates of a point on the surface, and the derivatives are taken in the direction of the outward normal to the surface over which the double integral extends. The values of ϕ_i are given by Equations [4] to [9], and those of $\partial \phi_i / \partial n$ by the boundary conditions[2]

$$\left.\begin{aligned} \frac{\partial \phi_1}{\partial n} &= -\sin\gamma & \frac{\partial \phi_4}{\partial n} &= 0 \\ \frac{\partial \phi_2}{\partial n} &= \cos\theta\cos\gamma & \frac{\partial \phi_5}{\partial n} &= -\sin\theta\,(x\cos\gamma + r\sin\gamma) \\ \frac{\partial \phi_3}{\partial n} &= \sin\theta\cos\gamma & \frac{\partial \phi_6}{\partial n} &= \cos\theta\,(x\cos\gamma + r\sin\gamma) \end{aligned}\right\} \quad [15]$$

The application of Equation [14] will be discussed in detail in a subsequent section

PRESSURE DISTRIBUTIONS

We may assume that the pressure is zero at infinity. Then, in the simplest case, when a body is at rest in a stream of velocity U_1 in the negative x-direction, the Bernoulli equation is

$$p + \frac{1}{2}\rho U_1^2 u_{1s}^2 = \frac{1}{2}\rho U_1^2$$

and the pressure coefficient

$$C_p = \frac{p}{\frac{1}{2}\rho U_1^2} \quad [16]$$

becomes

$$C_p = 1 - u_{1s}^2 \quad [17]$$

Next consider the case when the body is at an angle of attack in a uniform stream, i.e., the body is at rest in a uniform stream with components U_1 and U_2 in the negative x- and y-directions. The Bernoulli equation is now

$$p + \frac{1}{2}\rho\left[(U_1 u_{1s} + U_2 u_{2s})^2 + U_2^2 u_{2\theta}^2\right] = \frac{1}{2}\rho\,(U_1^2 + U_2^2)$$

and the pressure coefficient becomes

$$C_p = \frac{p}{\frac{1}{2}\rho\,(U_1^2 + U_2^2)} = 1 - \frac{(U_1 u_{1s} + U_2 u_{2s})^2 + U_2^2 u_{2\theta}^2}{U_1^2 + U_2^2} \quad [18]$$

If, on the other hand, the fluid is at rest at infinity and the body is undergoing a nonuniform translation with components $U_1(t)$, $U_2(t)$, $U_3(t)$, the Bernoulli equation, expressed in the form for a moving coordinate system,[5] becomes

$$\frac{p}{\rho} + \frac{\partial \Phi}{\partial t} + \frac{1}{2}\left[(u - U_1)^2 + (v - U_2)^2 + (w - U_3)^2\right] = \frac{1}{2}\left(U_1^2 + U_2^2 + U_3^2\right) \quad [19]$$

where u, v, w are the components of the velocity vector $\bar{v}$ of a fluid particle. On the surface of the body it is convenient to express these in terms of the components U_s, U_n, and U_θ, which is readily accomplished by means of the table of direction cosines between the directions of increasing s, n, and θ, and the x, y, z axes:

	u	v	w
U_s	$\cos\gamma$	$\cos\theta\sin\gamma$	$\sin\theta\sin\gamma$
U_n	$-\sin\gamma$	$\cos\theta\cos\gamma$	$\sin\theta\cos\gamma$
U_θ	0	$-\sin\theta$	$\cos\theta$

Thus we obtain

$$\left.\begin{aligned} u &= U_s\cos\gamma - U_n\sin\gamma \\ v &= U_s\cos\theta\sin\gamma + U_n\cos\theta\cos\gamma - U_\theta\sin\theta \\ w &= U_s\sin\theta\sin\gamma + U_n\sin\theta\cos\gamma + U_\theta\cos\theta \end{aligned}\right\} \quad [20]$$

But, from Equations [10], [11], and [12], we have

$$\begin{aligned} U_s &= U_1(u_{1s} + \cos\gamma) + (U_2\cos\theta + U_3\sin\theta)(\sin\gamma + u_{2s}) \\ U_n &= -U_1\sin\gamma + (U_2\cos\theta + U_3\sin\theta)\cos\gamma \\ U_\theta &= (U_2\sin\theta - U_3\cos\theta)(u_{2\theta} - 1) \end{aligned}$$

which, substituted into Equation [20], yield

$$\left.\begin{aligned} u - U_1 &= U_1 u_{1s}\cos\gamma + (U_2\cos\theta + U_3\sin\theta)u_{2s}\cos\gamma \\ v - U_2 &= U_1 u_{1s}\cos\theta\sin\gamma + (U_2\cos\theta + U_3\sin\theta)u_{2s}\sin\gamma\cos\theta \\ &\quad - (U_2\sin\theta - U_3\cos\theta)u_{2\theta}\sin\theta \\ w - U_3 &= U_1 u_{1s}\sin\theta\sin\gamma + (U_2\cos\theta + U_3\sin\theta)u_{2s}\sin\theta\sin\gamma \\ &\quad + (U_2\sin\theta - U_3\cos\theta)u_{2\theta}\cos\theta \end{aligned}\right\} \quad [21]$$

We also have, from Equation [2],

$$\frac{\partial \Phi}{\partial t} = \phi_1 \frac{dU_1}{dt} + \phi_2 \frac{dU_2}{dt} + \phi_3 \frac{dU_3}{dt} \qquad [22]$$

in which ϕ_1, ϕ_2, ϕ_3 are given by Equations [4], [5], and [6]. Thus the pressure can be obtained from Equations [19], [21], and [22] when the values of U_1, U_2, U_3 and their time derivatives are known.

Finally, let us consider the case when, in addition, the body is rotating at an angular velocity $\bar{\omega}$, with components U_4, U_5, U_6. The Bernoulli equation for a moving coordinate system now assumes the form

$$\frac{p}{\rho} + \frac{\partial \Phi}{\partial t} + \frac{1}{2}\left[(u-U_1)^2 + (v-U_2)^2 + (w-U_3)^2\right] + \bar{v} \cdot \bar{r} \times \bar{\omega} = \frac{1}{2}\left(U_1^2 + U_2^2 + U_3^2\right) \qquad [23]$$

where now

$$\frac{\partial \Phi}{\partial t} = \phi_1 \frac{dU_1}{dt} + \phi_2 \frac{dU_2}{dt} + \ldots + \phi_6 \frac{dU_6}{dt} \qquad [24]$$

and the last term in the left member of Equation [23] is the triple scalar product

$$\bar{v} \cdot \bar{r} \times \bar{\omega} = u\,(yU_6 - zU_5) + v\,(zU_4 - xU_6) + w\,(xU_5 - yU_4)$$

As in the previous case, the pressures on the surface of the body can be expressed in terms of the velocity functions, which now are u_{1s}, $u_{2\theta}$, u_{2s}, $u_{R\theta}$, u_{Rs}, the linear and angular velocity components U_1, U_2, ... U_6 and their derivatives, since, from Equations [10], [11], [12] and [20], we obtain

$$\left.\begin{aligned}
u - U_1 &= U_1 u_{1s} \cos\gamma + (U_2 \cos\theta + U_3 \sin\theta)\, u_{2s} \cos\gamma \\
&\quad + (U_5 \sin\theta - U_6 \cos\theta)\left[(x\cos\gamma + r\sin\gamma)\sin\gamma - u_{Rs}\cos\gamma\right] \\
v - U_2 &= U_1 u_{1s} \cos\theta \sin\gamma + (U_2 \cos\theta + U_3 \sin\theta)\, u_{2s} \sin\gamma \cos\theta \\
&\quad - (U_2 \sin\theta - U_3 \cos\theta)\, u_{2\theta} \sin\theta - U_5 \sin\theta \cos\theta \left[u_{Rs} \sin\gamma \right. \\
&\quad \left. + (x\cos\gamma + r\sin\gamma)\cos\gamma + u_{R\theta}\right] + U_6\left[u_{Rs}\cos^2\theta \sin\gamma \right. \\
&\quad \left. + (x\cos\gamma + r\sin\gamma)\cos^2\theta\cos\gamma - u_{R\theta}\sin^2\theta\right]
\end{aligned}\right\} \qquad [25]$$

$$\left.\begin{aligned} w - U_3 = {} & U_1 u_{1s} \sin\theta \sin\gamma + (U_2 \cos\theta + U_3 \sin\theta)\, u_{2s} \sin\theta \sin\gamma \\ & + (U_2 \sin\theta - U_3 \cos\theta)\, u_{2\theta} \cos\theta - U_5 \left[u_{Rs} \sin^2\theta \sin\gamma \right. \\ & + (x\cos\gamma + r\sin\gamma)\sin^2\theta\cos\gamma + u_{R\theta}\cos^2\theta \left.\right] \\ & + U_6 \sin\theta\cos\theta \left[u_{Rs}\sin\gamma + (x\cos\gamma + r\sin\gamma)\cos\gamma + u_{R\theta}\right] \end{aligned}\right\} \quad [25]$$

For elongated bodies the velocity $\bar{v}$ is small except in the neighborhood of the stagnation points, and a useful approximation is given by the linearized version of the Bernoulli Equation [23],

$$\frac{p}{\rho} + \frac{\partial\Phi}{\partial t} = u\,(U_1 - yU_6 + zU_5) + v\,(U_2 - zU_4 - xU_6) + w\,(U_3 - xU_5 + yU_4) \quad [26]$$

It is interesting to observe that the right member of Equation [26] is the scalar product of the velocity of the fluid and the velocity of the surface at a point having position vector $\bar{r}$.

DESCRIPTION OF TMB SERIES 58

The TMB Series 58 is a family of bodies of revolution with meridian sections represented by polynomials of the sixth degree, having coefficients that are functions of the geometry of the body. These are of the form

$$r^2(x) = \sum_{n=0}^{6} C_n x_n \quad [27]$$

in which the coefficients C_n depend upon the following six geometric properties:

ℓ	the length of the body
d	the maximum diameter
$1 - x_m$	the distance of the maximum section from the nose
R_0	the radius of curvature of a meridian section at the nose
R_1	the radius of curvature at the tail
V	the volume of the body

These quantities determine the following dimensionless characteristics of the body:

$$\lambda = \frac{\ell}{d}, \quad m = \frac{1 - x_m}{\ell}, \quad r_0 = \frac{R_0\ell}{d^2}, \quad r_1 = \frac{R_1\ell}{d^2}, \quad \varphi = \frac{4V}{\pi d^2 \ell}$$

the last quantity, φ, is the prismatic coefficient.

A family of 30 bodies of the series, for which the foregoing coefficients are given in Table 1, was selected for study. Among these the one designated Body 4 is treated as a "parent" form, the common members of the several series obtained by holding four of the five dimensionless parameters constant and by varying the fifth. In a few cases, more than one parameter was varied.

The coordinates of the bodies are given in Table 2 and their meridian sections are presented in Figures 2 to 8. These are shown with the nose to the right since, for the present purpose, the body is moving with six degrees of freedom and the positive sense of the axial motion is to the right. Thus the tail is at $x = -1$, the nose at $x = +1$, and the length of a body is $\ell = 2$.

It will be convenient to designate a body by means of its values of m, r_0, r_1, φ, and λ. For example, the parent form, Body 4, is designated by the serial number 40 50 10 65 70 indicating that $m = 0.40$, $r_0 = 0.5$, $r_1 = 0.1$, $\varphi = 0.65$ and $\ell/d = 7.0$.

THE VELOCITY FUNCTIONS

RESULTS FOR SERIES 58

Values of u_{1s}, $u_{1s} \sec \gamma$, $u_{2\theta}$, u_{2s}, $u_{R\theta}$, u_{Rs} for the Series 58 bodies, computed with the UNIVAC at the Model Basin, are given in Tables 3–32. In the original program, u_{2s} and u_{RS} were computed, by numerical differentiation, from the formulas

$$u_{2s} = -\frac{d}{dx}(ru_{2\theta}) \cos \gamma \qquad u_{Rs} = -\frac{d}{dx}(ru_{R\theta}) \cos \gamma \qquad [28]$$

which are identical with the definitions in Equation [13]. Near the end points, however, the expressions, Equation [27], become indeterminate, and the results obtained by applying Equation [28] directly suffer in accuracy. Thus it was necessary to recompute the values of u_{2s} and u_{Rs} at the first and last three points of each body by using Equation [13]. These corrected values are included in Table 3.

The quantity $u_{1s} \sec \gamma$ is included in the tabulations and in the subsequent graphs for several reasons. Firstly, it is the quantity one obtains by solving the integral equation for longitudinal flow, u_{1s} being derived from it. Secondly, whereas u_{1s} varies very rapidly near the ends of the body, $u_{1s} \sec \gamma$ varies slowly over the entire body length and, indeed, is a constant for ellipsoids. This is a very useful property in the analysis of pressure distributions on a body.

Graphs of the tabulated values are shown in Figures 9 to 38. Each figure contains the set of six curves for one body. In addition, the dimensionless pressure distributions on the bodies for axial flow are plotted in Figures 39 to 45.

ELLIPSOIDS

To compare the foregoing solutions with those for ellipsoids of similar dimensions, the velocity functions u_{1s}, $u_{2\theta}$, u_{2s}, $u_{R\theta}$, u_{Rs} have been calculated for prolate spheroids of length-diameter ratios $\lambda = 2, 2.5, 3, 4, 5, 6, 7, 8, 9$, and 10. These functions are given by the formulas

$$u_{1s} = \frac{\cos \gamma}{\zeta_0 \left[\frac{1}{2} (\zeta_0^2 - 1) \Lambda - \zeta_0\right]} \qquad [29]$$

$$u_{2\theta} = \frac{4}{\zeta_0 (\zeta_0^2 - 1) \Lambda - 2 \zeta_0^2 + 4} \qquad [30]$$

$$u_{2s} = - u_{2\theta} \sin \gamma \qquad [31]$$

$$u_{R\theta} = - \frac{[3 \zeta_0 (\zeta_0^2 - 1) \Lambda - 6 \zeta_0^2 + 4]}{\zeta_0 [3 (2\zeta_0^2 - 1) (\zeta_0^2 - 1) \Lambda - 2 \zeta_0 (6 \zeta_0^2 - 7)} \qquad [32]$$

$$u_{Rs} = u_{R\theta} \frac{2\mu^2 - 1}{\mu^2} \sin \gamma \qquad [33]$$

where

$$\zeta_0 = \frac{\lambda}{\sqrt{\lambda^2 - 1}} \qquad [34]$$

$$\Lambda = \ell n \frac{\zeta_0 + 1}{\zeta_0 - 1} = 2 \ell n (\lambda + \sqrt{\lambda^2 - 1}) \qquad [35]$$

$$\sin \gamma = - \mu \sqrt{\frac{\zeta_0^2 - 1}{\zeta_0^2 - \mu^2}}, \quad \cos \gamma = \zeta_0 \sqrt{\frac{1 - \mu^2}{\zeta_0^2 - \mu^2}} \qquad [36]$$

These spheroids may be represented by

$$y^2 = \frac{1}{\lambda^2} (1 - x^2) \qquad [37]$$

Thus it is seen that they are members of the family of bodies under consideration for which

$$C_0 = -C_2 = \frac{1}{\lambda^2}, \qquad C_1 = C_3 = C_4 = C_5 = C_6 = 0$$

Graphs of the meridian sections, the velocity functions, and the pressure distributions for the prolate spheroids are plotted in Figures 46, 47a to 47j, and 48, respectively.

ACCURACY OF CALCULATIONS

A simple test of the accuracy of the calculations is furnished by the famous paradox of d'Alembert, that the drag of a body moving with constant velocity through an otherwise undisturbed and unbounded inviscid fluid is zero. The drag given by the pressures on the body is

$$D = \iint p \sin \gamma \, dS \qquad [38]$$

where p is the pressure and the integration extends over the surface of the body. Setting $dS = 2\pi r ds$, and applying Equation [1] and the Bernoulli Equation [17], we obtain

$$D = \frac{\pi}{2} \rho U_1^2 \int_{-1}^{1} (1 - u_{1s}^2) \frac{d(r^2)}{dx} dx = -\frac{\pi}{2} \rho U_1^2 \int_{-1}^{1} u_{1s}^2 \frac{d(r^2)}{dx} dx \qquad [39]$$

Upon introduction of the drag coefficient $C_D = D / \left(\frac{1}{2} \rho U_1^2 \cdot \frac{\pi d^2}{4} \right)$, Equation [38] takes the form

$$C_D = -\frac{4}{d^2} \int_{-1}^{1} u_{1s}^2 \frac{d(r^2)}{dx} dx \qquad [40]$$

Assume now that the computed values of u_{1s} are in error and that the exact values are $u_{1s} + \epsilon$. Since the correct value of the drag coefficient is zero, we obtain from Equation [40]

$$-\frac{4}{d^2} \int_{-1}^{1} (u_{1s} + \epsilon)^2 \frac{d(r^2)}{dx} dx = 0$$

which, if the square of ϵ is neglected, yields for C_D

$$C_D = \frac{8}{d^2}\int_{-1}^{1} \epsilon\, u_{1s}\, \frac{d(r^2)}{dx}\, dx \qquad [41]$$

Let m denote the abscissa corresponding to the maximum ordinate $y = d/2$. Then we may write

$$C_D = \frac{8}{d^2}\left[\int_{-1}^{m} \epsilon\, u_{1s}\, \frac{d(r^2)}{dx}\, dx + \int_{m}^{1} \epsilon\, u_{1s}\, \frac{d(r^2)}{dx}\, dx\right]$$

$$= -\frac{8}{d^2}\left[\epsilon_1 \int_{-1}^{m} u_{1s}\, \frac{d(r^2)}{dx}\, dx + \epsilon_2 \int_{m}^{1} u_{1s}\, \frac{d(r^2)}{dx}\, dx\right]$$

where ϵ_1 and ϵ_2 are mean values of ϵ in the first and second integrals according to the theorem of the mean. Since u_{1s} is approximately equal to unity except near the end points, where it approaches zero, it suffices, for an approximate evaluation of the error, to replace u_{1s} by unity in the last two integrals, whence we obtain

$$C_D = 2(\epsilon_1 - \epsilon_2)$$

Then

$$C_D \leq 2(|\epsilon_1| + |\epsilon_2|) = 4\bar{\epsilon} \qquad [42]$$

where $\bar{\epsilon}$ is the mean of ϵ_1 and ϵ_2.

Inequality [42] furnishes a measure of the accuracy of the computed values of u_{1s}. For example, application of Equation [40] to the parent form, Body 4 of the series, gives the value $C_D = 0.00148$. Hence the errors in u_{1s} are of the order of magnitude $\bar{\epsilon} = 0.00148 \times 0.25 \doteq 0.00037$. The values of $\bar{\epsilon}$ obtained from Equations [40] and [42] for the series of 30 bodies are shown in Table 33.

MINIMUM PRESSURE COEFFICIENTS

For the purpose of determining conditions under which cavitation would ensue, it is necessary to study the magnitude and location of the minimum pressures on the bodies. When the body is at rest in a uniform stream U_1 in the negative x-direction, the minimum values of the pressure coefficient C_p can be read from the curves of pressure distribution in Figures 39 to 45. Analysis of these values has yielded the empirical formula [6]

$$(C_p)_{min} = -k_1[2.30 + 40(m - \tfrac{1}{2})^2 + 1.70(r_0 - \tfrac{1}{2})^2] \qquad [43]$$

where k_1 is the added-mass coefficient[6]

$$k_1 = k_e \left[1 + 17.02 \left(\varphi - \frac{2}{3} \right)^2 + 2.490 \left(m - \frac{1}{2} \right)^2 + 0.2828 \left(r_0 - \frac{1}{2} \right)^2 + \left(r_1 - \frac{1}{2} \right)^2 \right] \quad [44]$$

and k_e is the added-mass coefficient in longitudinal motion for a prolate spheroid of the same length and volume as the body.

Next, suppose that a body is at an angle of attack in a uniform stream composed of components U_1 and U_2 in the negative x- and y-directions. The pressure coefficient is now given by Equation [18], which, when $U_2 < U_1$, may be expanded in the series

$$C_p = 1 - {u_{1s}}^2 - 2 \frac{U_2}{U_1} u_{1s} u_{2s} + \frac{{U_2}^2}{{U_1}^2} ({u_{1s}}^2 - {u_{2s}}^2 - {u_{2\theta}}^2) + \ldots \quad [45a]$$

For small angles of attack α, since $U_2/U_1 \approx \alpha$, we obtain from Equation [45a]

$$\left(\frac{\partial C_p}{\partial \alpha} \right)_{\alpha = 0} = -2 u_{1s} u_{2s} \quad [45b]$$

from which the rate of change of the minimum pressure coefficient from its value at a zero angle of attack can be computed. Values of $(C_p)_{min}$, their rates of change with angle of attack from Equation [45b], and the corresponding abscissas x_{min} are given in Table 34.

To obtain the minimum pressure coefficients at larger angles of attack (these were computed for all bodies of the series for the values $U_2/U_1 = 0.2$ and 0.4), the method described in Reference 6 was used. Curves showing the variation of $(C_p)_{min}$ with angle of attack, derived from the slope at $\alpha = 0$ and computed values at $\alpha =$ arctan 0.2 and arctan 0.4, are presented in Figure 49.

A more detailed study of the minimum pressure characteristics was made on the parent form, Body 4. By applying the method of Reference 6, the minimum pressure coefficients were obtained at each of the various sections for the body at various angles of attack. These minimum pressure coefficients are shown in Figure 50 as functions of longitudinal distance x, and in Figure 51 as overall coefficients over the forward part of the body for various angles of attack.

The minimum pressure coefficient in each section of the body, and the corresponding θ, for $\alpha =$ arctan 0.1 are presented in Figure 52. The line of minimum pressures coincides with the meridian profile $\theta = \pi$ up to a certain point downstream from the nose. At $x = 0.747$ it divides into a pair of symmetrically situated lines winding around the body. Close to the tail, at $x = -0.762$ both lines coincide again with the meridian profile $\theta = 0$.

VELOCITY POTENTIALS IN FLOW FIELD

It has already been indicated that the velocity potentials at a point of the fluid can be obtained by means of Green's formula, Equation [14]. In a previous report[7] this formula had been reduced, for bodies of revolution, to a simple integral with the intergrands for the various potentials expressed in terms of elliptic functions. Numerical results were obtained, however, only for points on the axis of the body.

When it was attempted, in the course of the present work, to apply [14], it was found to be difficult to obtain accurate numerical results in the neighborhood of the body because of the nature of the integrand. For longitudinal flow this difficulty was overcome to a great extent by modifying the integrand so as to make it more suitable for numerical quadrature and, in addition, the variation of the potential in the neighborhood of the surface was obtained independently as a Taylor Series. These two complementary methods will be described. A FORTRAN program for computing the velocity potential in the flow field will be presented and applied to Body 4.

TAYLOR SERIES FOR POTENTIAL NEAR SURFACE

For the purpose of expanding the velocity potential ϕ_1 in the neighborhood of the surface, let us introduce the system of orthogonal, parallel coordinates[8] s, n, θ, generated by surfaces parallel and perpendicular to the given surface, shown in Figure 53. The radial distance from the axis of revolution to a point will be denoted by $r(s, n)$, and by $r_0(s) = r(s,0)$ when the point lies in the surface. Then, as is seen from Figure 42, we have

$$r = r_0 + n \cos \gamma$$

and hence

$$\frac{\partial r}{\partial s} = (1 + Kn) \sin \gamma, \qquad \frac{\partial r}{\partial n} = \cos \gamma \qquad [46]$$

where K is the curvature

$$K = -\frac{d\gamma}{ds}$$

Then the quantities h_1, h_2, h_3 which occur in the expressions $h_1 ds$, $h_2 dn$, and $h_3 d\theta$ for the elements of arc in the directions of increasing s, n, and θ are[8]

$$h_1 = 1 + Kn, \quad h_2 = 1, \quad h_3 = r \qquad [47]$$

and LaPlace's equation in this system of coordinates becomes

$$\frac{\partial}{\partial s}\left(\frac{r}{1+Kn}\,\frac{\partial\phi}{\partial s}\right)+\frac{\partial}{\partial n}\left[r(1+Kn)\,\frac{\partial\phi}{\partial n}\right]=0 \qquad [48]$$

Hence, performing the indicated differentiations and then substituting $n = 0$, we obtain for values on the surface, where $\partial\phi/\partial n$ is given by Equation [15],

$$r_0\left(\frac{\partial^2\phi_1}{\partial s^2}\right)_0+\sin\gamma\left(\frac{\partial\phi_1}{\partial s}\right)_0+r_0\left(\frac{\partial^2\phi_1}{\partial n^2}\right)_0=\sin\gamma\,(r_0K+\cos\gamma)$$

whence we obtain

$$\left(\frac{\partial^2\phi_1}{\partial n^2}\right)_0=-\left(\frac{\partial^2\phi_1}{\partial s^2}\right)_0+\left[K+\frac{\cos\gamma-\left(\frac{\partial\phi_1}{\partial s}\right)_0}{r_0}\right]\sin\gamma \qquad [49]$$

Since it is the derivatives with respect to r, rather than n, that are desired, we now write

$$\frac{\partial\phi_1}{\partial r}=\frac{\partial\phi_1}{\partial s}\,\frac{\partial s}{\partial r}+\frac{\partial\phi_1}{\partial n}\,\frac{\partial n}{\partial r} \qquad [50]$$

But, from the relations among direction cosines of orthogonal coordinate systems, we have

$$h_1\frac{\partial s}{\partial r}=\frac{1}{h_1}\,\frac{\partial r}{\partial s}\,,\quad \frac{\partial n}{\partial r}=\frac{\partial r}{\partial n} \qquad [51]$$

whence Equation [50] becomes

$$\frac{\partial\phi_1}{\partial r}=\frac{1}{h_1{}^2}\,\frac{\partial\phi_1}{\partial s}\,\frac{\partial r}{\partial s}+\frac{\partial\phi_1}{\partial n}\,\frac{\partial r}{\partial n} \qquad [52]$$

or, from Equations [46] and [47],

$$\frac{\partial\phi_1}{\partial r}=\frac{1}{h_1}\,\frac{\partial\phi_1}{\partial s}\,\sin\gamma+\frac{\partial\phi_1}{\partial n}\cos\gamma \qquad [53]$$

Similarly, we derive

$$\frac{\partial^2\phi_1}{\partial r^2}=\frac{\partial}{\partial s}\left(\frac{\partial\phi_1}{\partial r}\right)\frac{1}{h_1}\,\sin\gamma+\frac{\partial}{\partial n}\left(\frac{\partial\phi_1}{\partial r}\right)\cos\gamma$$

or

$$\frac{\partial^2\phi_1}{\partial r^2} = \left[\frac{1}{h_1}\frac{\partial^2\phi_1}{\partial s^2}\sin\gamma - \frac{K}{h_1}\frac{\partial\phi_1}{\partial s}\cos\gamma - \frac{n}{h_1^2}\frac{dK}{ds}\frac{\partial\phi_1}{\partial s}\sin\gamma + \frac{\partial^2\phi_1}{\partial s\partial n}\cos\gamma + K\frac{\partial\phi_1}{\partial n}\sin\gamma\right]\frac{1}{h_1}\sin\gamma + \left[\frac{1}{h_1}\frac{\partial^2\phi_1}{\partial s\partial n}\sin\gamma - \frac{K}{h_1^2}\frac{\partial\phi_1}{\partial s}\sin\gamma + \frac{\partial^2\phi_1}{\partial n^2}\cos\gamma\right]\cos\gamma \quad [54]$$

The values of the derivatives at the surface can now be obtained by setting $n = 0$ in [53] and [54] and applying [15]. We have from [53]

$$\left(\frac{\partial\phi_1}{\partial r}\right)_0 = \left(\frac{\partial\phi_1}{\partial s} - \cos\gamma\right)\sin\gamma \quad [55]$$

Furthermore, from [15], we have

$$\left(\frac{\partial^2\phi_1}{\partial s\partial n}\right)_0 = -\frac{\partial}{\partial s}\sin\gamma = K\cos\gamma$$

Hence we obtain from [54]

$$\left(\frac{\partial^2\phi_1}{\partial r^2}\right)_0 = \left(\frac{\partial^2\phi_1}{\partial s^2}\right)_0\sin^2\gamma - 2K\left(\frac{\partial\phi_1}{\partial s}\right)_0\sin\gamma\cos\gamma + 2K\sin\gamma\cos^2\gamma - K\sin^3\gamma + \left(\frac{\partial^2\phi_1}{\partial n^2}\right)_0\cos^2\gamma$$

or by substituting from [49],

$$\left(\frac{\partial^2\phi_1}{\partial r^2}\right)_0 = -\left(\frac{\partial^2\phi_1}{\partial s^2}\right)_0\cos 2\gamma - \left(\frac{\partial\phi_1}{\partial s}\right)_0\left(2K + \frac{\cos\gamma}{r_0}\right)\sin\gamma\cos\gamma + K\sin 3\gamma + \frac{\sin\gamma\cos^3\gamma}{r_0} \quad [56]$$

Equations [55] and [56] may be put into a form more suitable for their numerical evaluation by applying the relation, obtained from [4],

$$\left(\frac{\partial\phi_1}{\partial s}\right)_0 = (1+g)\cos\gamma, \quad g = u_{1s}\sec\gamma \quad [57]$$

Then

$$\left(\frac{\partial^2 \phi_1}{\partial s^2}\right)_0 = g' \cos \gamma + K(1+g) \sin \gamma, \quad g' = \frac{dg}{ds} \qquad [58]$$

Hence [55] and [56] become

$$\left(\frac{\partial \phi_1}{\partial r}\right)_0 = g \sin \gamma \cos \gamma \qquad [59]$$

$$\left(\frac{\partial^2 \phi_1}{\partial r^2}\right)_0 = -g' \cos \gamma \cos 2\gamma - Kg \sin 3\gamma - \frac{g}{r_0} \sin \gamma \cos^3 \gamma \qquad [60]$$

The variation of ϕ_1 in the neighborhood of the surface is then given by

$$\phi_1 \approx (\phi_1)_0 + \left(\frac{\partial \phi_1}{\partial r}\right)_0 (r - r_0) + \frac{1}{2}\left(\frac{\partial^2 \phi_1}{\partial r^2}\right)_0 (r - r_0)^2 \qquad [61]$$

in which $\left(\frac{\partial \phi_1}{\partial r}\right)_0$ and $\left(\frac{\partial^2 \phi_1}{\partial r^2}\right)_0$ are obtained from [59] and [60], and the values of ϕ_1 on the surface, $(\phi_1)_0$, are given by [4] except for an additive arbitrary constant. In accordance with Green's formula, Equation [14], this constant has been selected so that the potential vanishes at infinity. Consequently, the absolute value of the potential $(\phi_1)_0$ may be obtained by modifying [4] to become

$$(\phi_1)_0 = \int_{-\infty}^{-1} u(x)\, dx + \int_{-1}^{x} u_{1s} \sec \gamma \, dx + x + 1 \qquad [62]$$

in which the first integral extends along the negative x-axis from minus infinity to the body, the second employs values of $u_{1s} \sec \gamma$ on the surface, and $u(x)$ denotes the velocity on the x-axis when the body is moving with unit velocity in the positive x-direction.

From Reference 7 we have for $u(x)$

$$u(x) = -\frac{1}{2} \int_{-1}^{1} u_{1s} \sec \gamma \, \frac{r_0^2(\xi)}{R^3} \, d\xi \qquad [63]$$

where

$$R^2 = (\xi - x)^2 + r_0^2(\xi)$$

Then we obtain

$$\int_{-\infty}^{-1} u(x) dx = -\frac{1}{2} \int_{-\infty}^{-1} \int_{-1}^{1} u_{1s} \sec \gamma \, \frac{r_0^2(\xi)}{R^3} \, dx d\xi$$

$$= -\frac{1}{2}\int_{-1}^{1} \frac{u_{1s}\sec\gamma\ r_0^{\,2}(\xi)\,d\xi}{\sqrt{(1+\xi)^2+r_0^{\,2}}\ \left[\sqrt{(1+\xi)^2+r_{02}^{\,2}}+1+\xi\right]} \qquad [64]$$

which, substituted into [62], permits the absolute values of the potentials on the surface to be derived from the values of the velocity function $u_{1s}\sec\gamma$.

EVALUATION OF GREEN'S FORMULA FOR THE VELOCITY POTENTIALS

The result obtained for ϕ_1 in Reference 7 by applying Green's formula, Equation [14], can be expressed in the form

$$4\pi\phi_1 = \int_{-1}^{1} \frac{k}{\sqrt{rr_0}}\left\{2r_0r_0'K + \phi_1(\xi)\left[-K + \frac{k^2E}{1-k^2}\ \frac{(x-\xi)^2+r^2-r_0^{\,2}-2r_0r_0'(x-\xi)}{4rr_0}\right]\right\} d\xi \qquad [65]$$

where

$$k = 2\sqrt{\frac{rr_0}{(x-\xi)^2+(r+r_0)^2}} \qquad [66]$$

and K and E are the complete elliptic integrals

$$K(k) = \int_0^{\frac{\pi}{2}} (1-k^2\sin^2\alpha)^{-1/2}\,d\alpha\,, \qquad E(k) = \int_0^{\frac{\pi}{2}} (1-k^2\sin^2\alpha)\,d\alpha \qquad [67]$$

The integrand in [65] is difficult to evaluate with accuracy for points in the neighborhood of the body since, when ξ is near x, k approaches unity and both terms in the integrand become very large but in opposite senses. Consequently, the integral was modified in the following manner. The integral of the first term may be written in the form

$$\int_{-1}^{1}\left[\frac{2kr_0r_0'K(k)}{\sqrt{rr_0}} - \frac{2k_Er_{0E}r_{0E}'K(k_E)}{\sqrt{rr_{0E}}}\right]d\xi + \int_{-1}^{1}\frac{2k_Er_{0E}r_{0E}'K(k_E)}{\sqrt{rr_{0E}}}\,d\xi$$

in which there has been added and subtracted the corresponding integral over the ellipse $r_{0E}(\xi)$

$$r_{0E}(\xi) = r_0(x)\sqrt{\frac{1-\xi^2}{1-x^2}} \qquad [68]$$

which coincides with the given body at its end points and at the point $(x,\ r_0)$. But, as is shown in Appendix A, the integral over the ellipse gives the value

$$\int_{-1}^{1}\frac{2k_Er_{0E}r_{0E}'K(k_E)}{\sqrt{rr_{0E}}}\,d\xi = -\frac{4\pi r_0^2\mu}{1-x^2-r_0^{\,2}}\left(\frac{\zeta}{2}\ell n\ \frac{\zeta+1}{\zeta-1} - 1\right) \qquad [69]$$

where μ and ζ are ellipsoidal coordinates given by

$$\mu = \frac{x\sqrt{2}}{[x^2 + r^2 + e^2 + \sqrt{(x^2 + r^2 + e^2)^2 - 4e^2x^2}]^{1/2}},$$
$$\zeta = \frac{x}{e\mu} \qquad [70]$$

and e is the eccentricity of the ellipse given by

$$e^2 = 1 - \frac{r_0^2(x)}{1-x^2} \qquad [71]$$

Thus the integral of the first term in [65] has been replaced by the sum of the expression in Equation [69] and an integral which is well behaved, in fact vanishes, at $x = \xi$.

Next we observe that the second term of the integrand of Equation [65] was derived from the surface integral

$$\iint \phi_1(\xi) \frac{\partial}{\partial n}\left(\frac{1}{R}\right) dS$$

But $1/R$ is the potential of a source at the point (x,y,z) outside the body, and hence, by Gauss's flux theorem, we have

$$\iint \frac{\partial}{\partial n}\left(\frac{1}{R}\right) dS = 0 \qquad [72]$$

Consequently, the integral of the second term of [65] may be written in the form

$$[\phi_1(\xi) - \phi_1(x)] \frac{k^2E}{1-k^2} \frac{(x-\xi)^2 + r^2 - r_0^2 - 2r_0r_0'(x-\xi)}{4rr_0} d\xi$$

the integrand of which also vanishes at $x = \xi$. Thus we have succeeded in transforming [65] into a form more suitable for numerical quadrature,

$$4\pi\phi_1 = -\frac{4\pi r_0^2\mu}{1-x^2-r_0^2}\left(\frac{\zeta}{2}\ell n \frac{\zeta+1}{\zeta-1} - 1\right) + \int_{-1}^{1}\left\{\frac{2kr_0r_0'K(k)}{\sqrt{rr_0}} - \frac{2k_Er_{0E}r_{0E}'K(k_E)}{\sqrt{rr_{0E}}}\right.$$
$$\left. + [\phi_1(\xi) - \phi_1(x)] \frac{k^2E}{1-k^2} \frac{(x-\xi)^2 + r^2 - r_0^2 - 2r_0r_0'(x-\xi)}{4rr_0}\right\} d\xi \qquad [73]$$

The expressions for ϕ_2 and ϕ_6 obtained in Reference 7, modified in accordance with the present convention that the fluid velocity is the positive gradient of the velocity potential, are

$$\phi_2 = \frac{1}{4\pi}\int_{-1}^{1}\left[J + r_0(1-u_{2\theta})\left(\frac{\partial J}{\partial r_0} - r_0'\frac{\partial J}{\partial \xi}\right)\right] r_0 \, d\xi \qquad [74]$$

$$\phi_6 = \frac{1}{4\pi} \int_{-1}^{1} \left[-(\xi + r_0 r_0')J + r_0 u_{R\theta} \left(\frac{\partial J}{\partial r_0} - r_0' \frac{\partial J}{\partial \xi} \right) \right] r_0 d\xi \qquad [75]$$

where

$$J = \int_0^{2\pi} \frac{\cos\theta}{R} d\theta \qquad [76]$$

Then

$$\frac{\partial J}{\partial r_0} = \frac{2\cos\theta}{r_0} \left\{ K \left[\frac{2r_0(r + r_0)}{Z^2} - \frac{Z}{2rr_0} \right] + \frac{K'}{\sqrt{rr_0}} \left[1 - \frac{2r_0(2r + r_0)}{Z^2} + \frac{4r_0^2 r(r + r_0)}{Z^4} \right] + \frac{ZE}{2rr_0} \right\} \qquad [77]$$

$$\frac{\partial J}{\partial \xi} = -\frac{4(x - \xi)\cos\theta}{Z^2} \left[\frac{K}{Z} - \frac{K'}{\sqrt{rr_0}} \left(1 - \frac{2rr_0}{Z^2} \right) \right] \qquad [78]$$

where

$$Z^2 = (x - \xi)^2 + (r + r_0)^2$$

and

$$K' = \frac{dK}{dk}$$

The formulas for ϕ_1 in Equation [73] and those for ϕ_2 and ϕ_6 in Equations [74] to [78] have been programmed for calculation with the IBM 7070 high-speed computer. For the two latter potentials no modifications were introduced to improve the accuracy of their numerical evaluation, and comparison between the exact and computed results, for a 7:1 prolate spheroid, indicated that the results obtained for ϕ_2 and ϕ_6 become inaccurate at distances less than about half the local body ordinate from the body, i.e., for $r < 1.5r_0$.

The program, written in IBM FORTRAN, is given in Appendix B. As a first stage, values of ϕ_1, ϕ_2, and ϕ_6 on the surface of the body are computed from given data for u_{1s}, $u_{2\theta}$, and $u_{R\theta}$, with $(\phi_1)_0$ taken equal to zero at $x = -1$. This relative value for $(\phi_1)_0$ suffices for computing ϕ_1 in the field from Equation [14]. Consequently, the calculation of the absolute values of $(\phi_1)_0$ from [62] and [64] was not programmed, but was subsequently performed with a desk calculator when the need for a more accurate evaluation of the velocity potential, by means of the Taylor expansion [61], became apparent.

Next, the program contains procedures for calculating the complete elliptic integrals, mainly by means of convergent series in the parameter k, except when k is nearly equal to unity, when it becomes necessary to use asymptotic series to obtain sufficient accuracy.

These values are then substituted into the integral expressions for ϕ_1, ϕ_2, and ϕ_6 and are evaluated by means of the Gauss quadrature formula for as many field points as desired.

The program does not give values of the potentials on the axis outside of the body. For ϕ_1 these can be derived from the integral of $u(x)$ in [63],

$$\phi_1 = -\frac{1}{2} \int_{-\infty}^{x} \int_{-1}^{1} u_{1s} \sec\gamma \frac{r_0^2(\xi)}{R^3} \, d\xi \, dx$$

$$\phi_1 = -\frac{1}{2} \int_{-1}^{1} \frac{u_{1s} \sec\gamma \cdot r_0^2(\xi) \, d\xi}{\sqrt{(x-\xi)^2 + r_0^2(\xi)} \; [\sqrt{(x-\xi)^2 + r_0^2(\xi)} + \xi - x]} \qquad [79]$$

After the validity of the program had been verified by applying it to a 7:1 prolate spheroid, the potential-flow field was computed for the parent form of the series, Body 4. The values at 476 points in the field were obtained from the IBM computer and, for ϕ_1, the values at 27 additional points on the axis were calculated from [74], and its variation near the body was computed at 16 points from [61]. The results are shown in Figures 54–59.

It was also of interest to obtain the velocity distribution along the axis for Body 4. The results, computed by applying the Gauss quadrature formula to [63], are shown in Figures 60 and the program, written in FORTRAN, is also given in Appendix B.

Finally, as an application of the potential-flow field, the flow pattern of equipotential and stream lines was derived from Figures 54 and 55. First the data of Figures 54 and 55, in which curves of ϕ_1 versus r for various values of x are given, were replotted to obtain the curves of ϕ_1 versus x for various values of y, shown in Figure 61. Points on the equipotential lines for the velocity potential ϕ_1 for the body at rest in a uniform stream were then obtained from Figure 62 as the intersections of the curves of the figure with the ϕ_1, x lines of unit slope

$$\phi_1 = x + \Phi_1 \qquad [80]$$

since [80] is the relation between the velocity potentials ϕ_1 and Φ_1 for steady and unsteady flow. The value of Φ_1 corresponding to a particular straight line was given by its intercept with the x-axis ($\phi_1 = 0$), since there we have $x = -\Phi_1$. The intersections with the curves of ϕ_1 then gave the coordinates (x, y) of the equipotentials Φ_1 = constant. The equipotential lines are shown in Figure 58.

For axisymmetric flow we have the relation between the Stokes stream function and the velocity potential,

$$\frac{1}{r}\frac{\partial\psi}{\partial n} = \frac{\partial\Phi_1}{\partial s} \qquad [81]$$

which may be solved for the normal distance Δn between streamlines to give the approximate formula

$$\Delta n \approx \frac{\Delta s}{r} \frac{\Delta \psi}{\Delta \Phi_1} \qquad [82]$$

Beginning with the body profile and the portions of the x-axis outside it as the streamline $\psi = 0$, points along a neighboring streamline $\Delta\psi$ = constant can be obtained from Figure 58 by applying [82]. For increased accuracy the radial distance r should be taken to the estimated center of the curvilinear rectangle formed by successive pairs of equipotential and streamlines. If the estimated location of this center is found to be in error, the calculation for Δn may be repeated with a corrected value for Δr. A more direct procedure consists of expressing r in terms of the distance r_i to the ith streamline and the increment Δr to the $(i + 1)$th streamline in the form

$$r = r_i + \frac{1}{2} \Delta r = r_i + \frac{1}{2} \Delta n \cos \gamma$$

which, substituted into [82], gives the quadratic equation

$$(\Delta n)^2 + 2r_i \Delta n \gamma - 2\Delta s \frac{\Delta \psi}{\Delta \Phi_1} \sec \gamma = 0$$

the solution of which may be expressed in the form

$$\Delta n = \frac{2(\Delta n)_0}{1 + \sqrt{1 + \frac{2}{r_i} (\Delta n)_0 \cos \gamma}} \quad , \quad (\Delta n)_0 = \frac{\Delta s}{r_i} \frac{\Delta \psi}{\Delta \Phi_i} \qquad [83]$$

Values of the stream function were selected by using the condition at infinity

$$\psi \approx - \frac{1}{2} r^2 \qquad [84]$$

For the first streamline the value $r_1 = 0.0025$ was selected. Eight additional streamlines were then obtained for the values of r

$$r_i = 2^{\frac{n-1}{2}} r_1$$

and corresponding values of the stream function

$$\psi_i \approx - 2^{n-2} r_1 \qquad [85]$$

For small values of r it is shown in Appendix C that the stream function $\psi(x,r)$ is approximately given by

$$\psi(x,r) = \frac{1}{2} u_0 r^2 - \frac{1}{8}\left(\frac{\partial^2 u}{\partial x^2}\right)_0 r^4 \qquad [86]$$

where the zero subscript refers to values when $r = 0$. When r is small, the last term in the right member of [86] may be neglected in comparison with the first (except near the stagnation point), and the equation of a streamline at a distance from the body is given by

$$\psi = \frac{1}{2} u_0 r^2 \qquad [87]$$

For larger values of r, and in the neighborhood of the stagnation point, Equation [86] may be considered as a quadratic equation, the solution of which expresses r^2 explicitly in terms of $\psi(x, r)$ and thus gives the equation of the corresponding streamline. The coefficient $\left(\frac{\partial^2 u}{\partial x^2}\right)_0$ can be obtained graphically (or numerically) from the known values of $u(x, 0)$.

In this way the flow pattern shown in Figure 62 was obtained.

ACKNOWLEDGMENTS

This project was begun in September 1960 under Contract N600(167)55727(x) with the David Taylor Model Basin, and essentially all of the pressure-distribution computations were conducted under TMB sponsorship. After June 1961, supplementary support was provided by the Office of Naval Research under Contract Nonr-1611(01) for the evaluation of the velocity potentials and the flow patterns. Additional computer time was provided without charge by the Computer Center of the State University of Iowa.

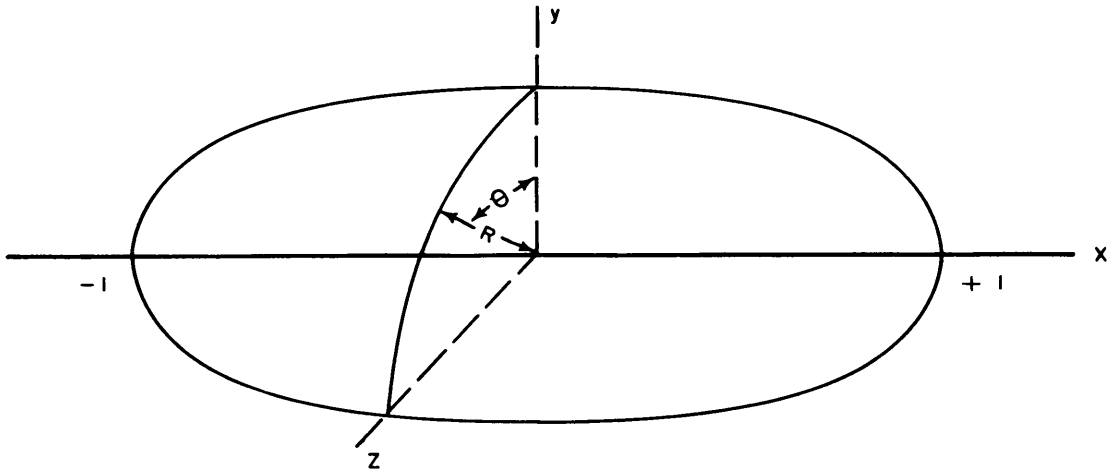

Figure 1 – Body of Revolution

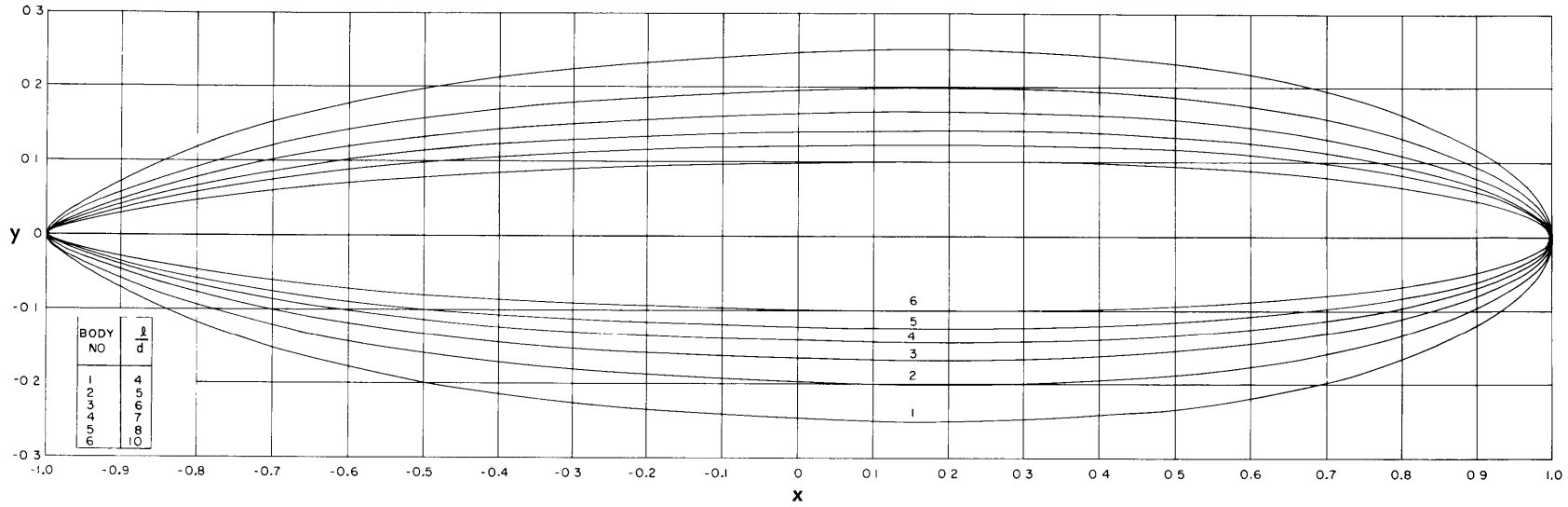

Figure 2 – Meridian Sections of Series 58 Bodies with Various Length/Diameter Ratios

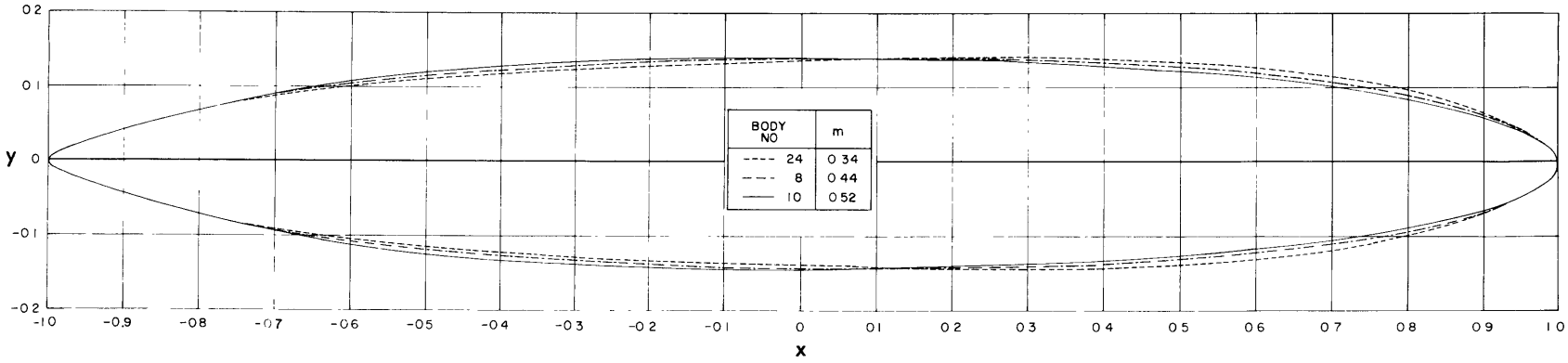

Figure 3 – Meridian Sections of Series 58 Bodies with Various Locations of Section of Maximum Thickness

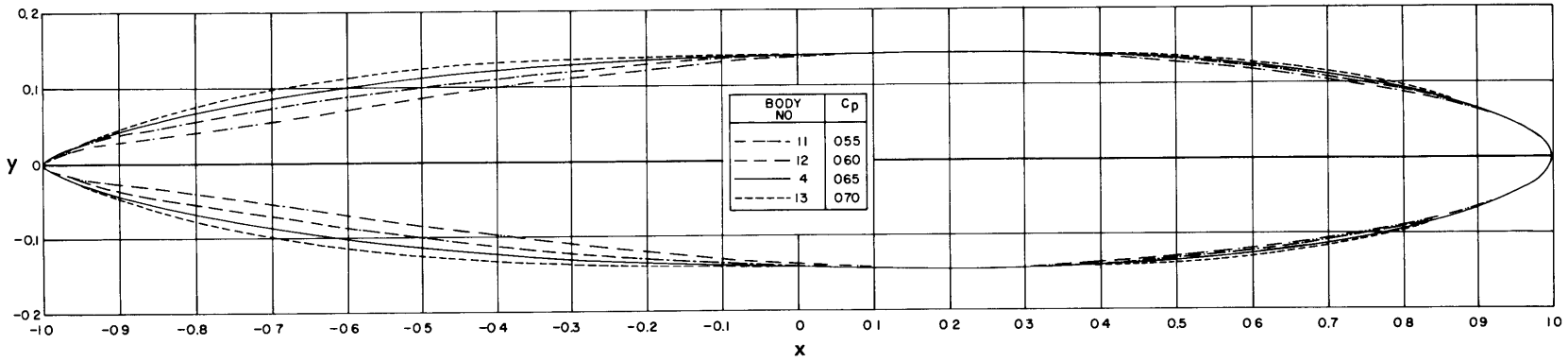

Figure 4 – Meridian Sections of Series 58 Bodies with Various Prismatic Coefficients

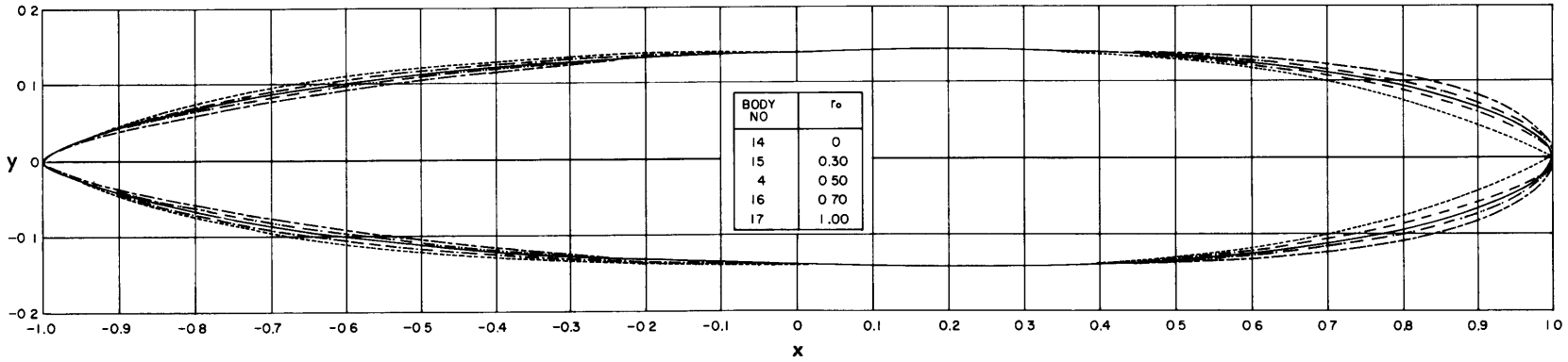

Figure 5 – Meridian Sections of Series 58 Bodies with Various Nose Radii

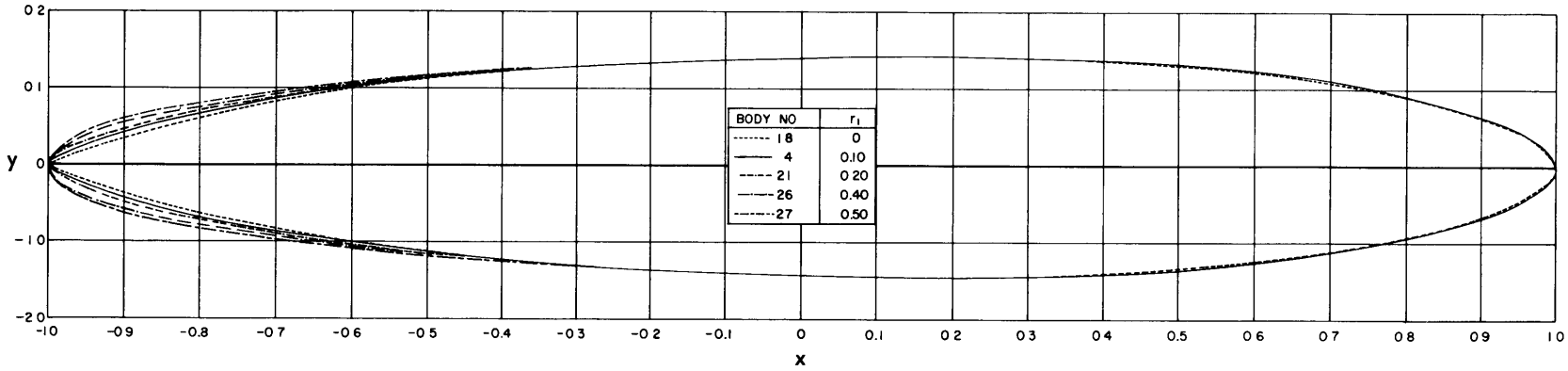

Figure 6 – Meridian Sections of Series 58 Bodies with Various Tail Radii

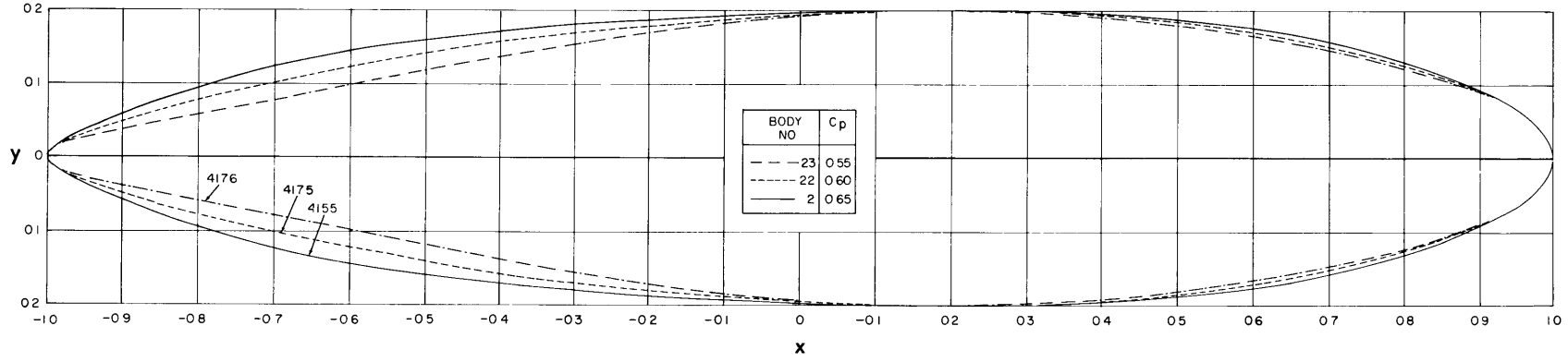

Figure 7 – Meridian Sections of Series 58 Bodies with Various Prismatic Coefficients

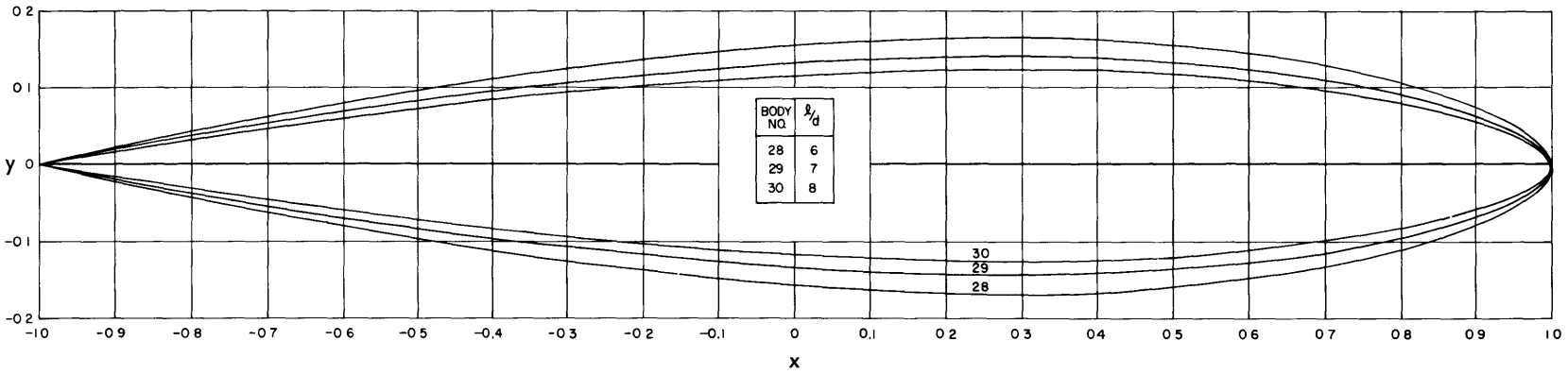

Figure 8 – Meridian Sections of Series 58 Bodies with Various Length/Diameter Ratios

Figures 9 through 38

Velocity Functions of Bodies 1 through 30

Values of u_{1s}, $u_{1s} \sec \gamma$, $u_{2\theta}$, u_{2s}, $u_{R\theta}$, and u_{Rs} versus x

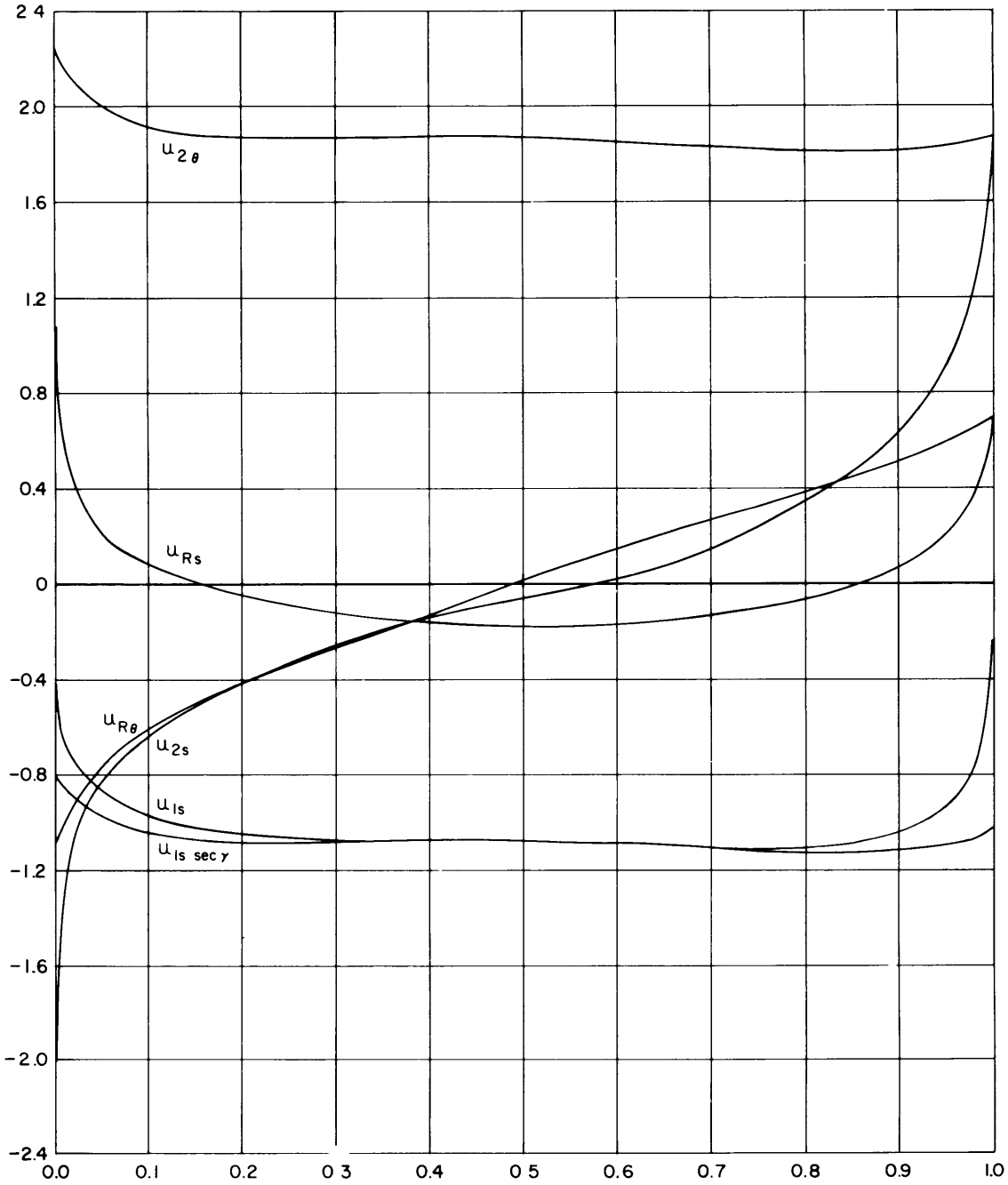

Figure 9 – Body 1

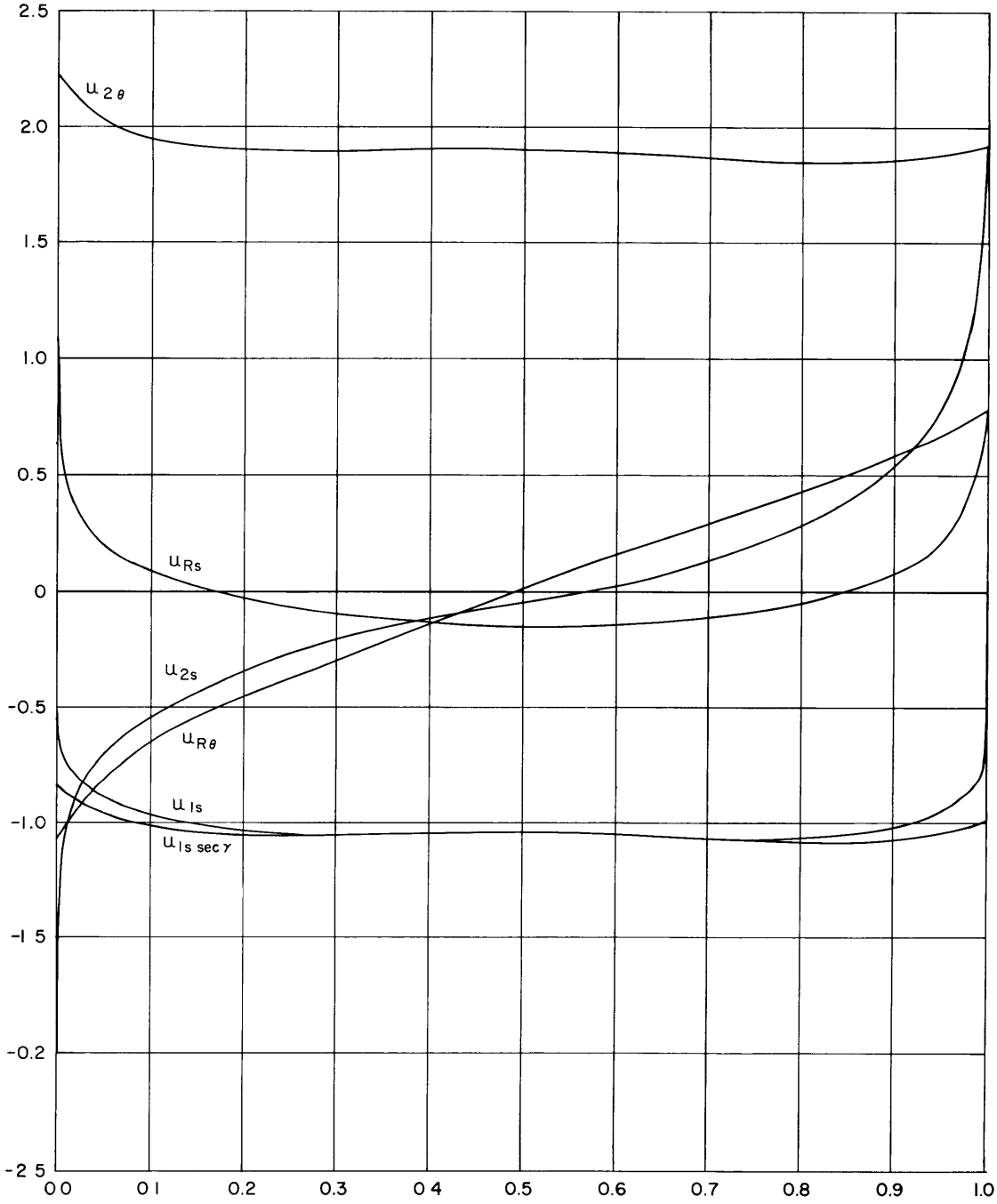

Figure 10 – Body 2

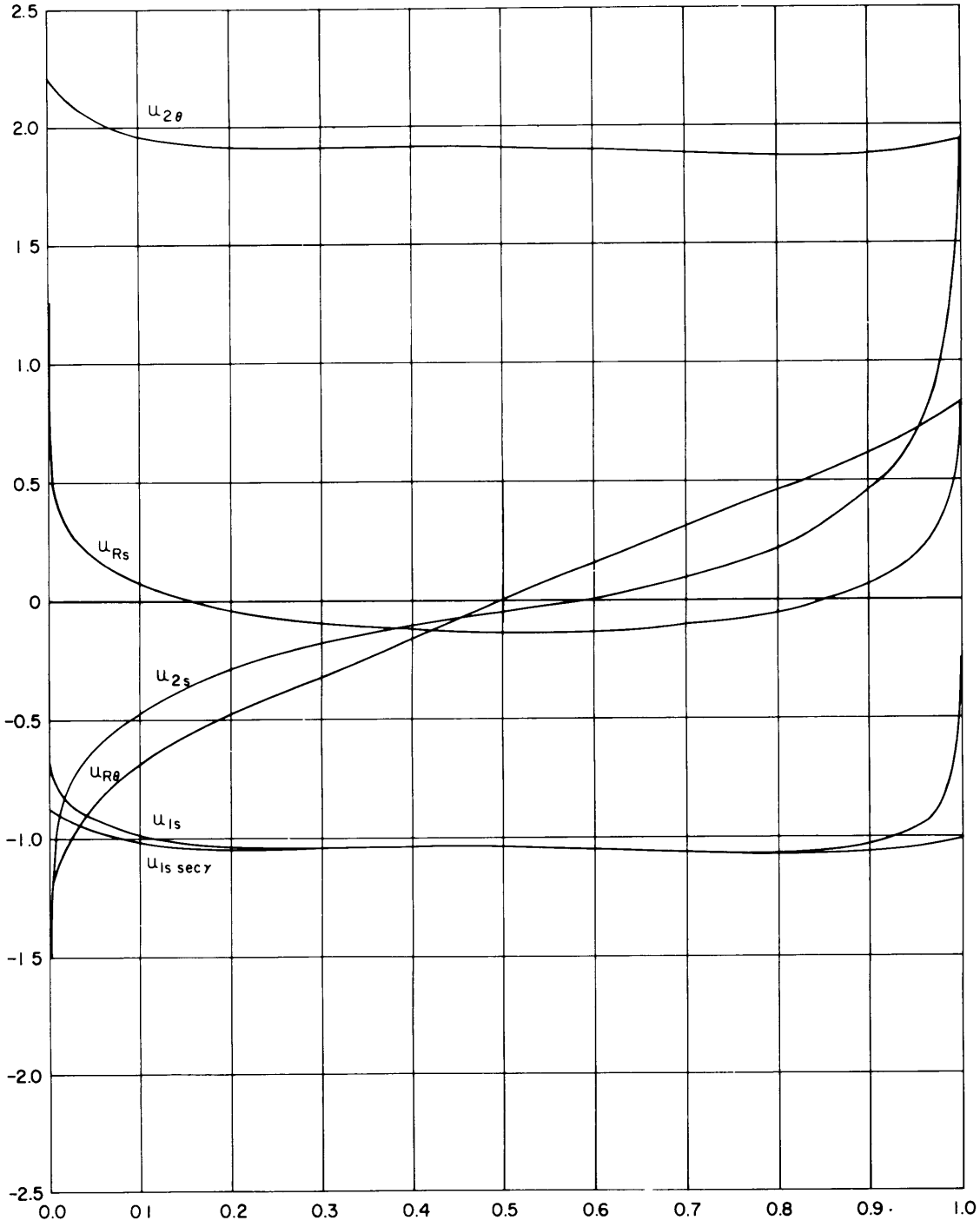

Figure 11 – Body 3

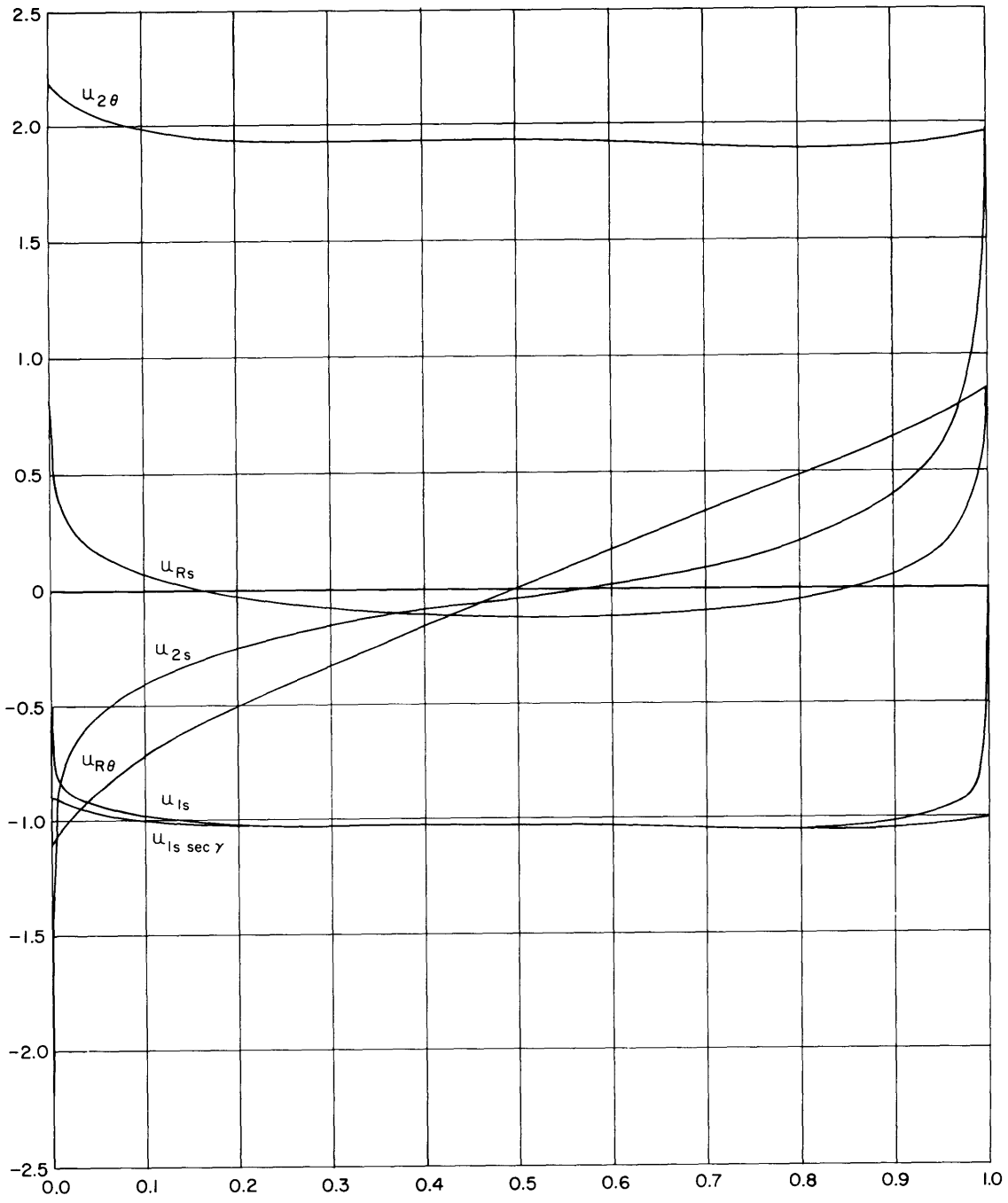

Figure 12 – Body 4

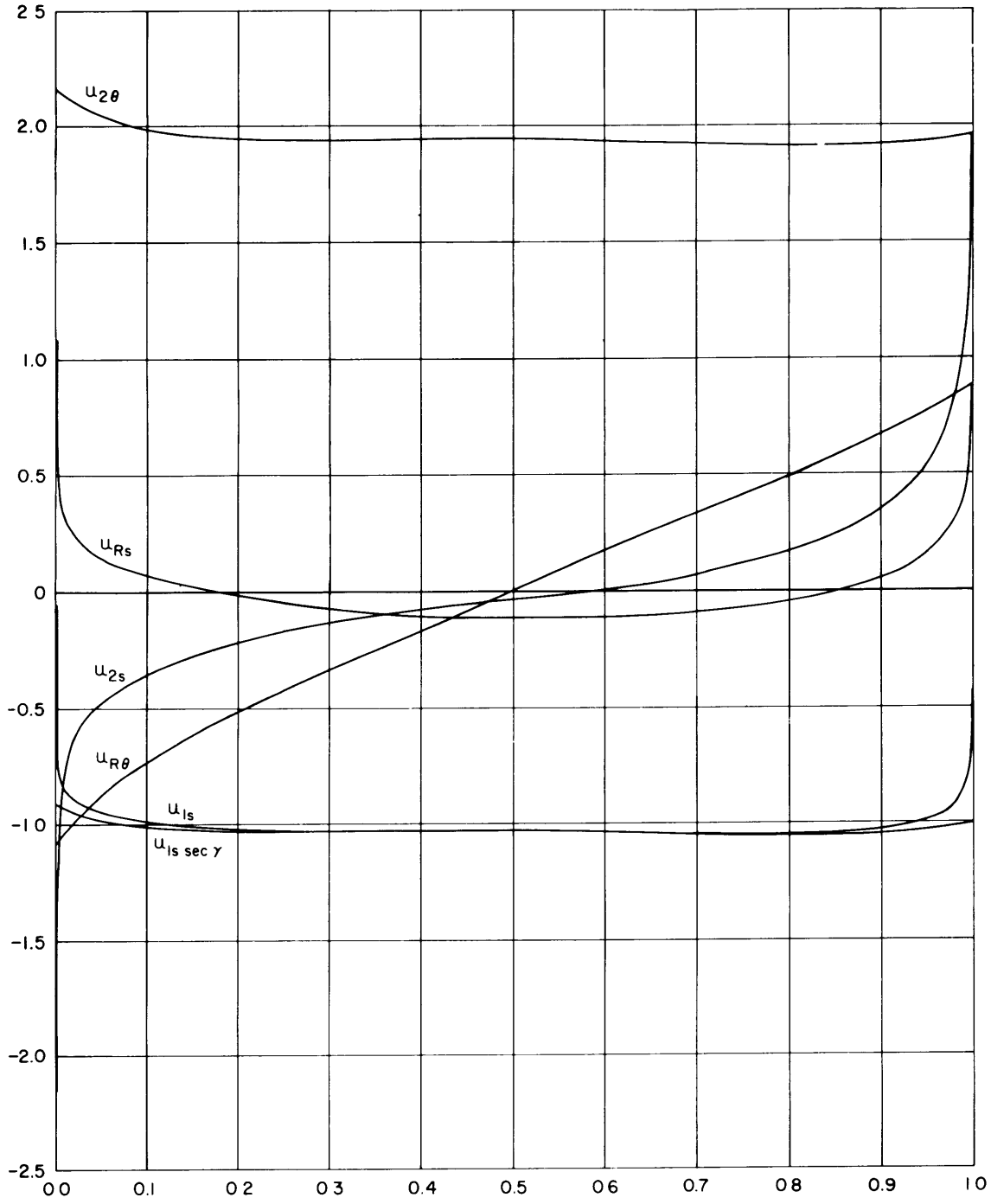

Figure 13 – Body 5

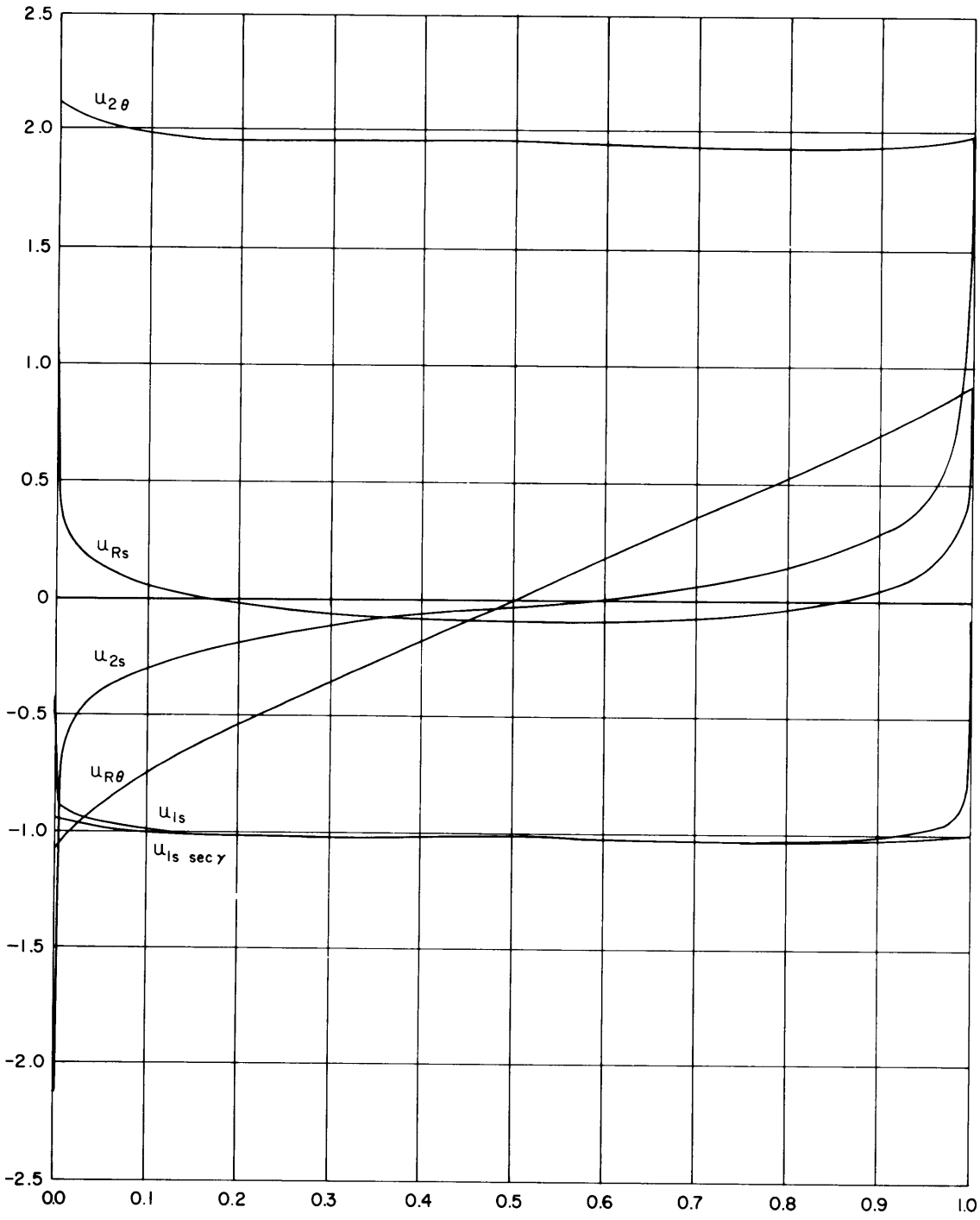

Figure 14 – Body 6

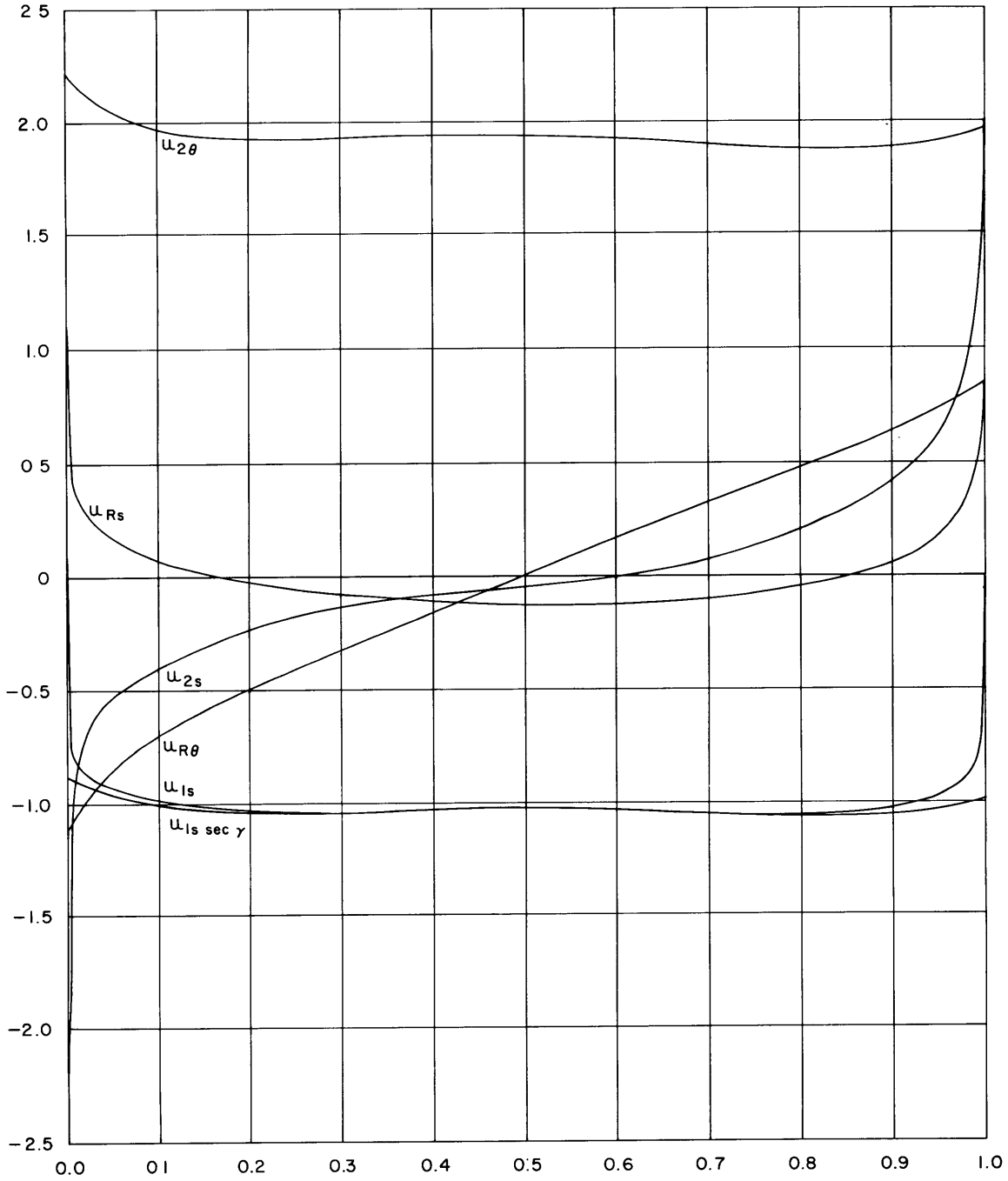

Figure 15 – Body 7

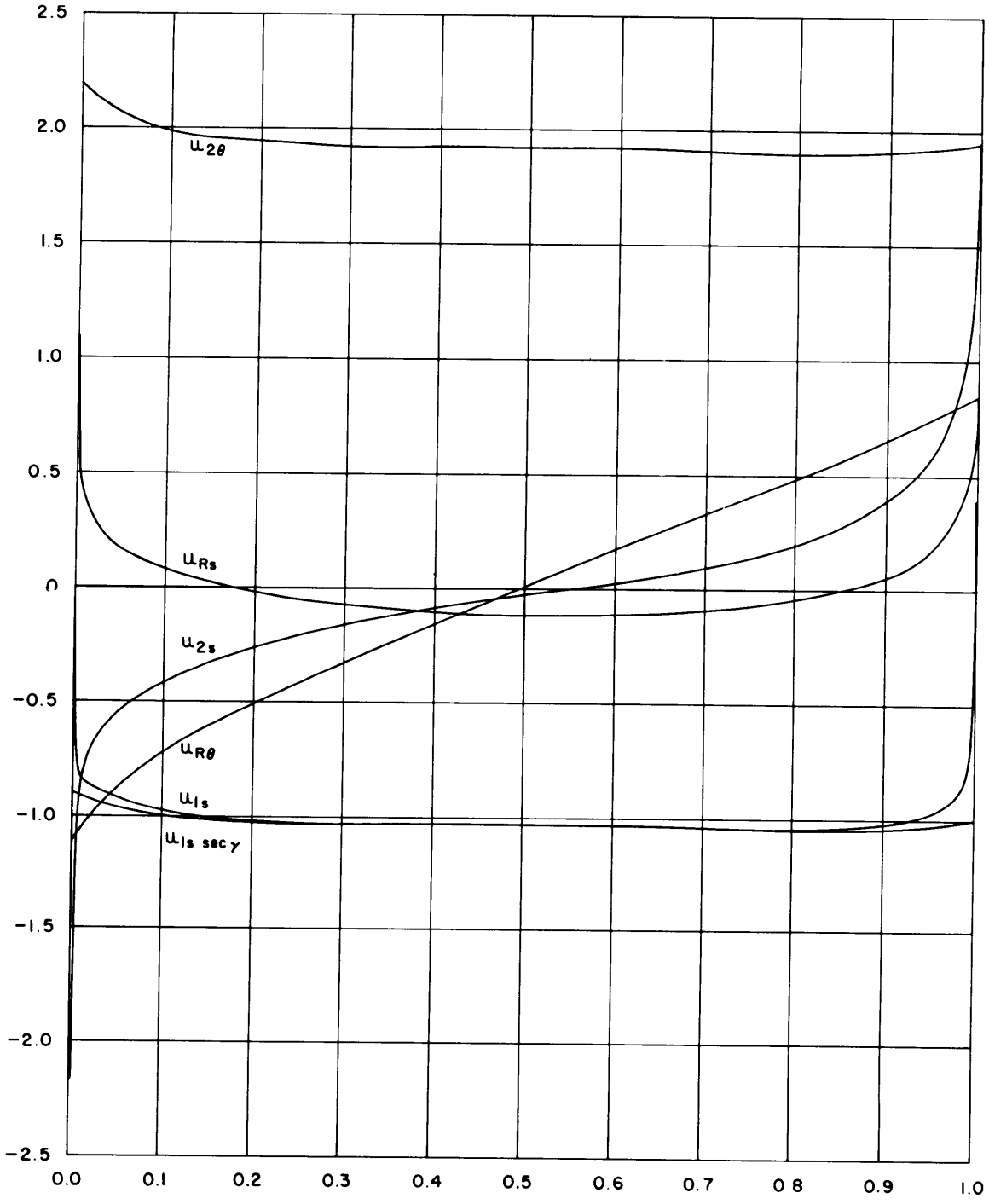

Figure 16 – Body 8

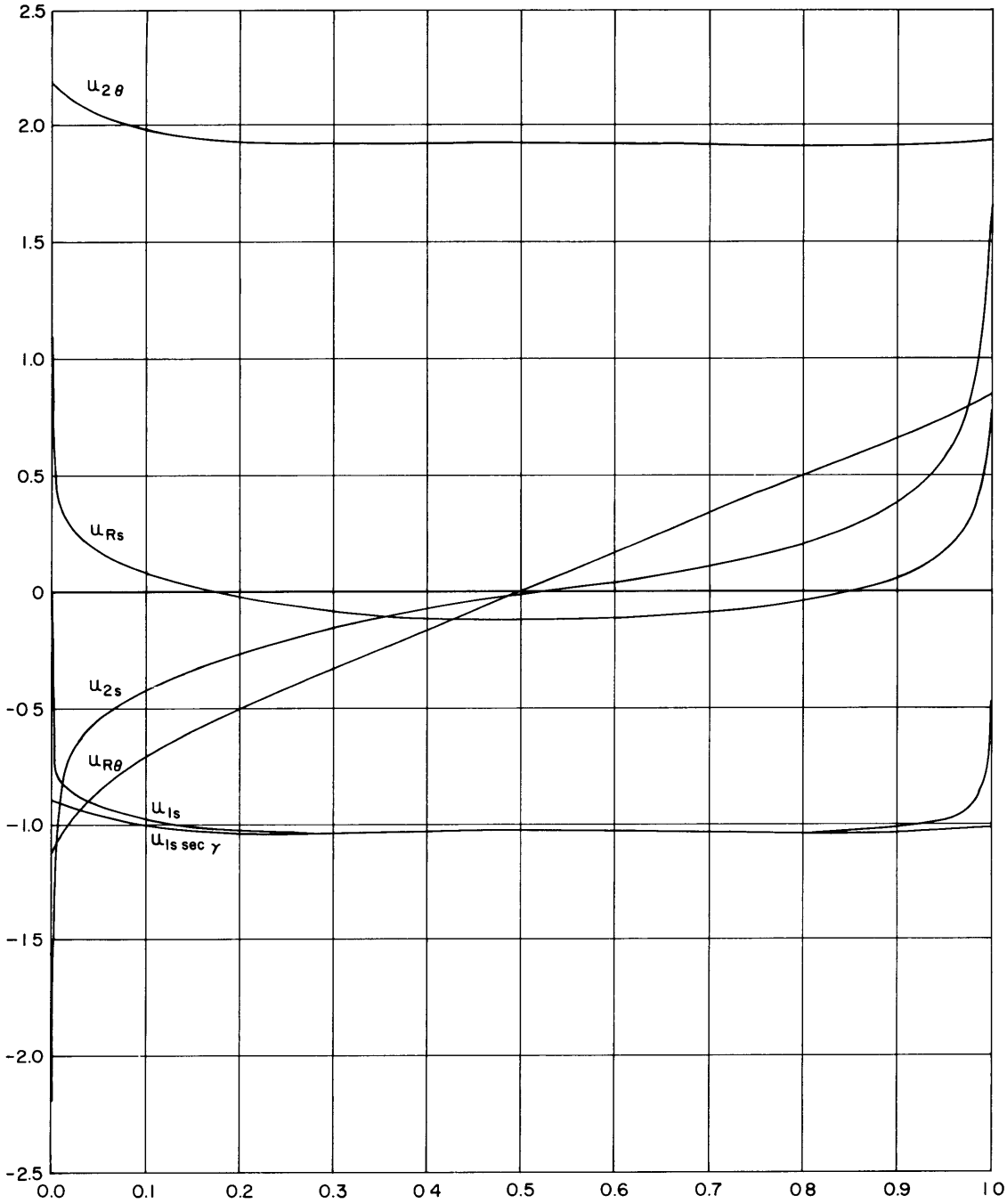

Figure 17 – Body 9

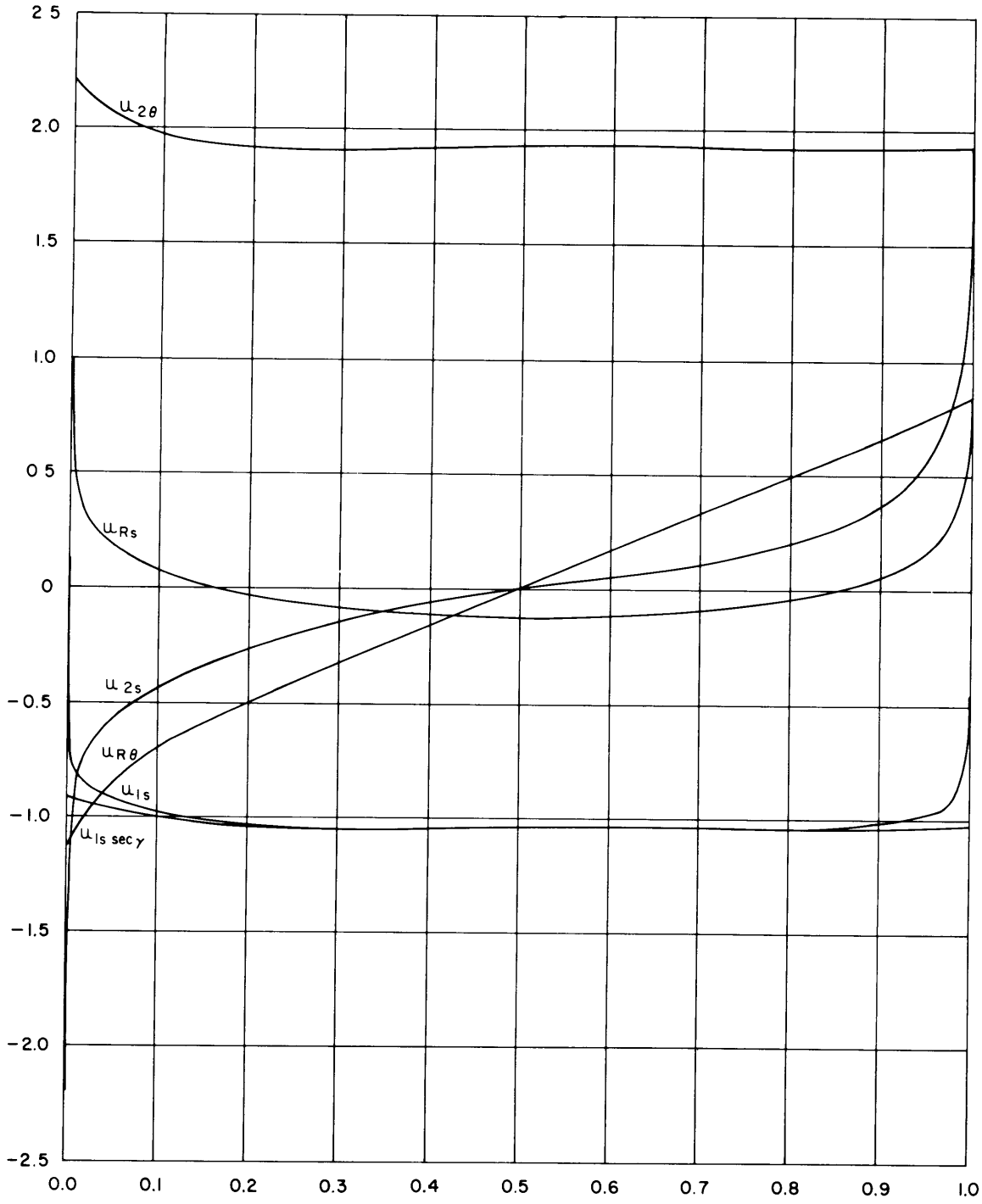

Figure 18 – Body 10

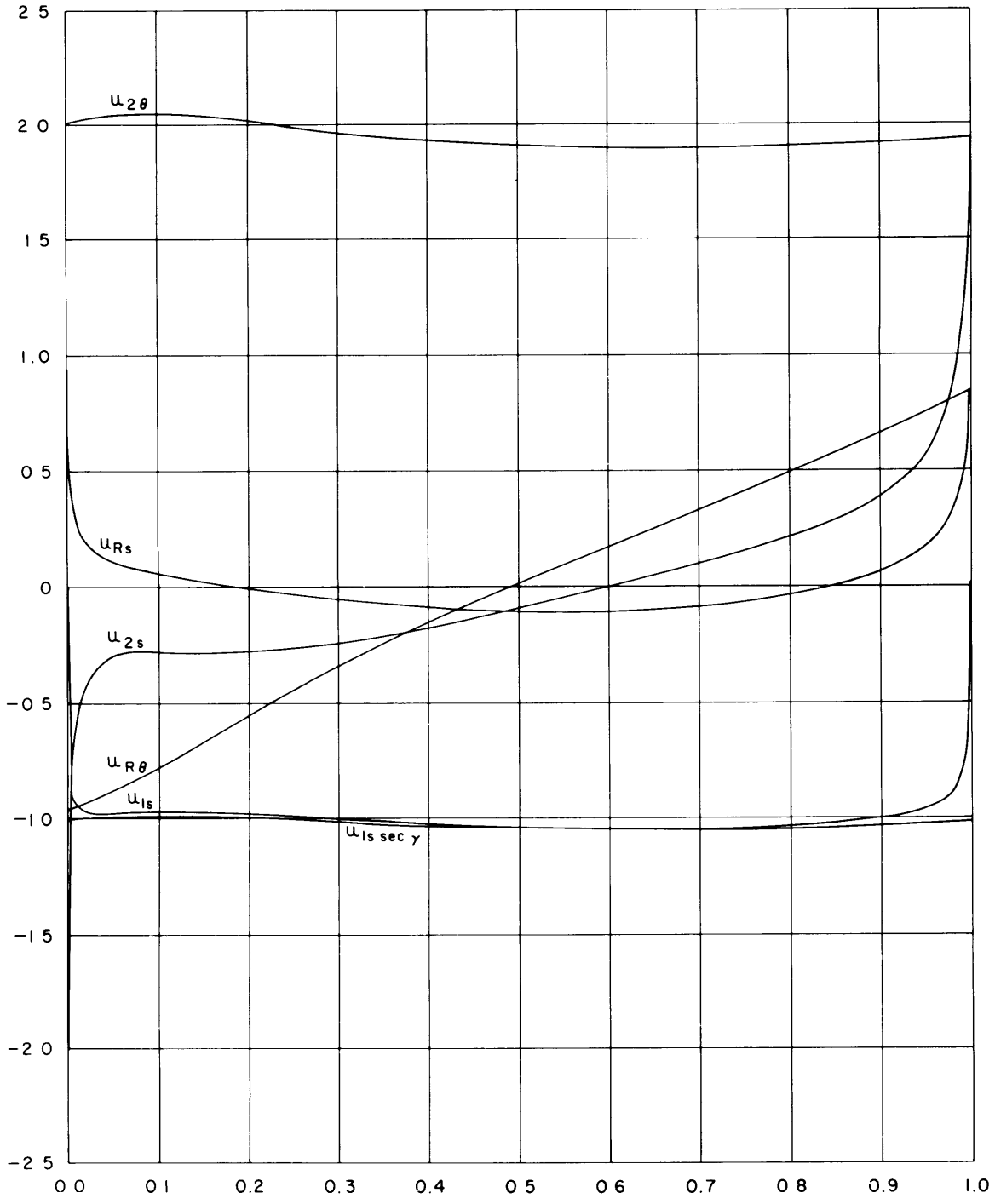

Figure 19 – Body 11

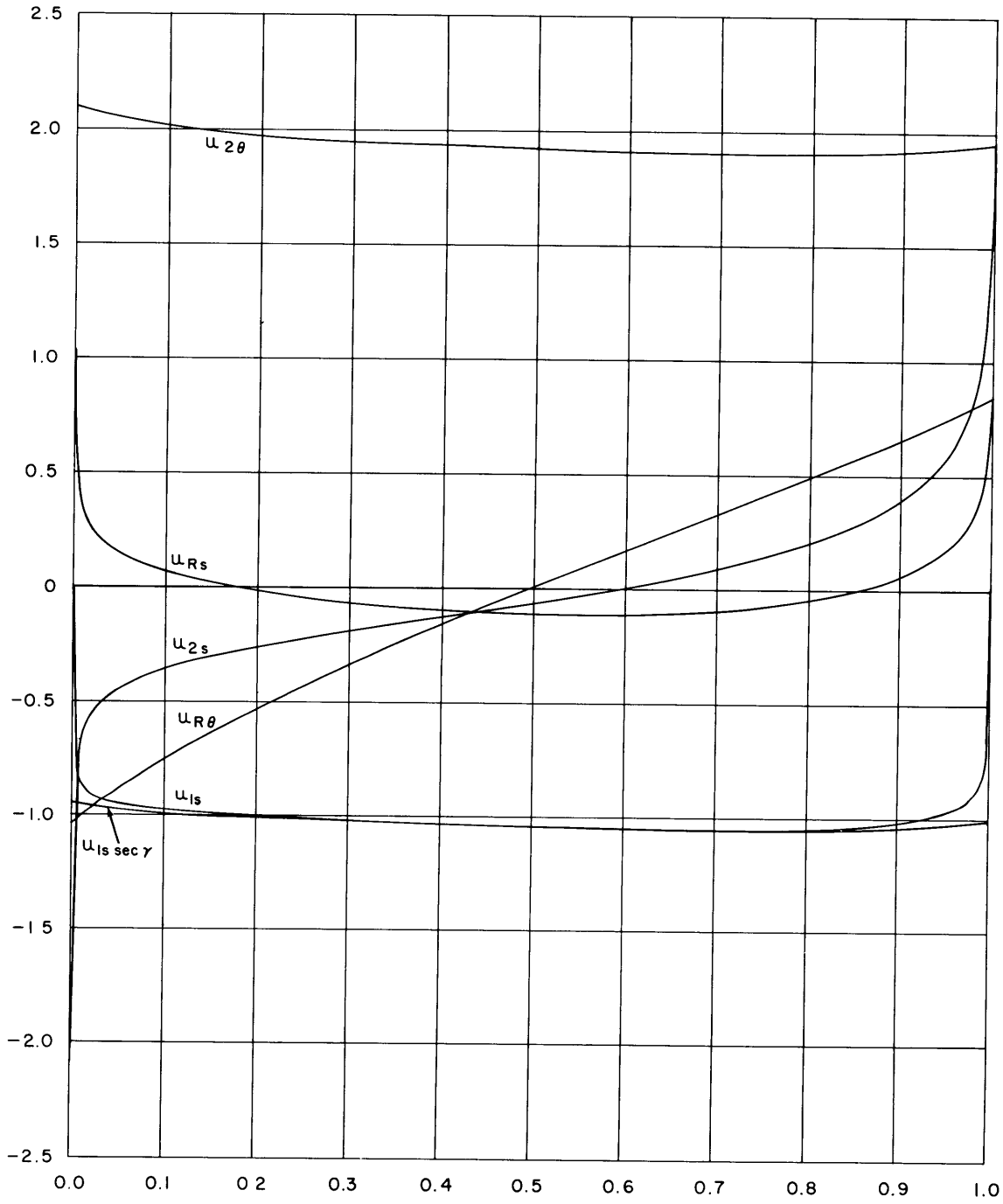

Figure 20 – Body 12

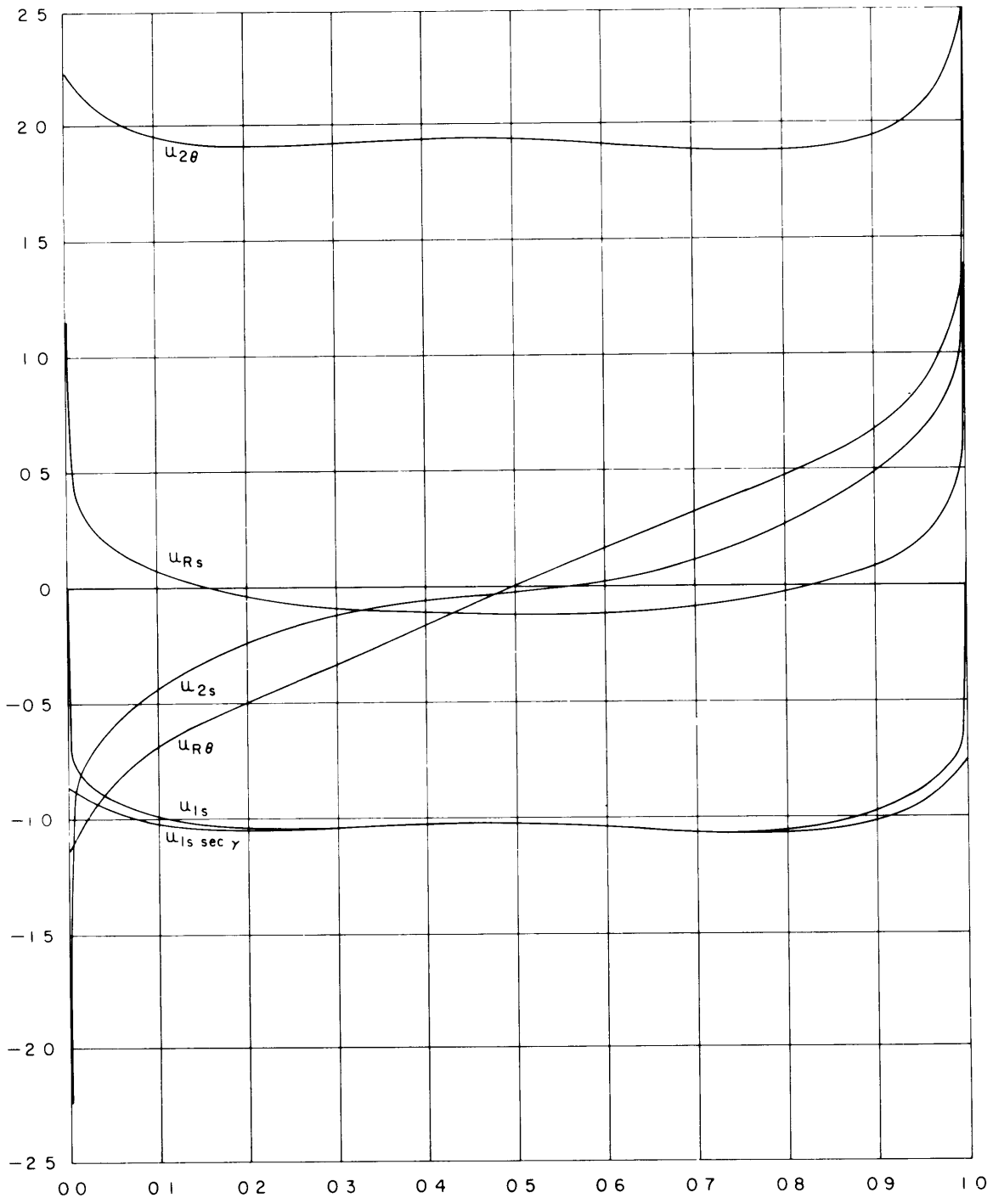

Figure 21 – Body 13

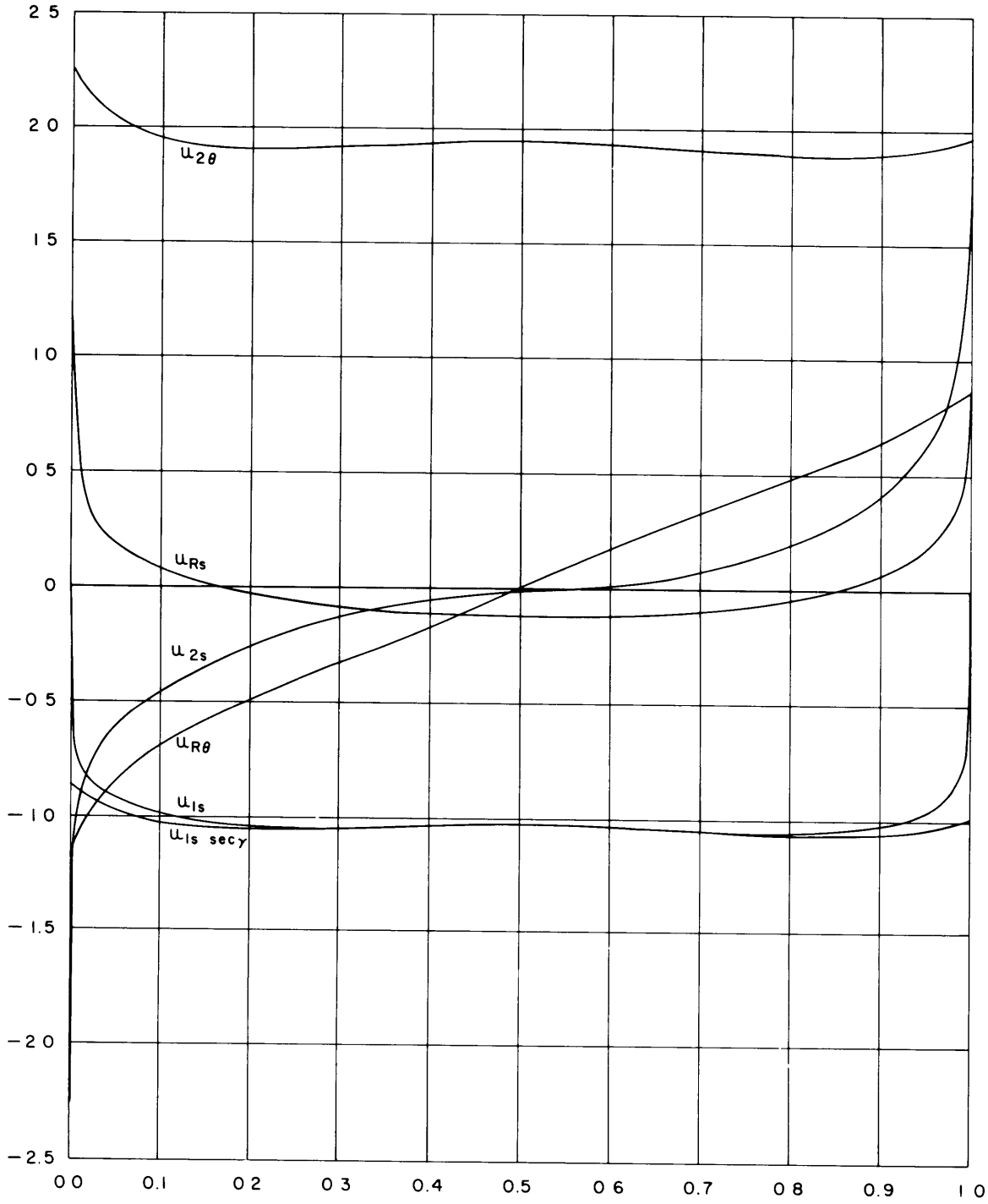

Figure 22 – Body 14

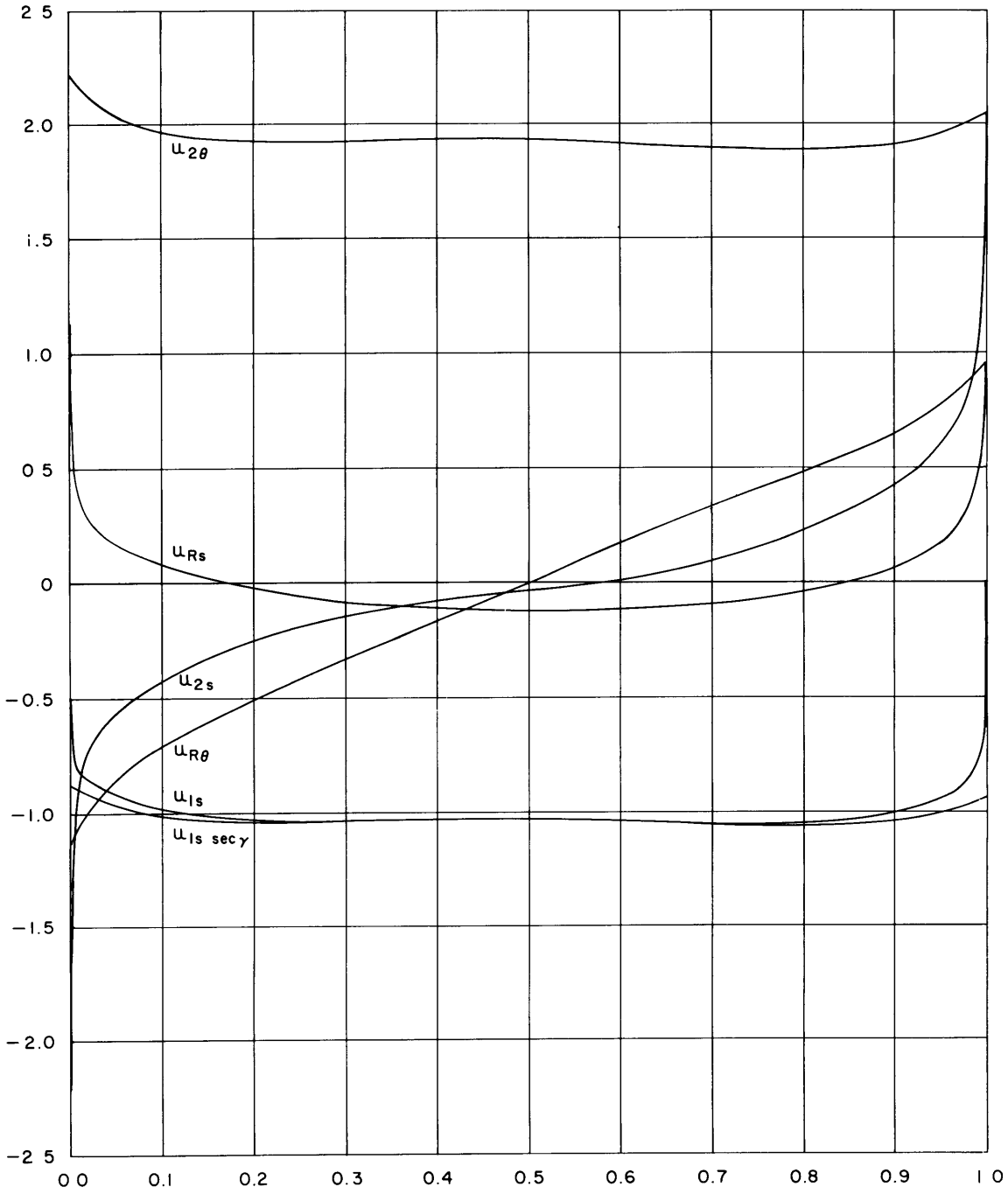

Figure 23 – Body 15

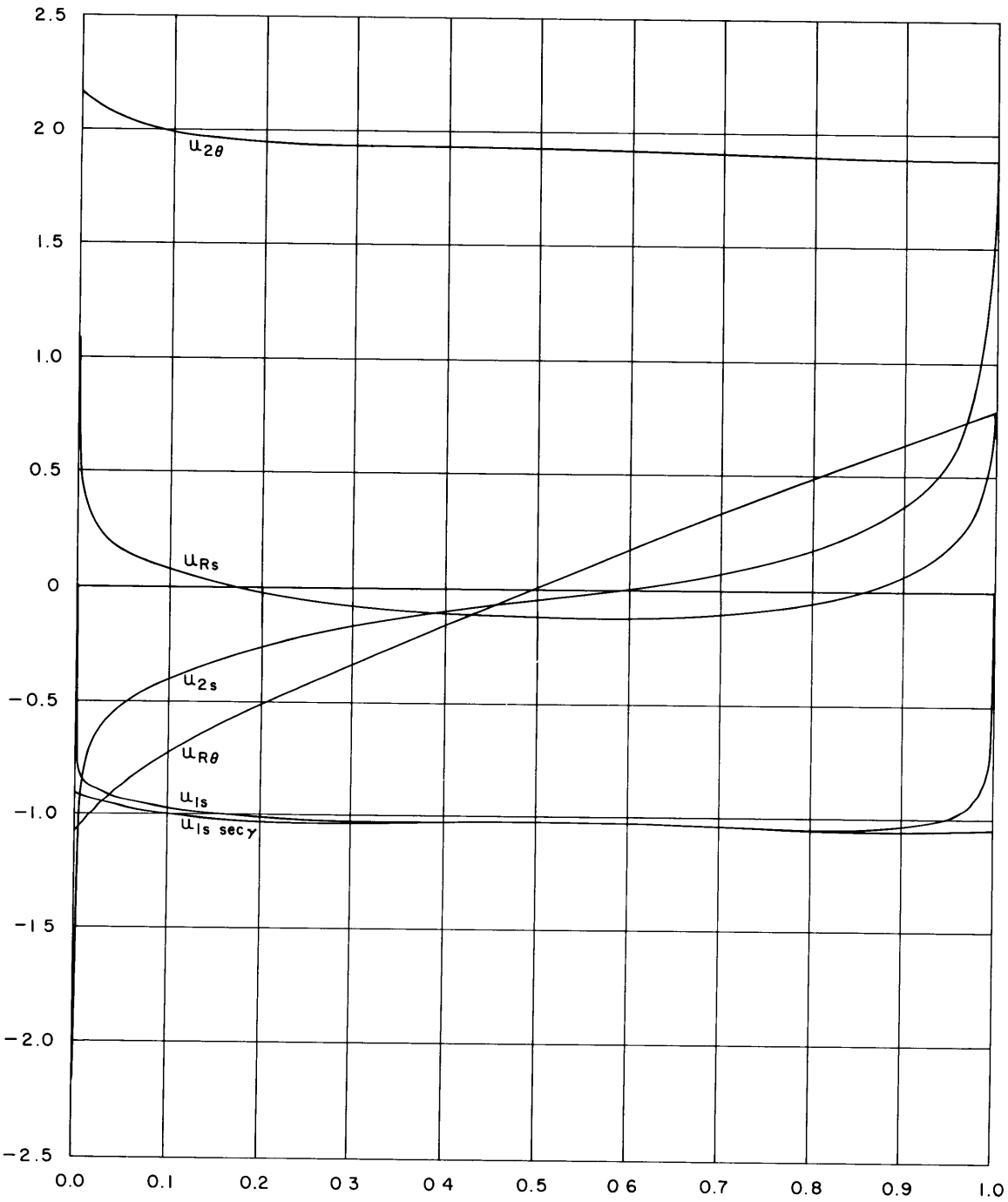

Figure 24 – Body 16

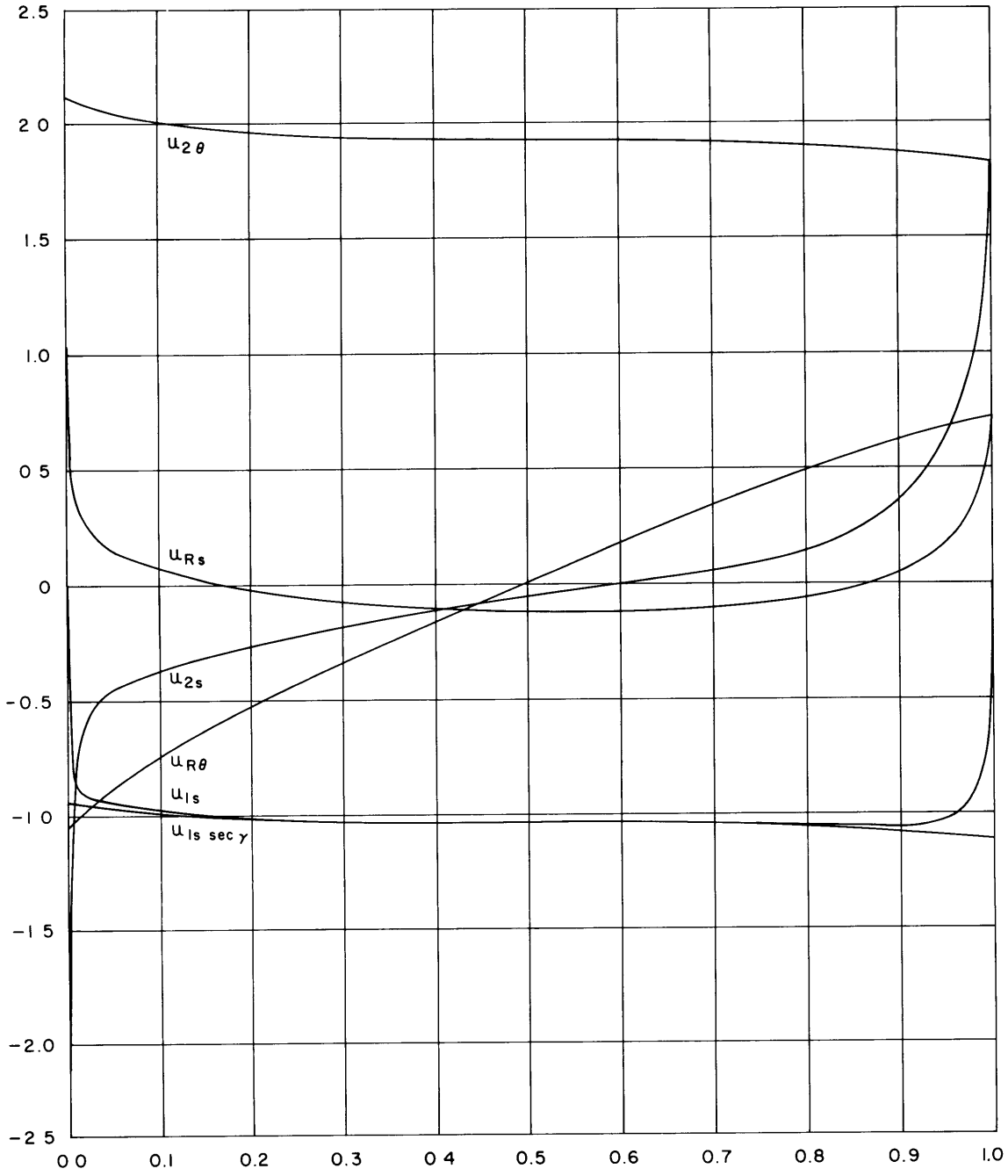

Figure 25 – Body 17

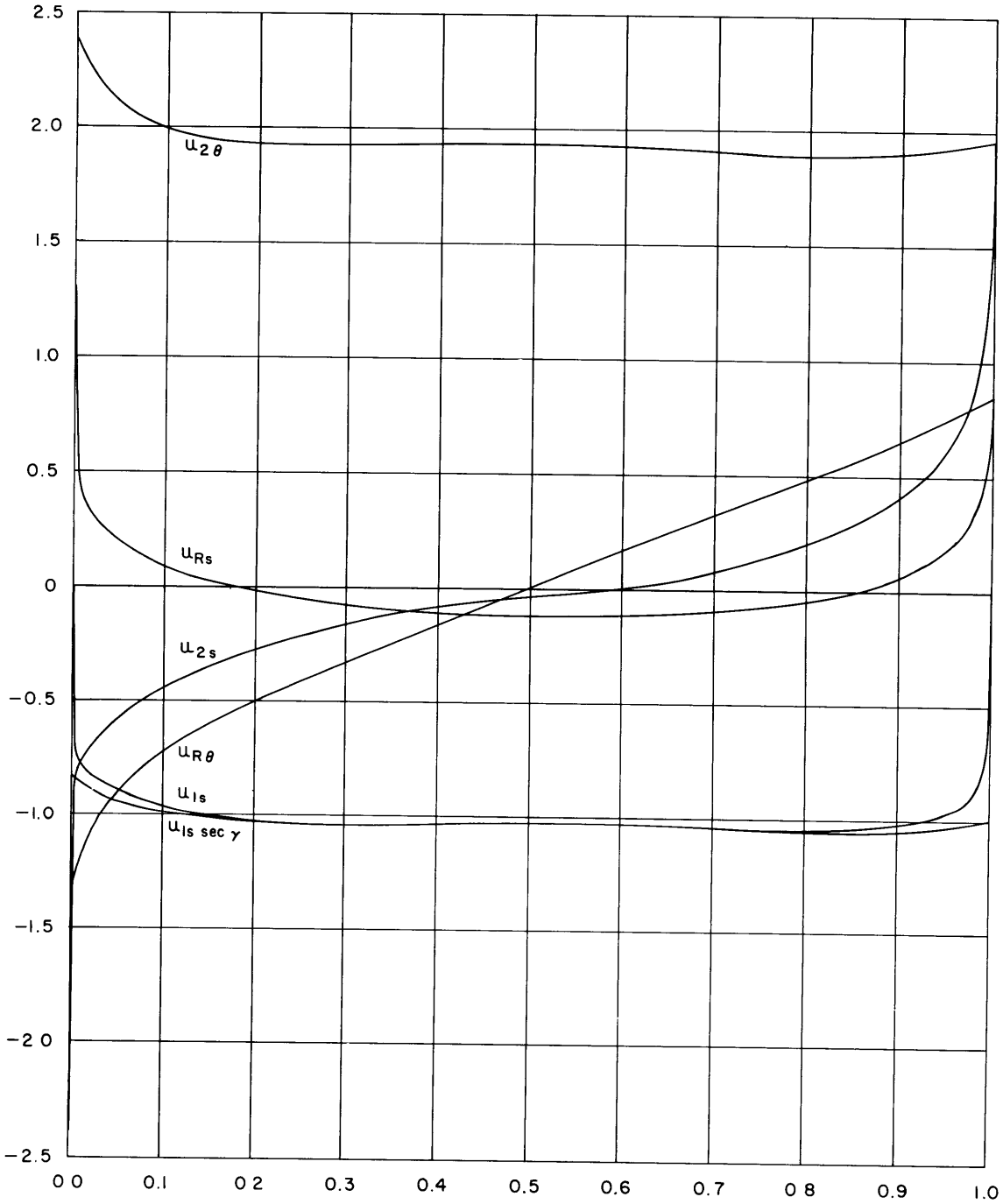

Figure 26 – Body 18

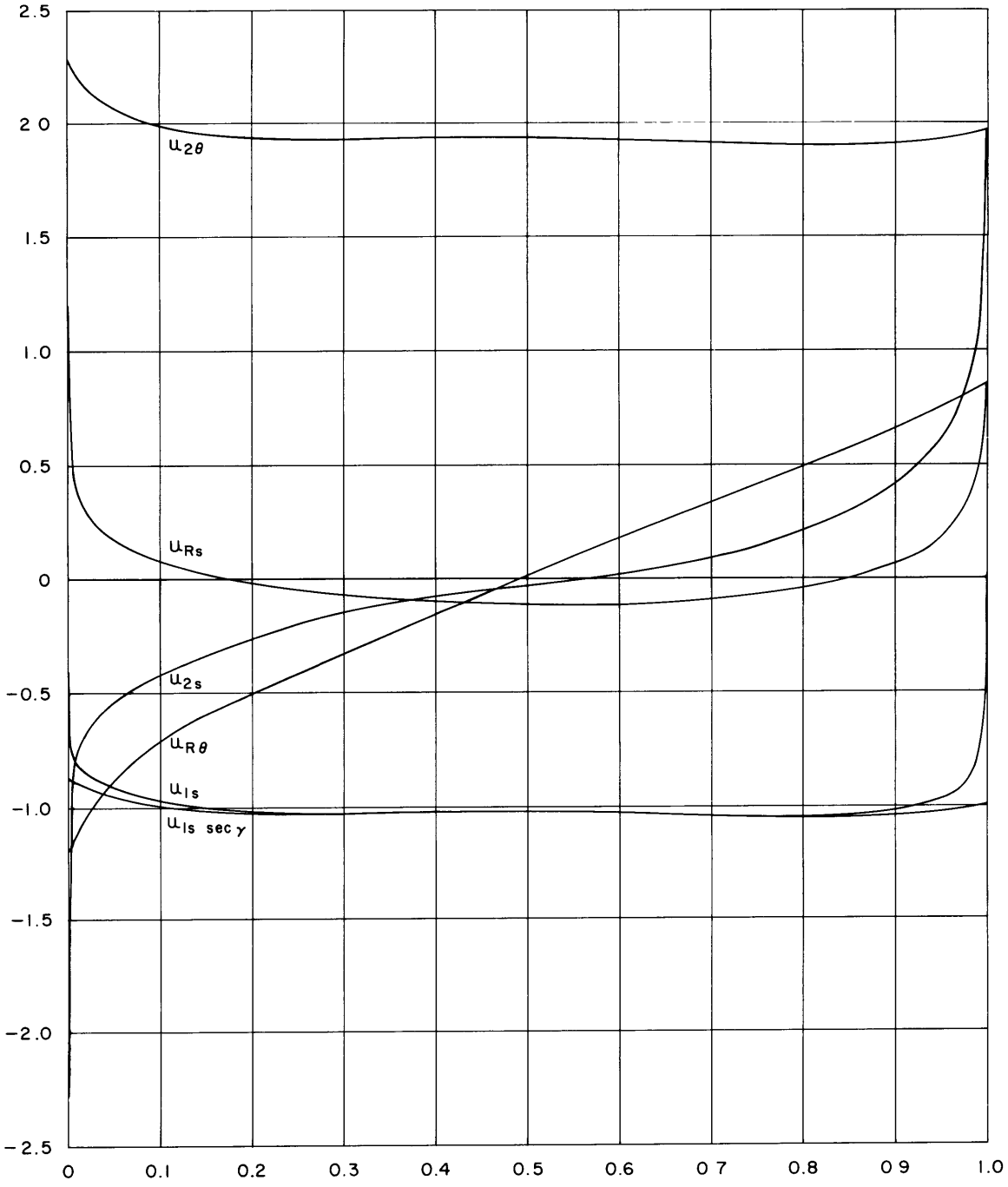

Figure 27 – Body 19

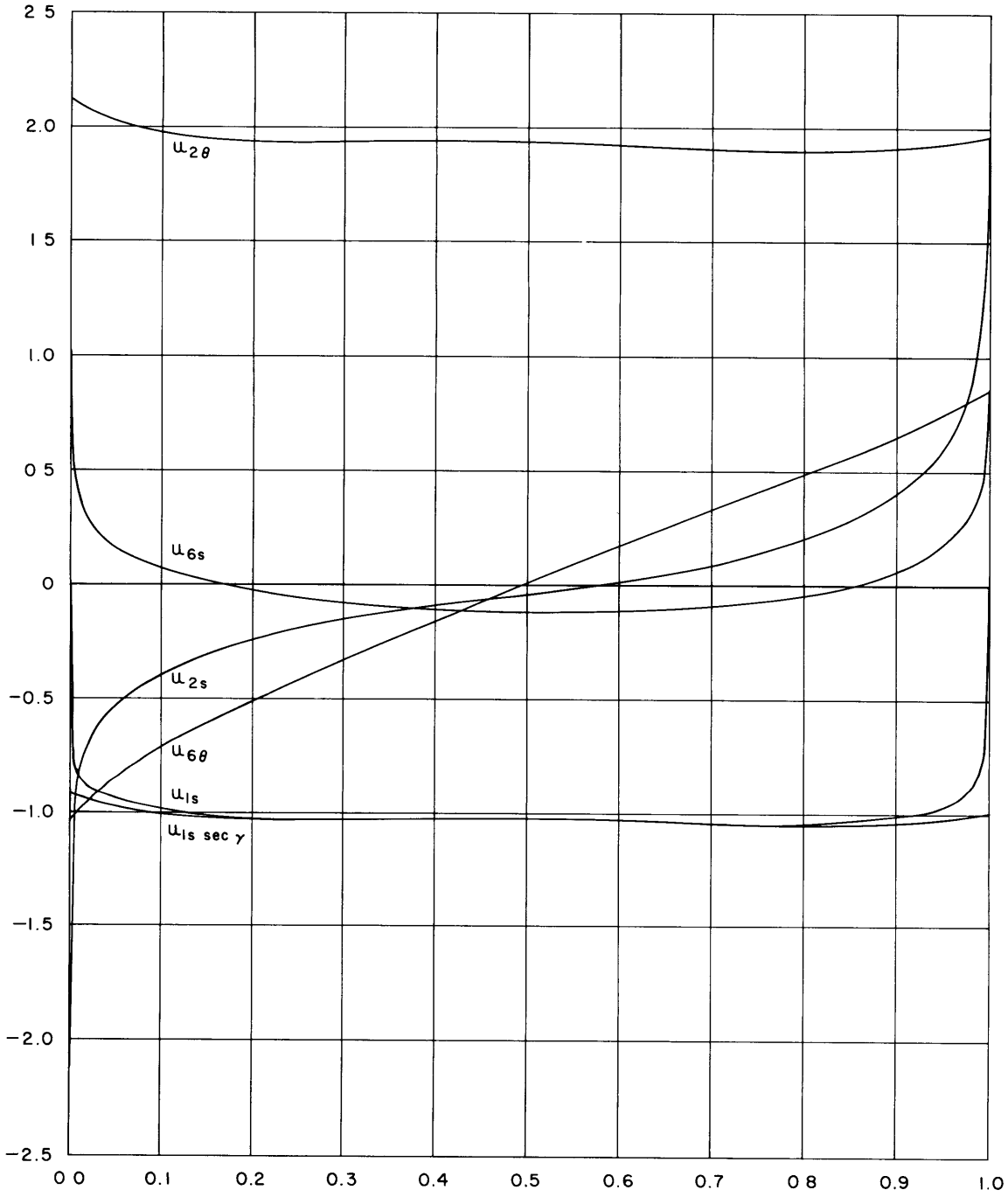

Figure 28 – Body 20

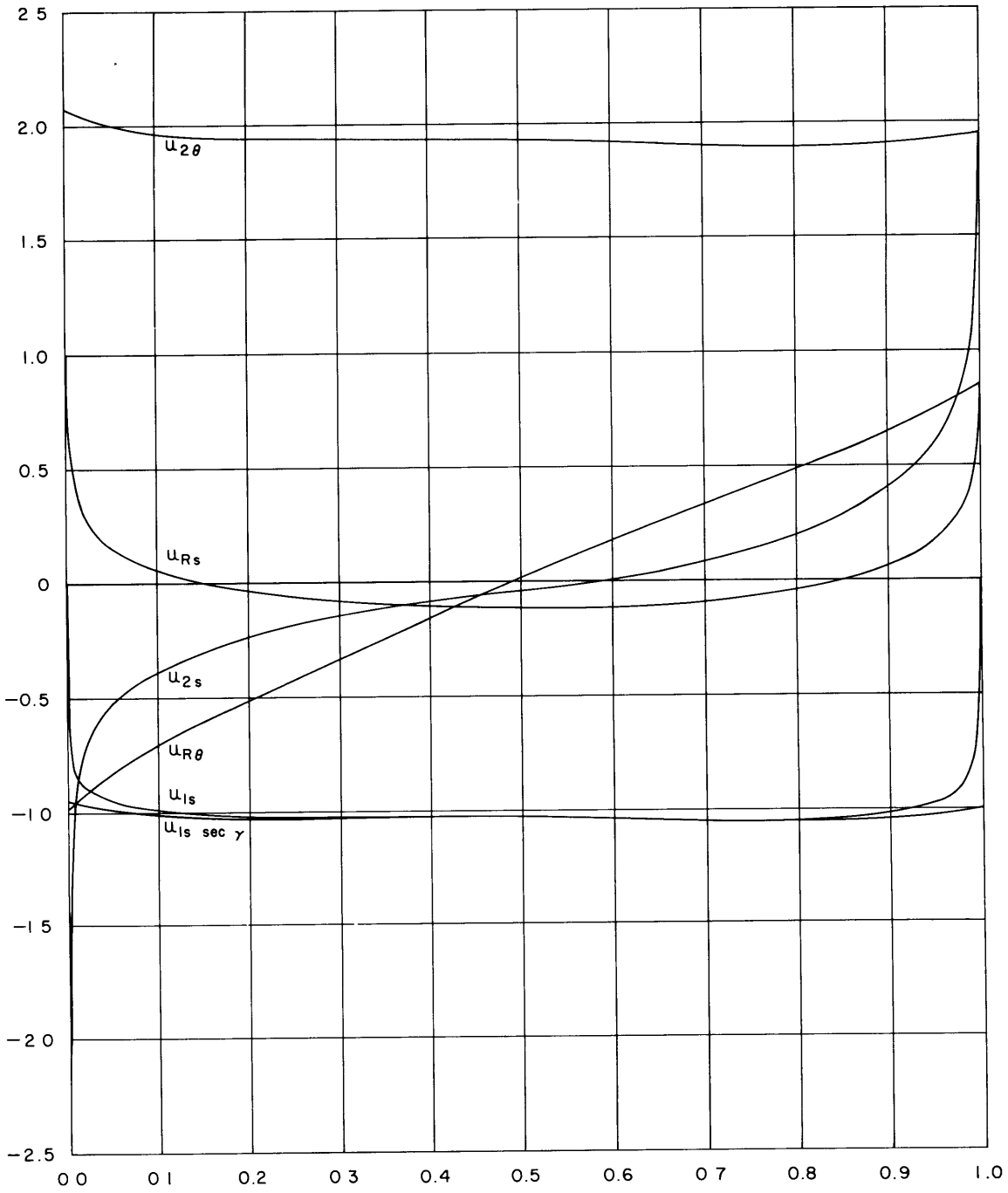

Figure 29 – Body 21

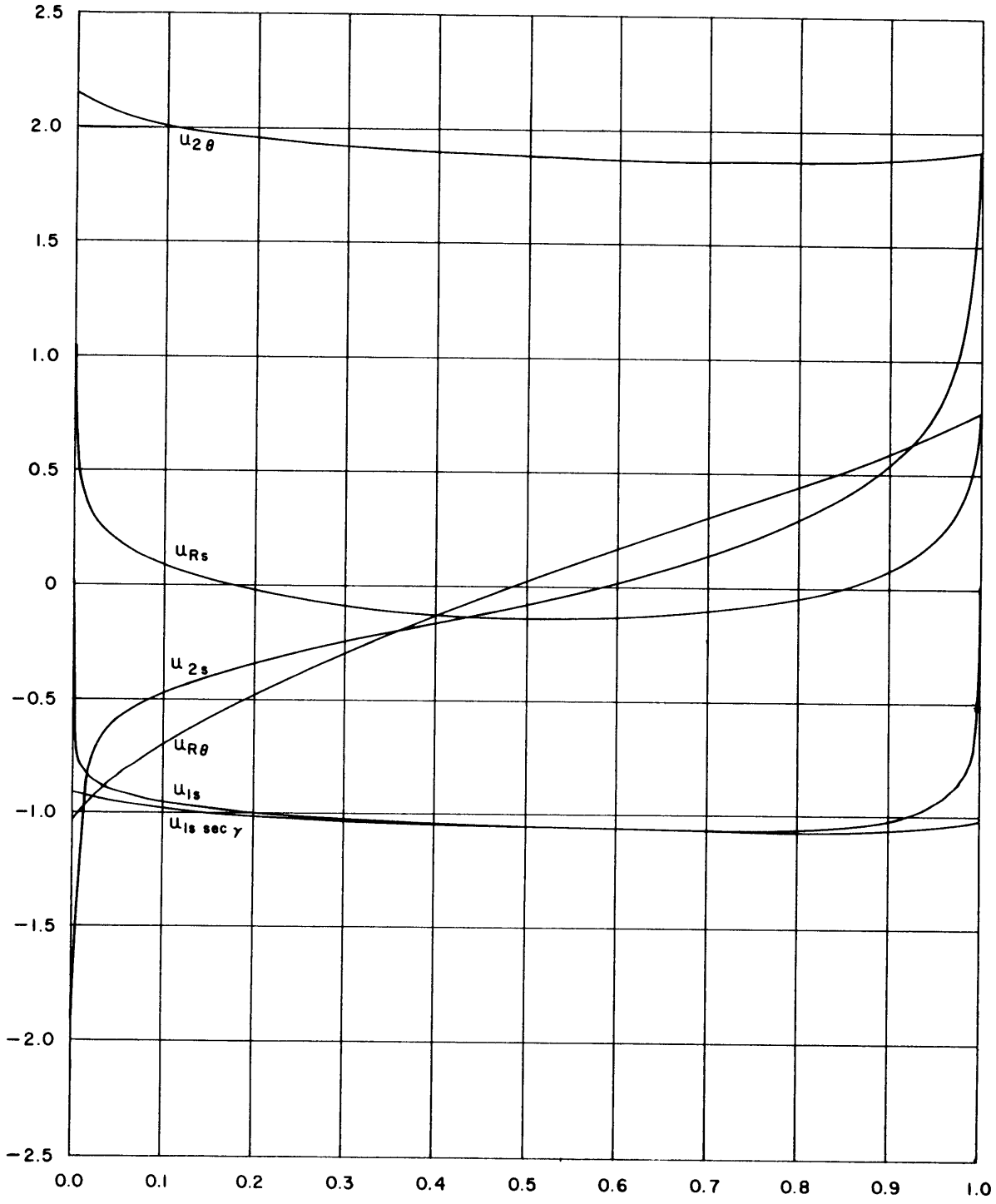

Figure 30 – Body 22

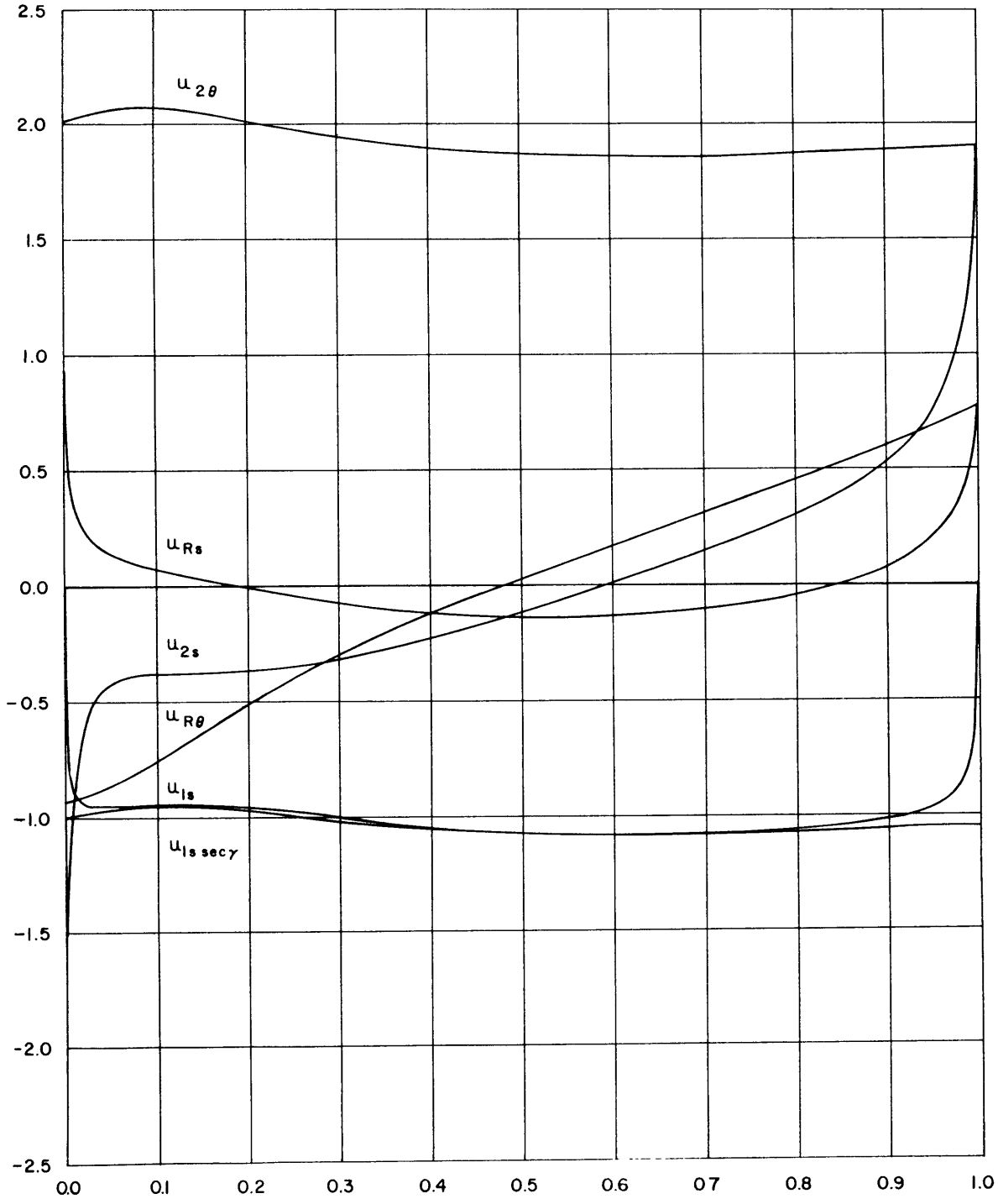

Figure 31 – Body 23

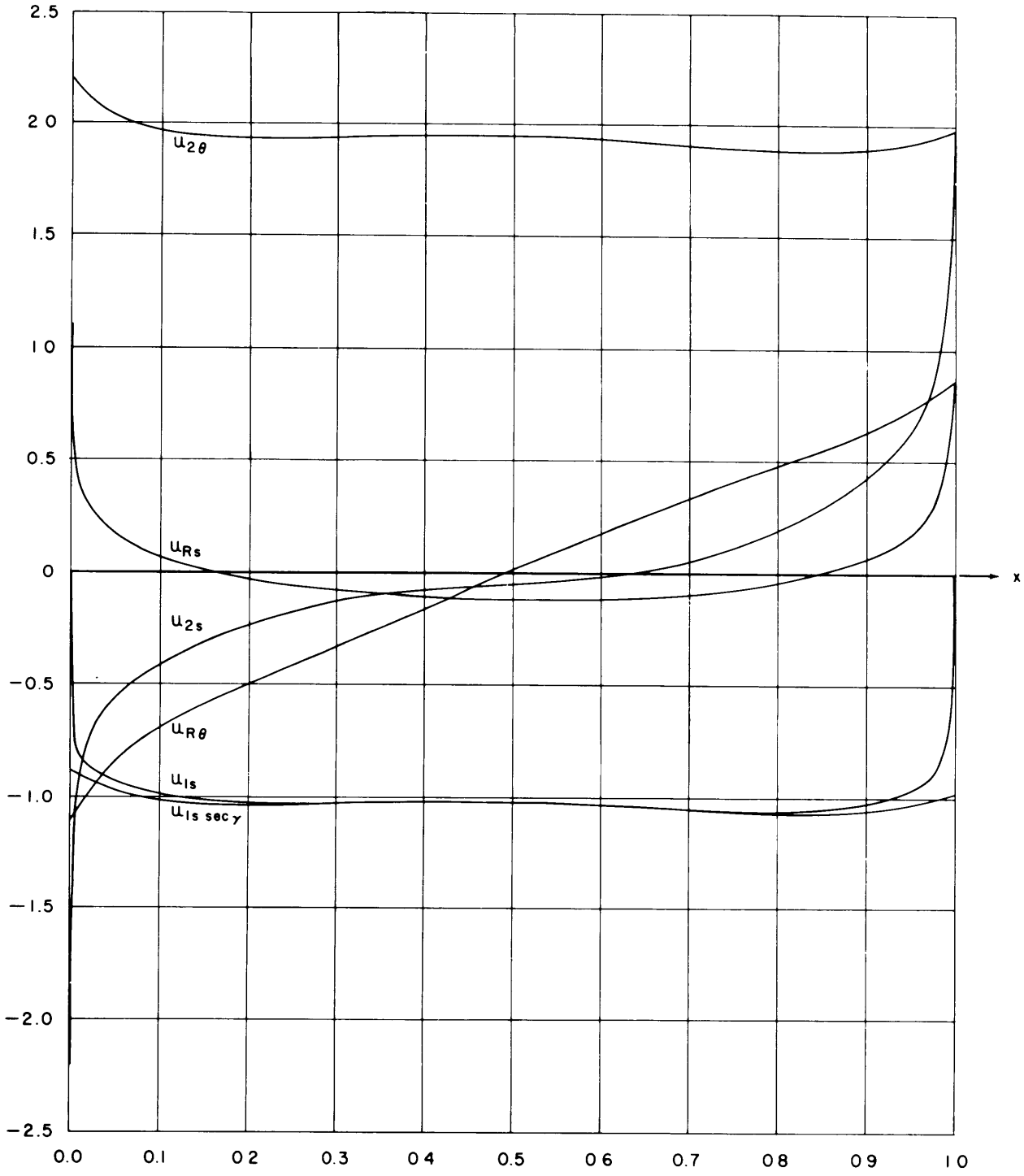

Figure 32 – Body 24

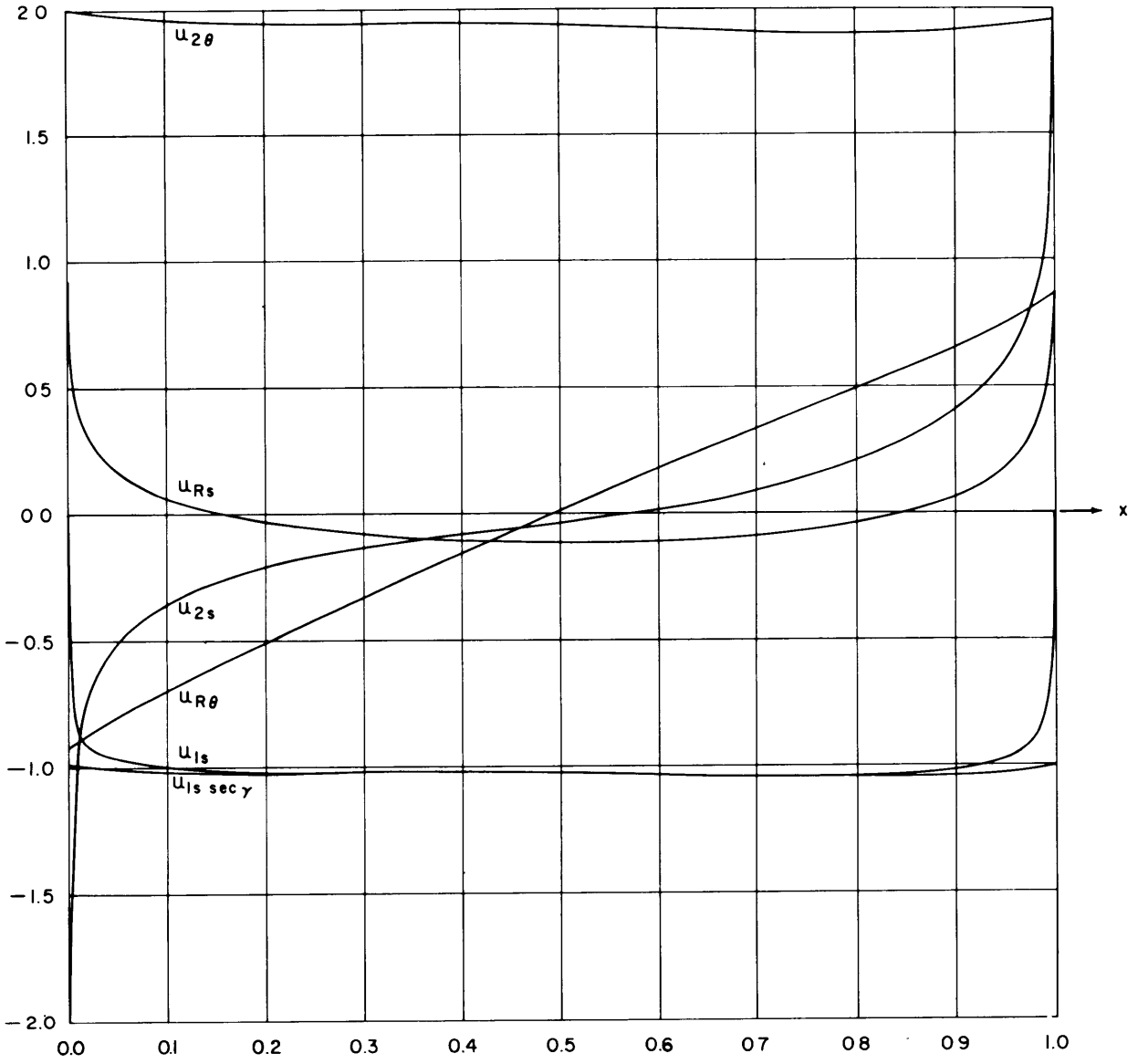

Figure 33 – Body 25

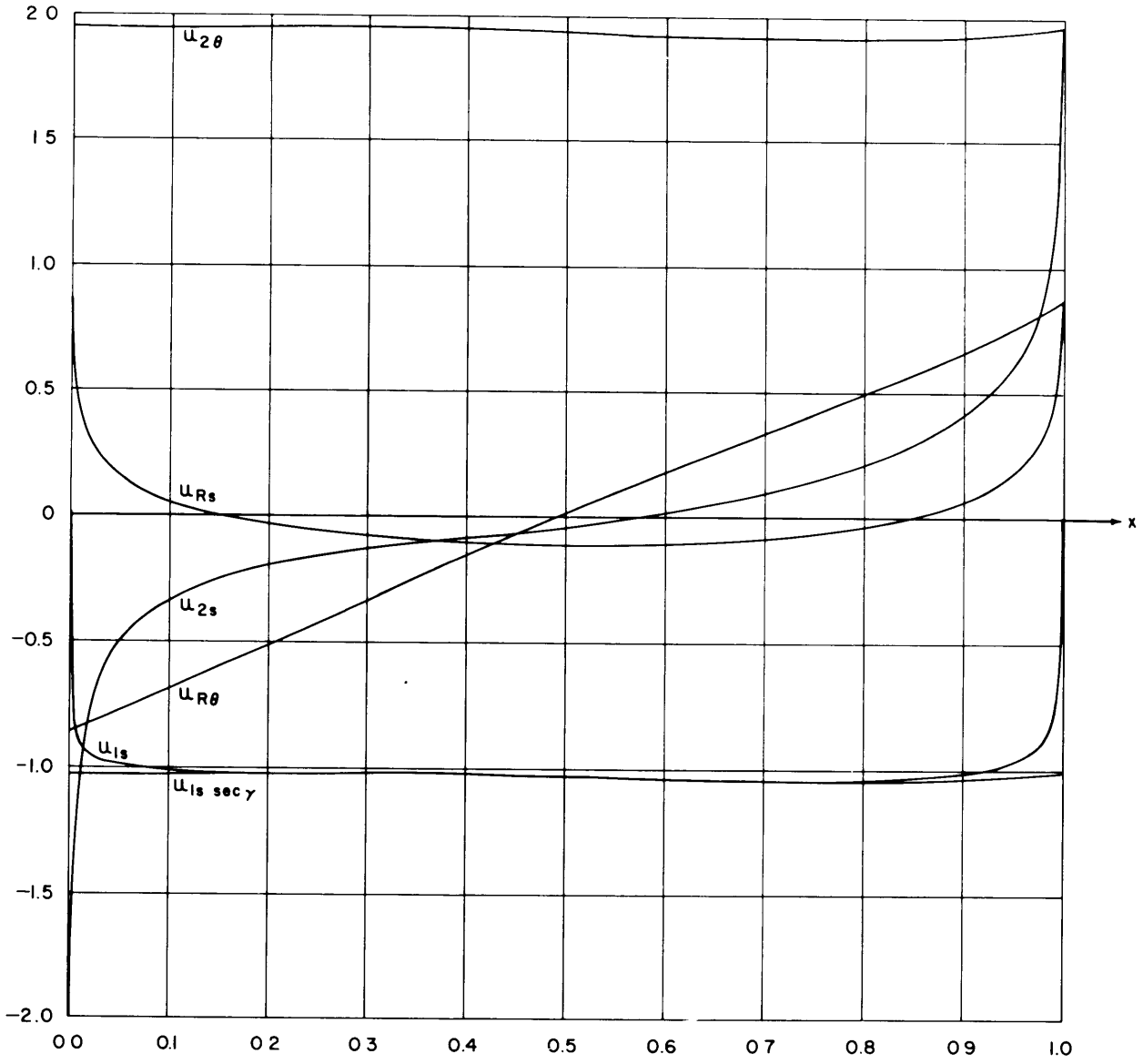

Figure 34 – Body 26

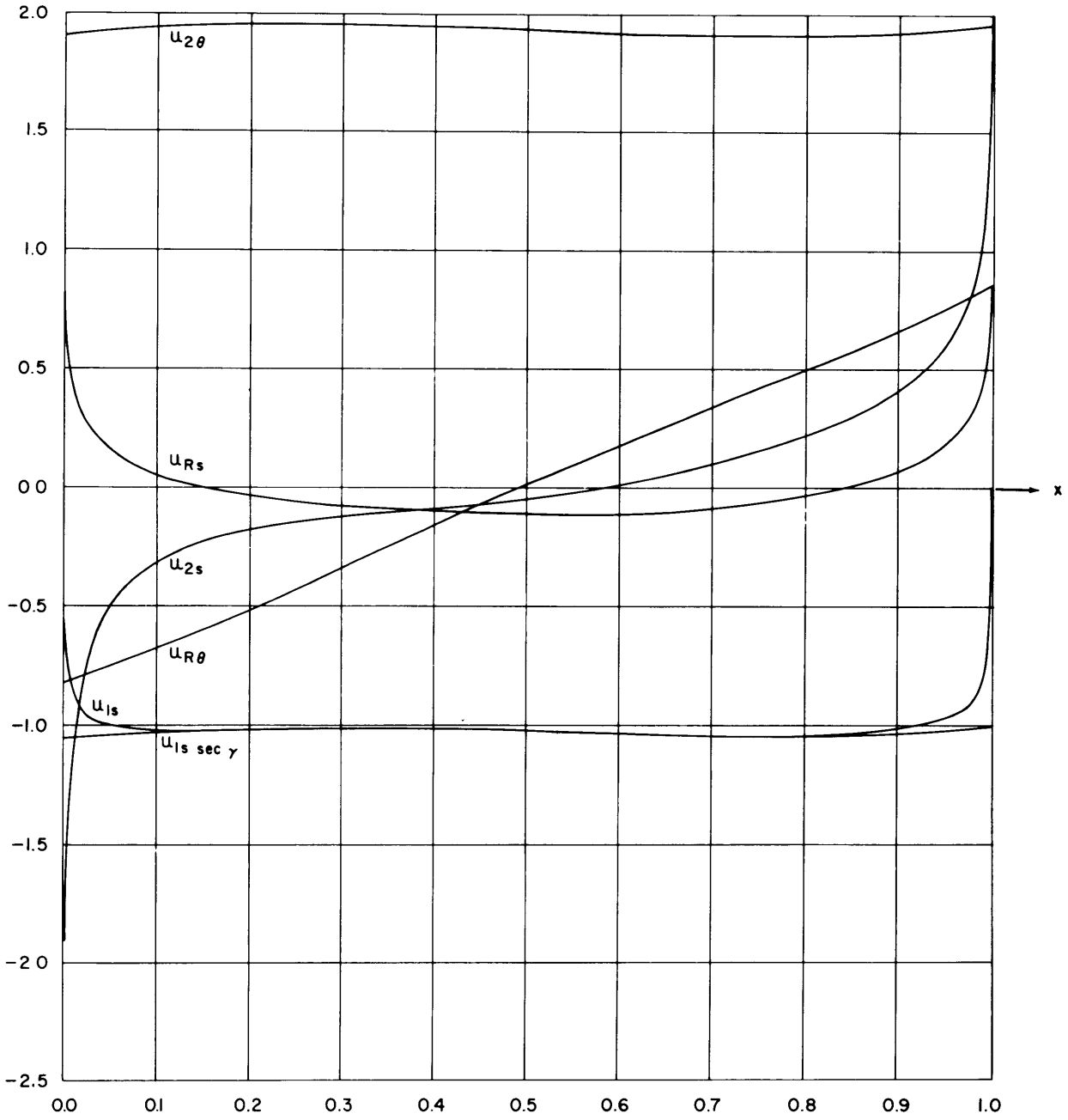

Figure 35 – Body 27

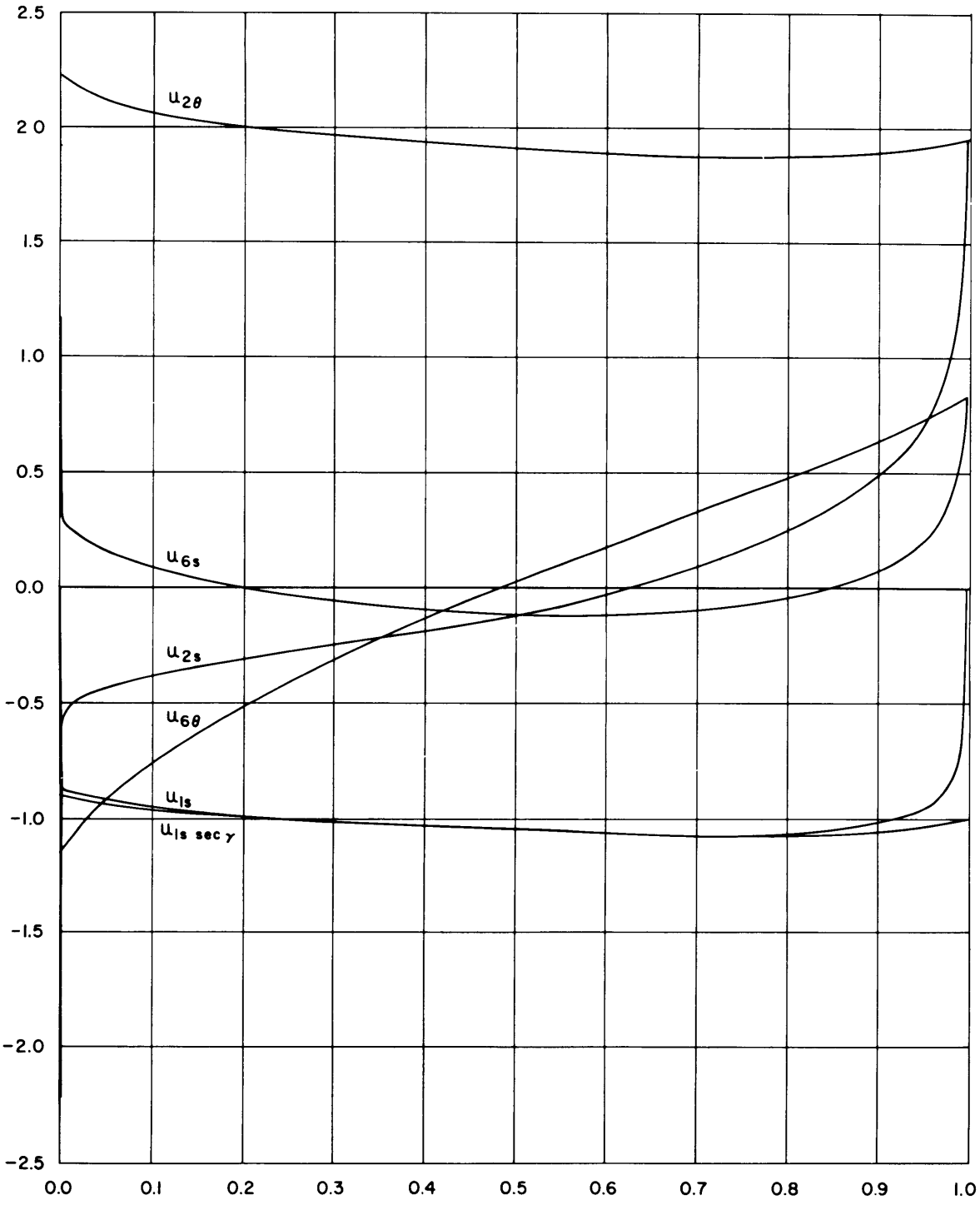

Figure 36 – Body 28

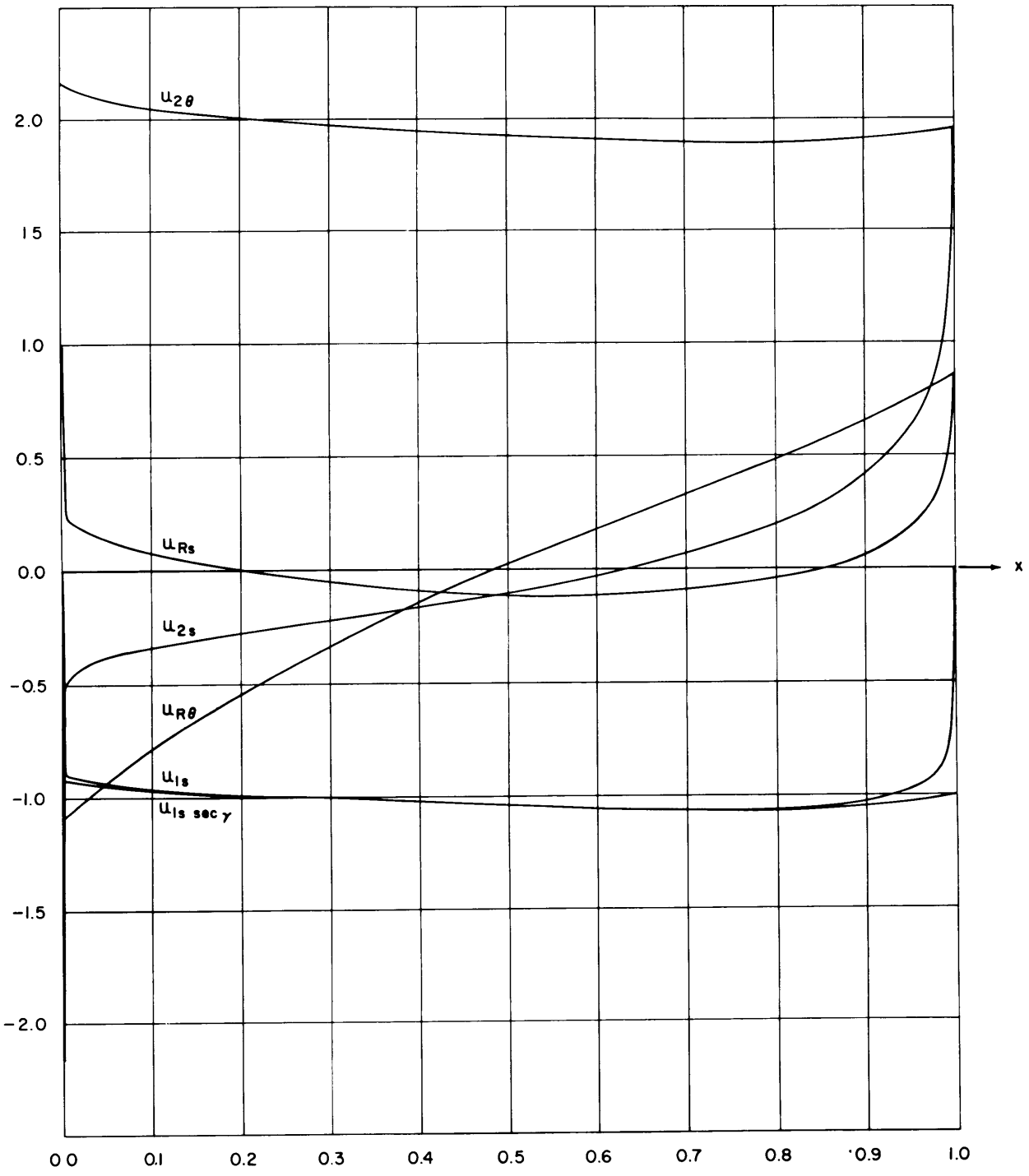

Figure 37 – Body 29

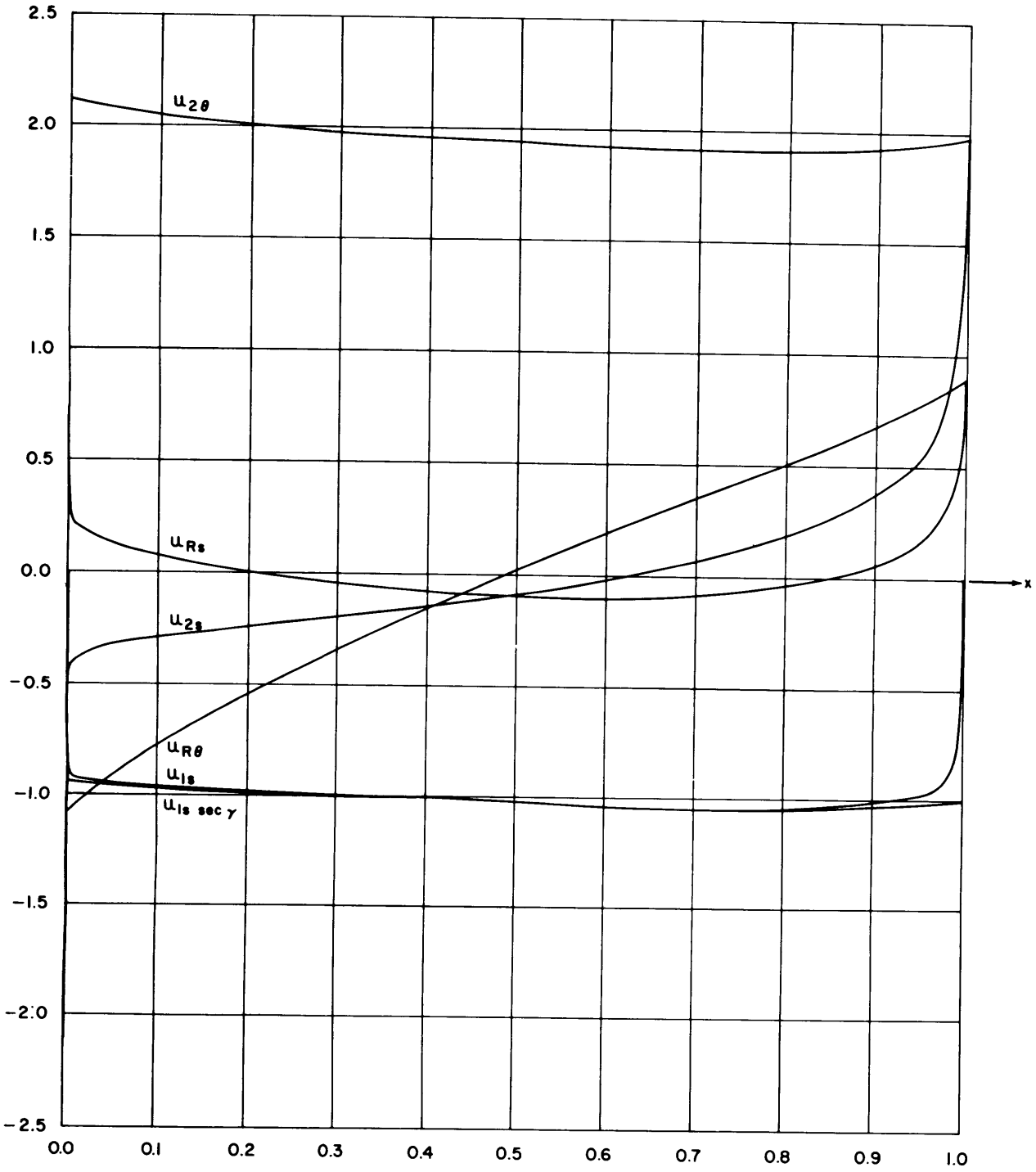

Figure 38 – Body 30

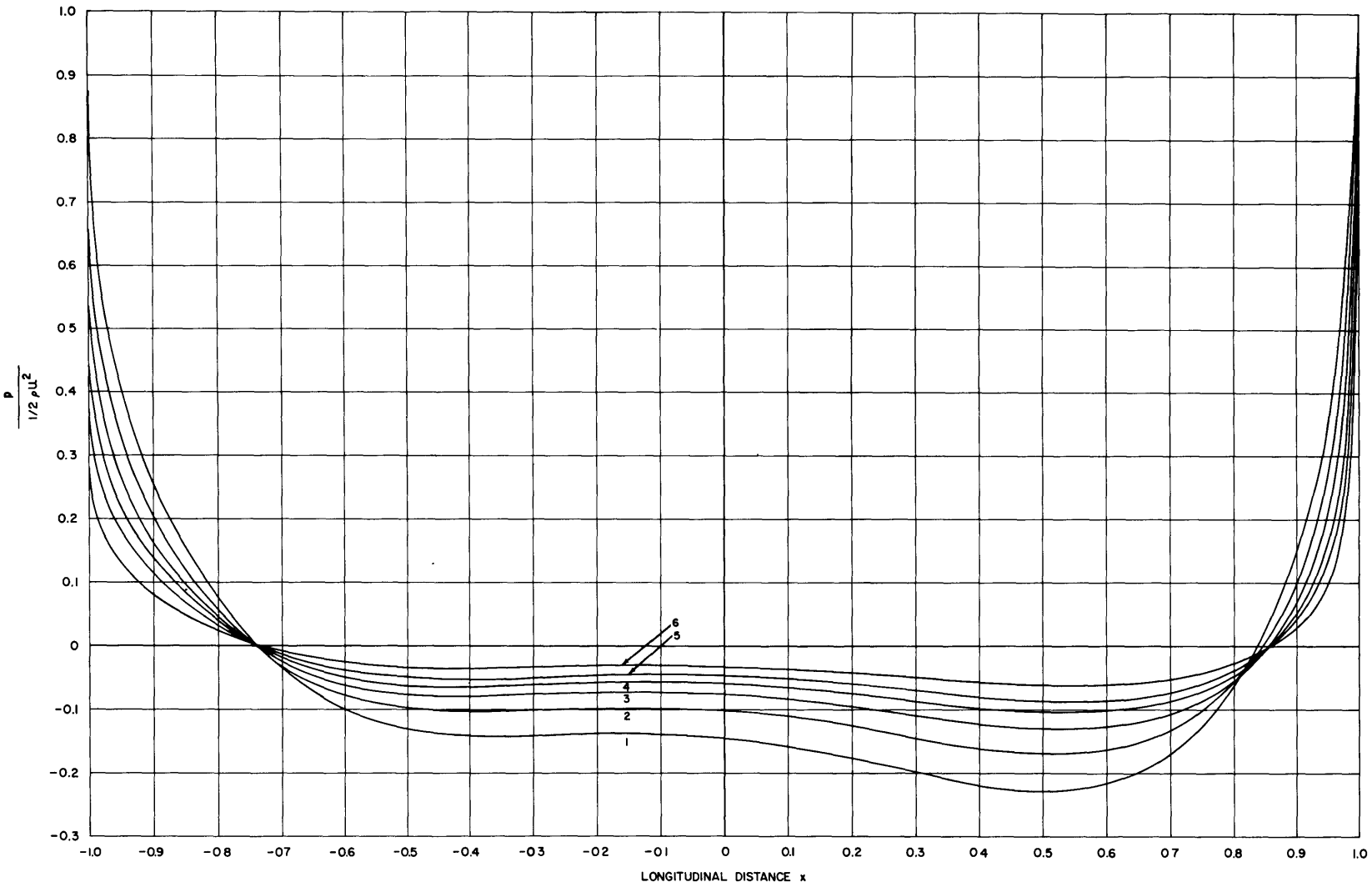

Figure 39 – Pressure Distributions for Longitudinal Flow for Series 58 Bodies with Various Length/Diameter Ratios

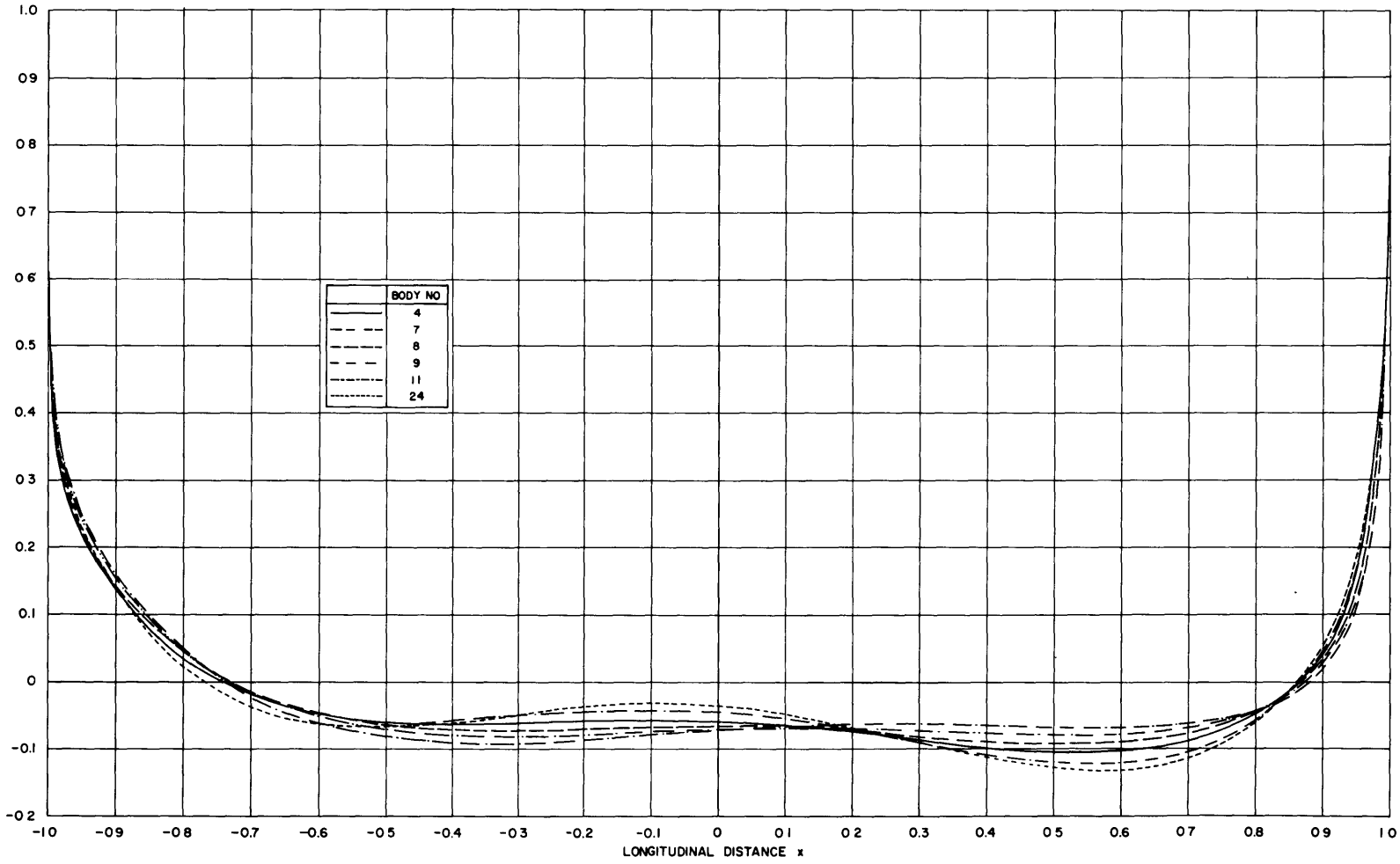

Figure 40 – Pressure Distributions for Longitudinal Flow for Series 58 Bodies with Various Locations of Maximum Section

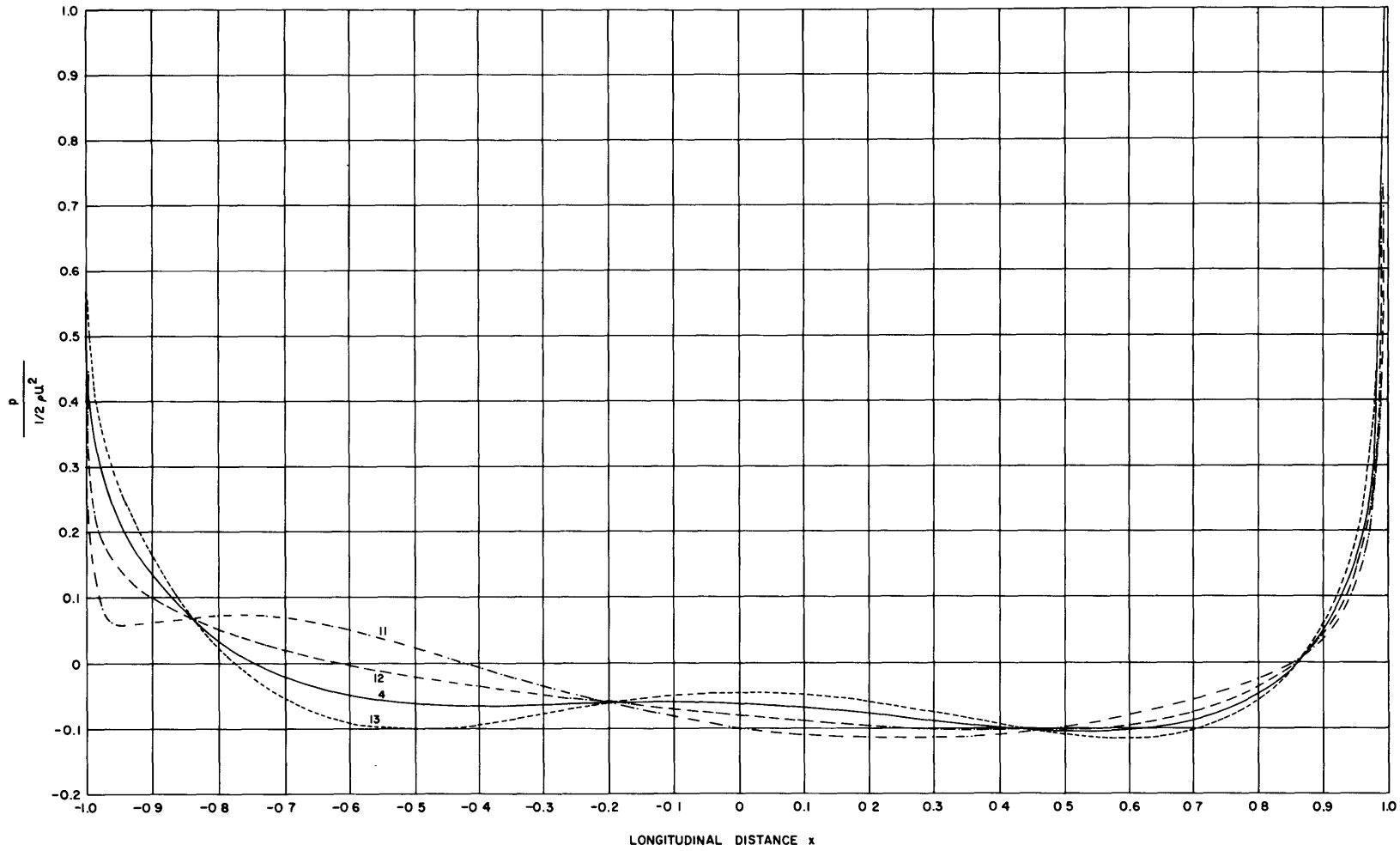

Figure 41 – Pressure Distributions for Longitudinal Flow for Series 58 Bodies with Various Prismatic Coefficients

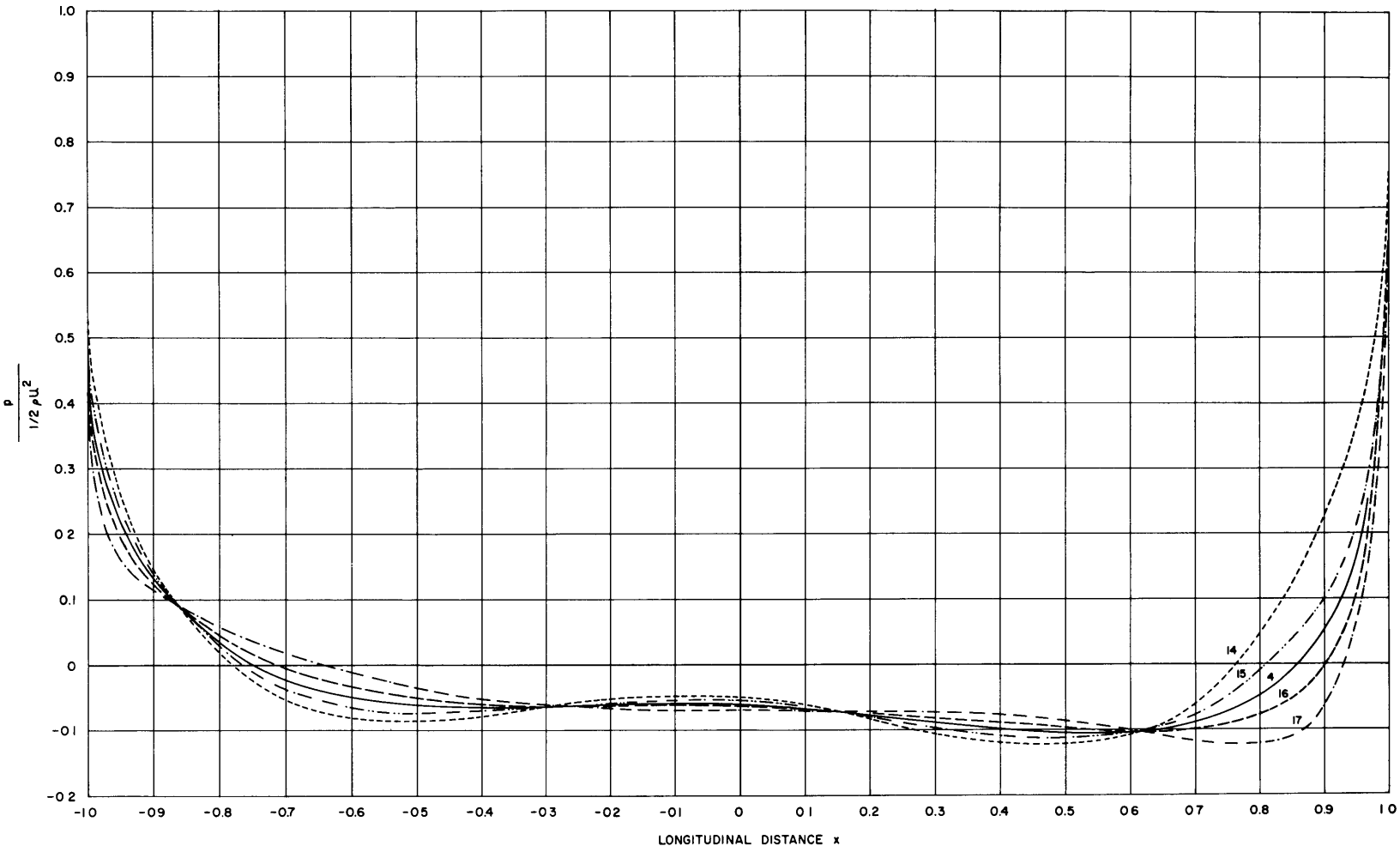

Figure 42 – Pressure Distributions for Longitudinal Flow for Series 58 Bodies with Various Nose Radii

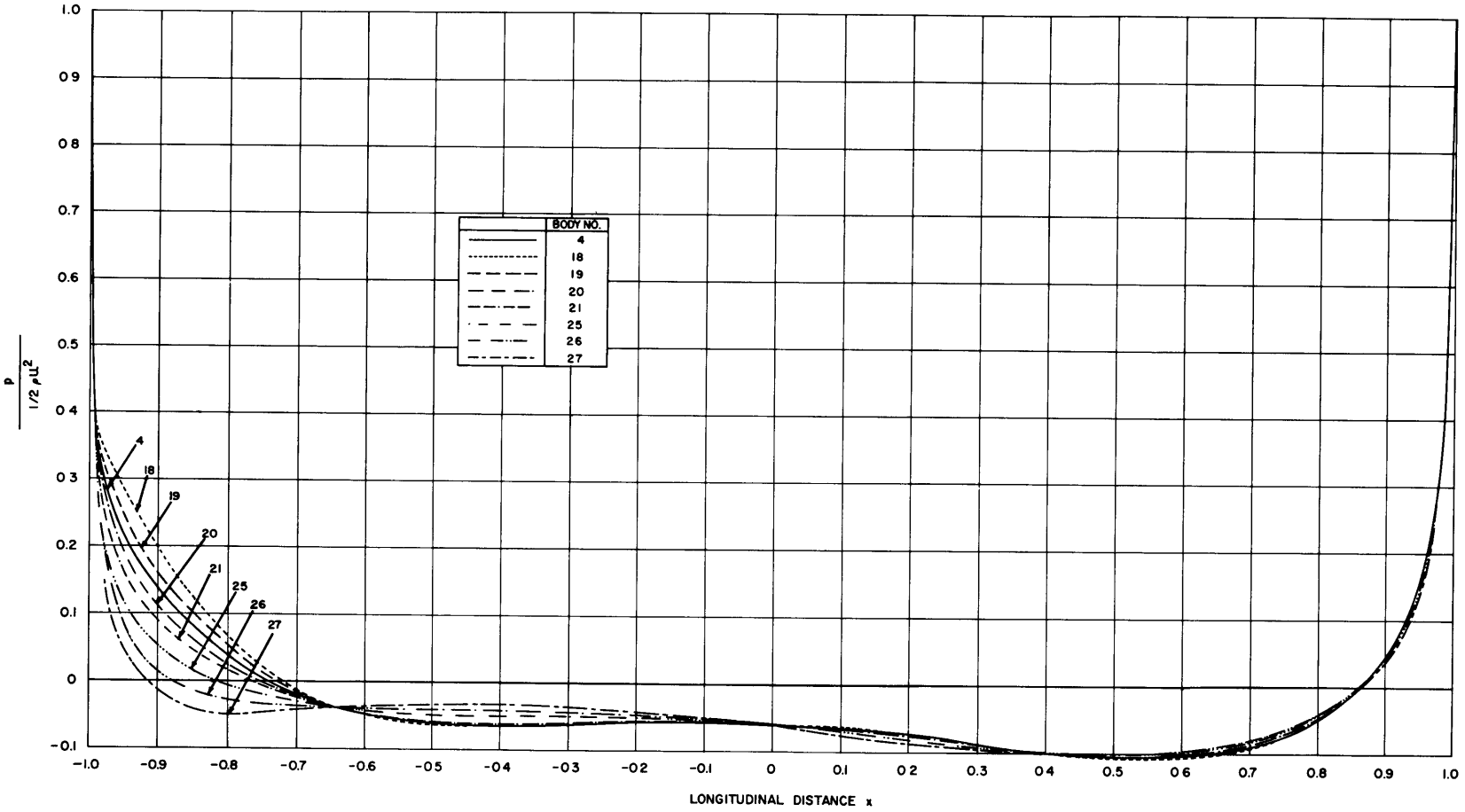

Figure 43 – Pressure Distributions for Longitudinal Flow for Series 58 Bodies with Various Tail Radii

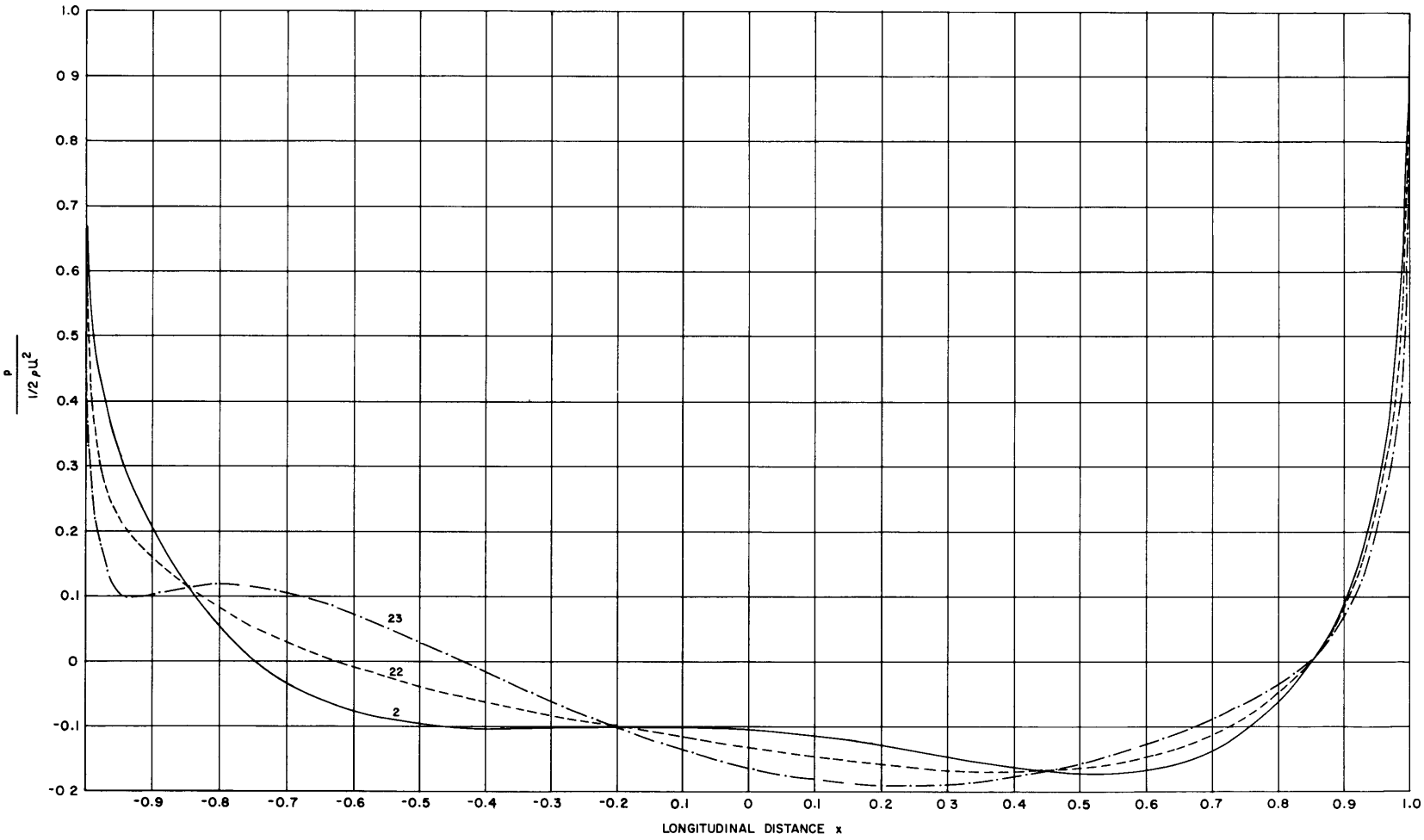

Figure 44 – Pressure Distributions for Longitudinal Flow for Series 58 Bodies with Various Prismatic Coefficients

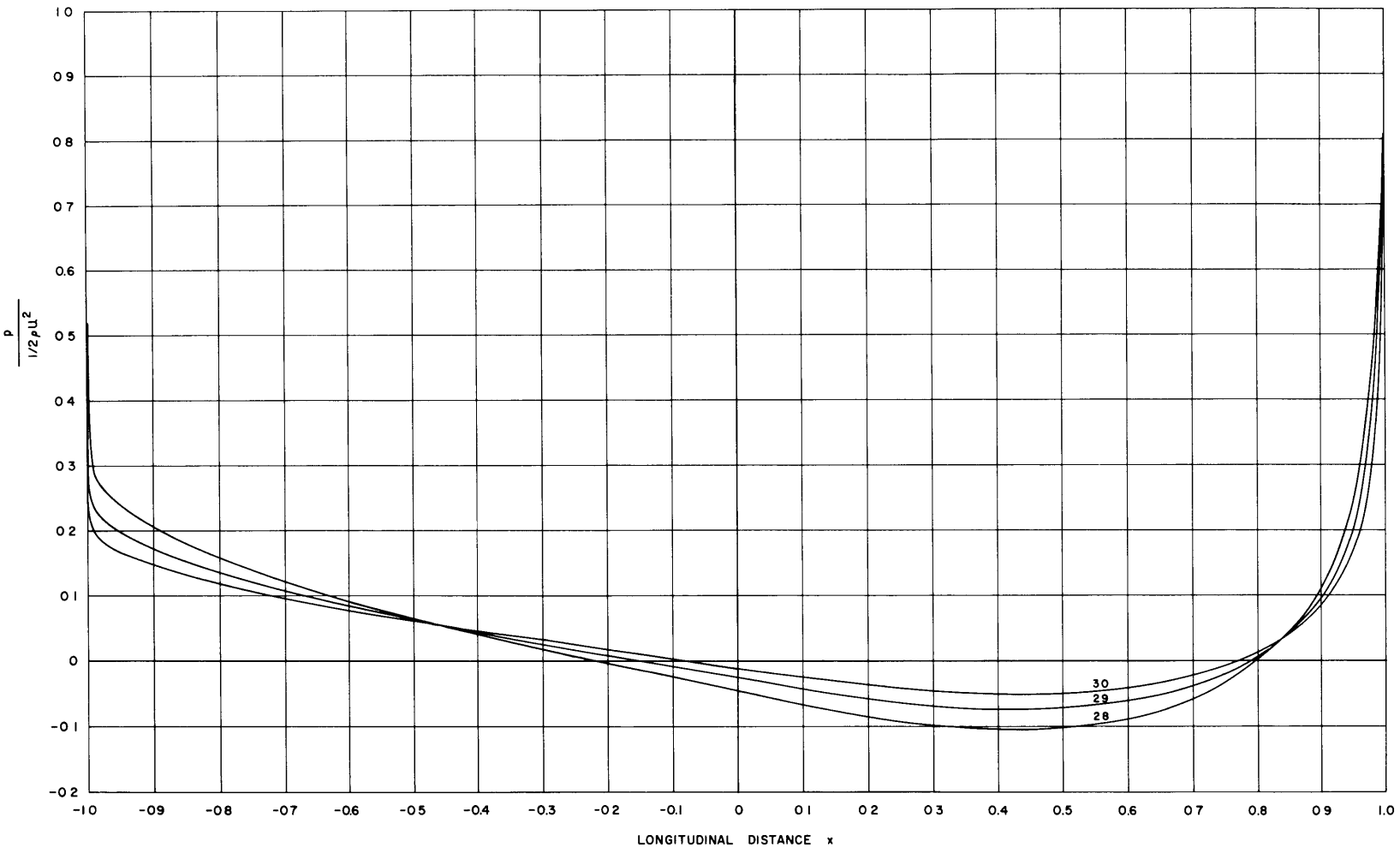

Figure 45 – Pressure Distributions for Longitudinal Flow for Series 58 Bodies with Various Length/Diameter Ratios

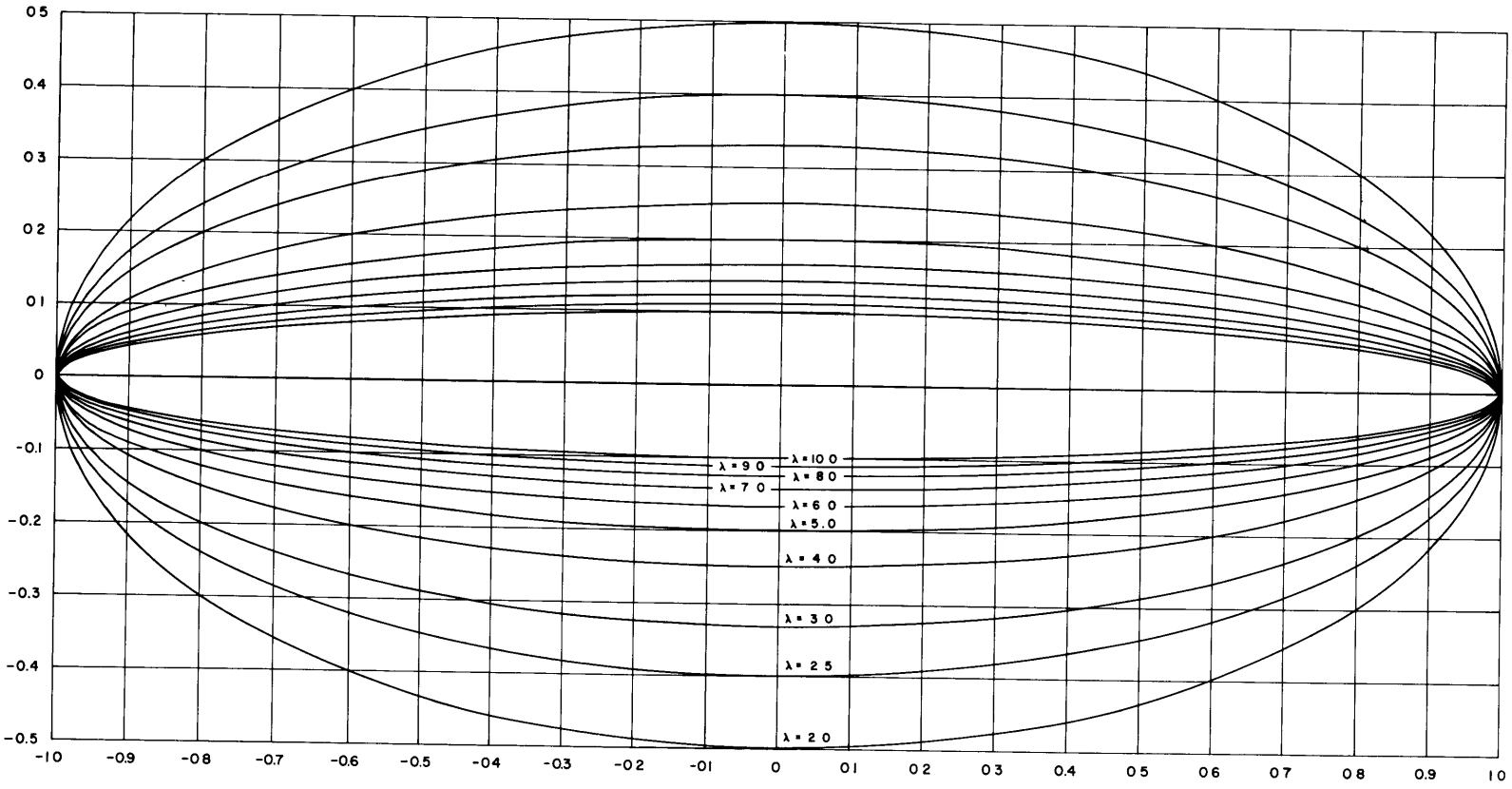

Figure 46 – Meridian Sections of Prolate Spheroids

Figure 47 – Velocity Functions of Prolate Spheroids

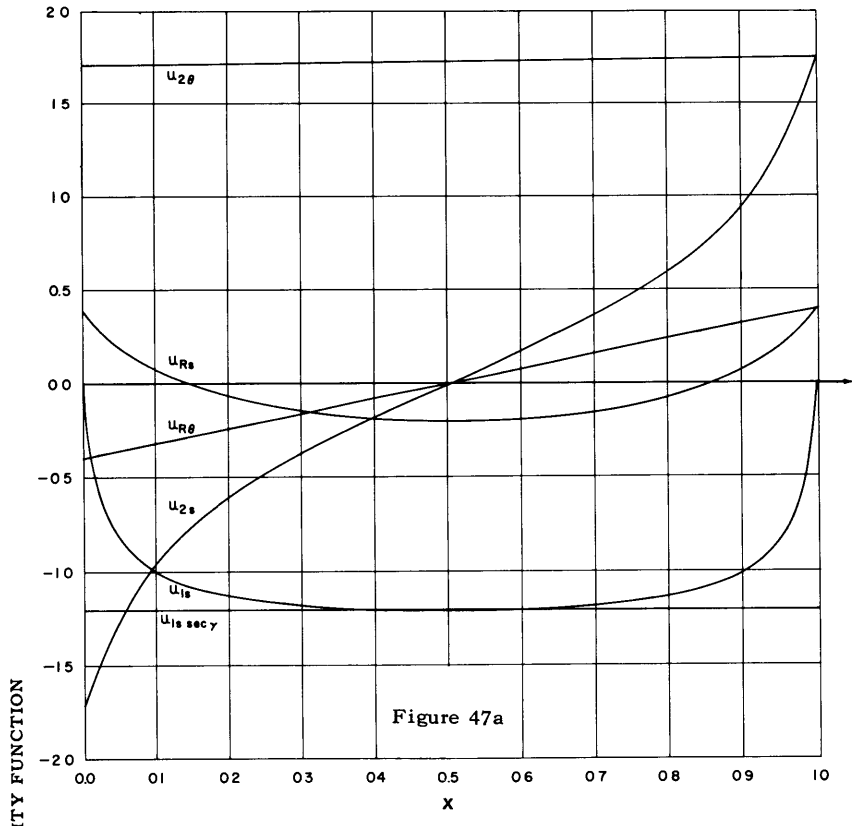

Figure 47a

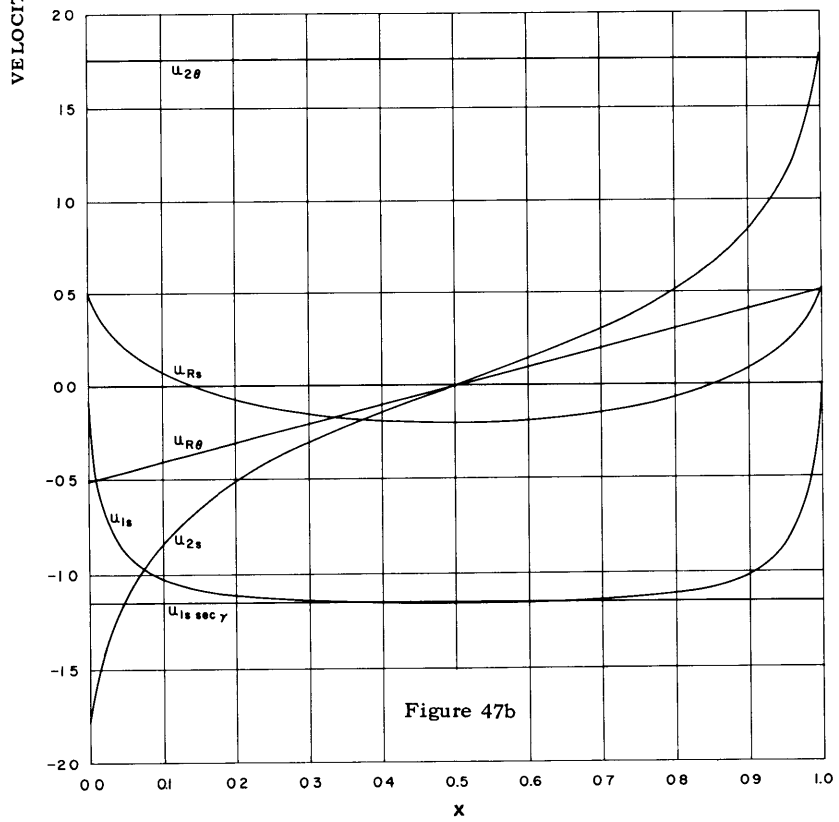

Figure 47b

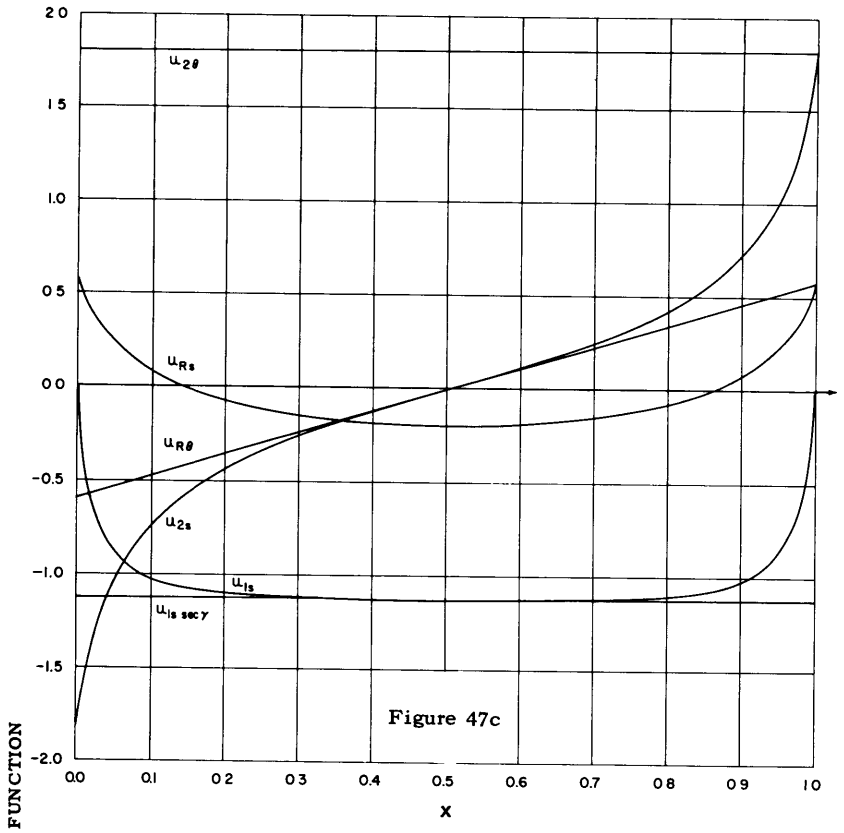

Figure 47c

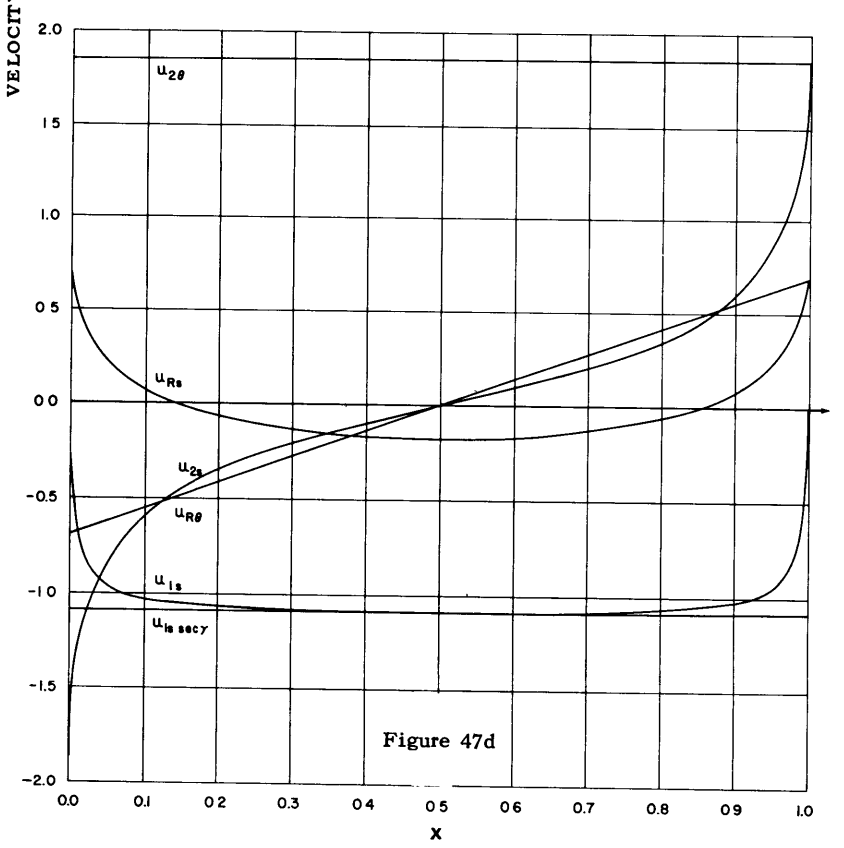

Figure 47d

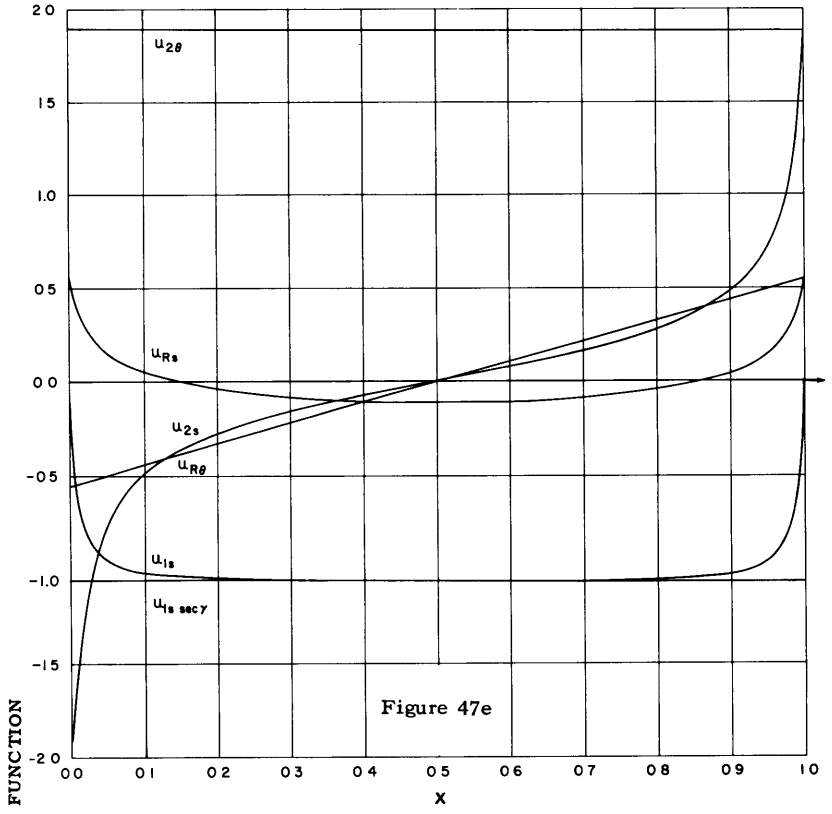

Figure 47e

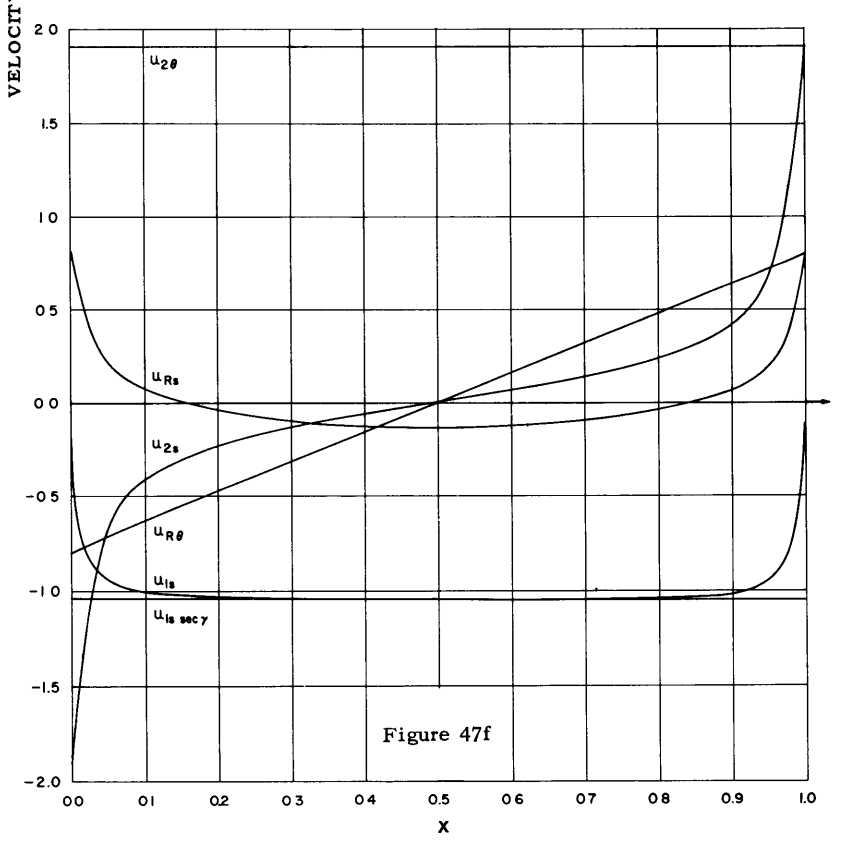

Figure 47f

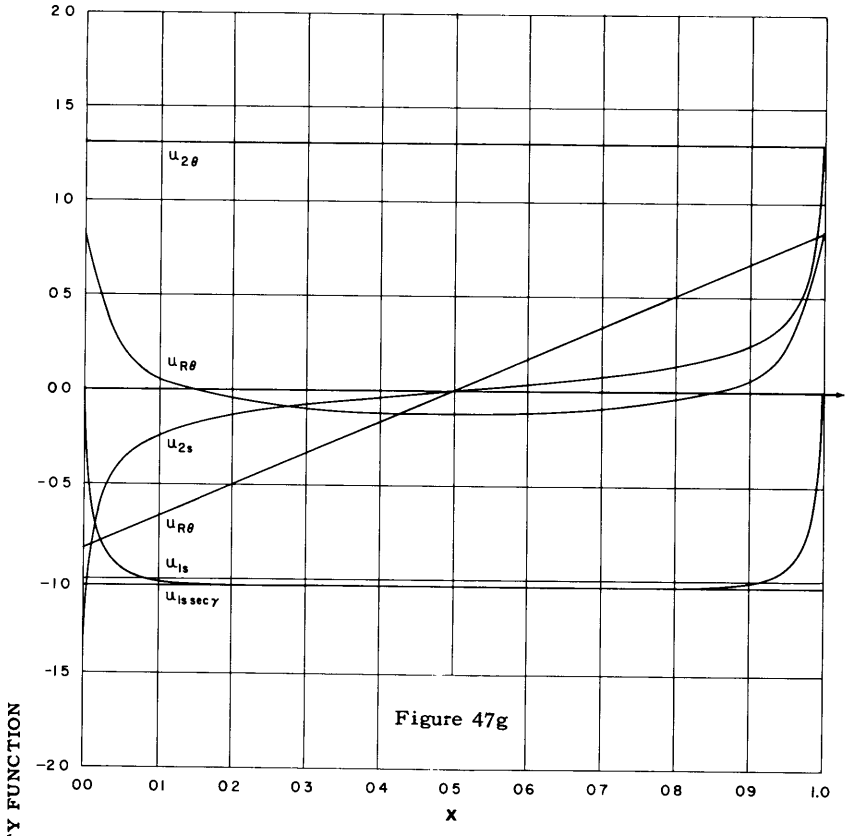

Figure 47g

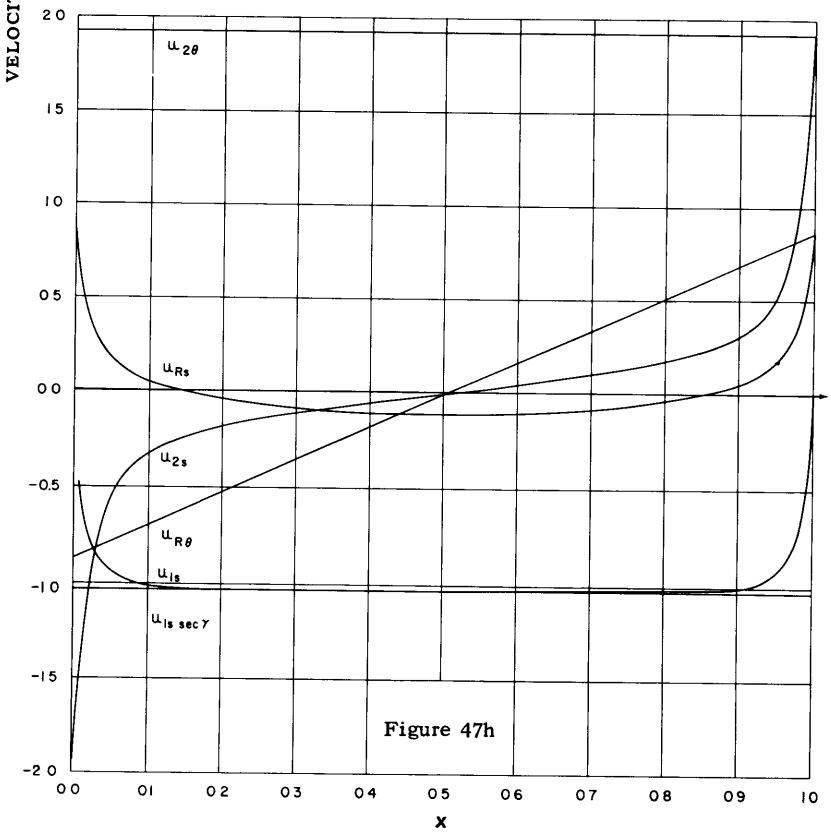

Figure 47h

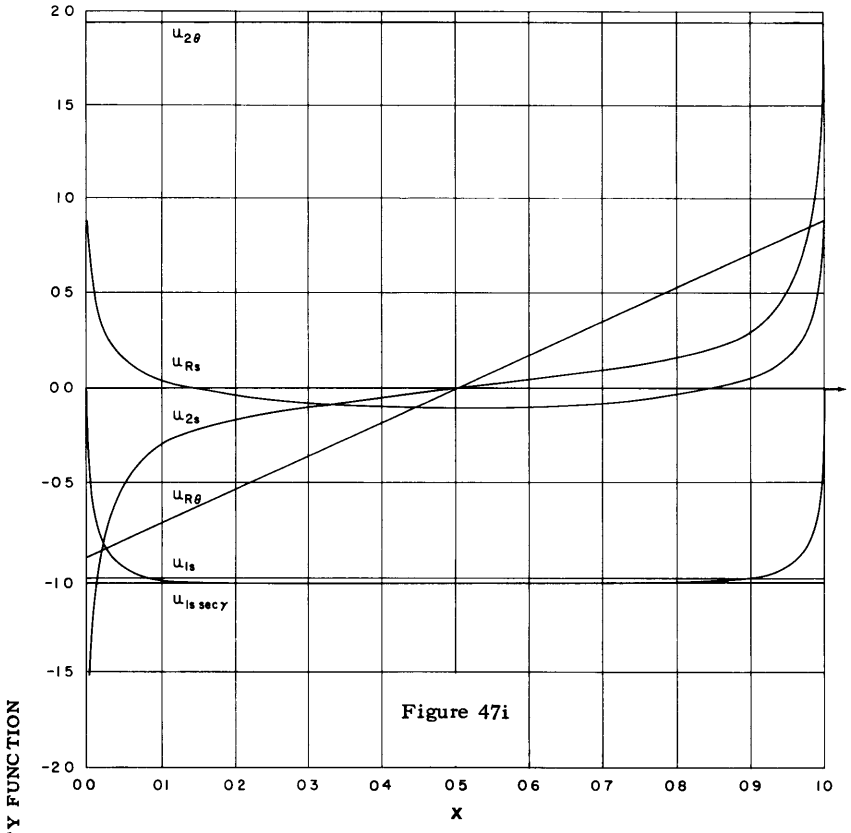

Figure 47i

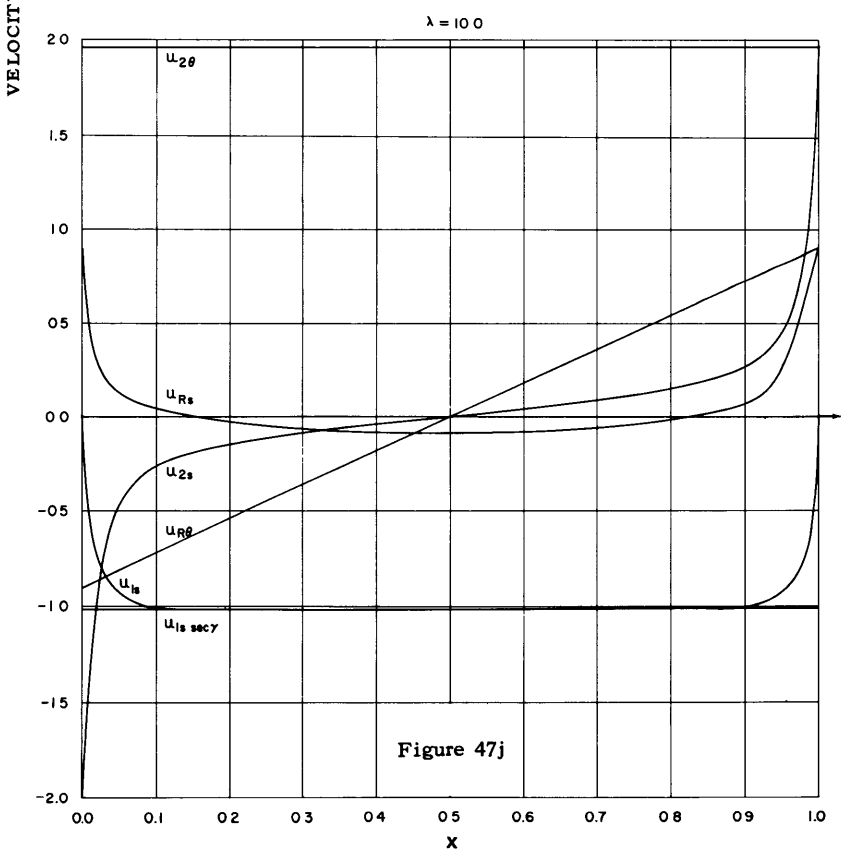

Figure 47j

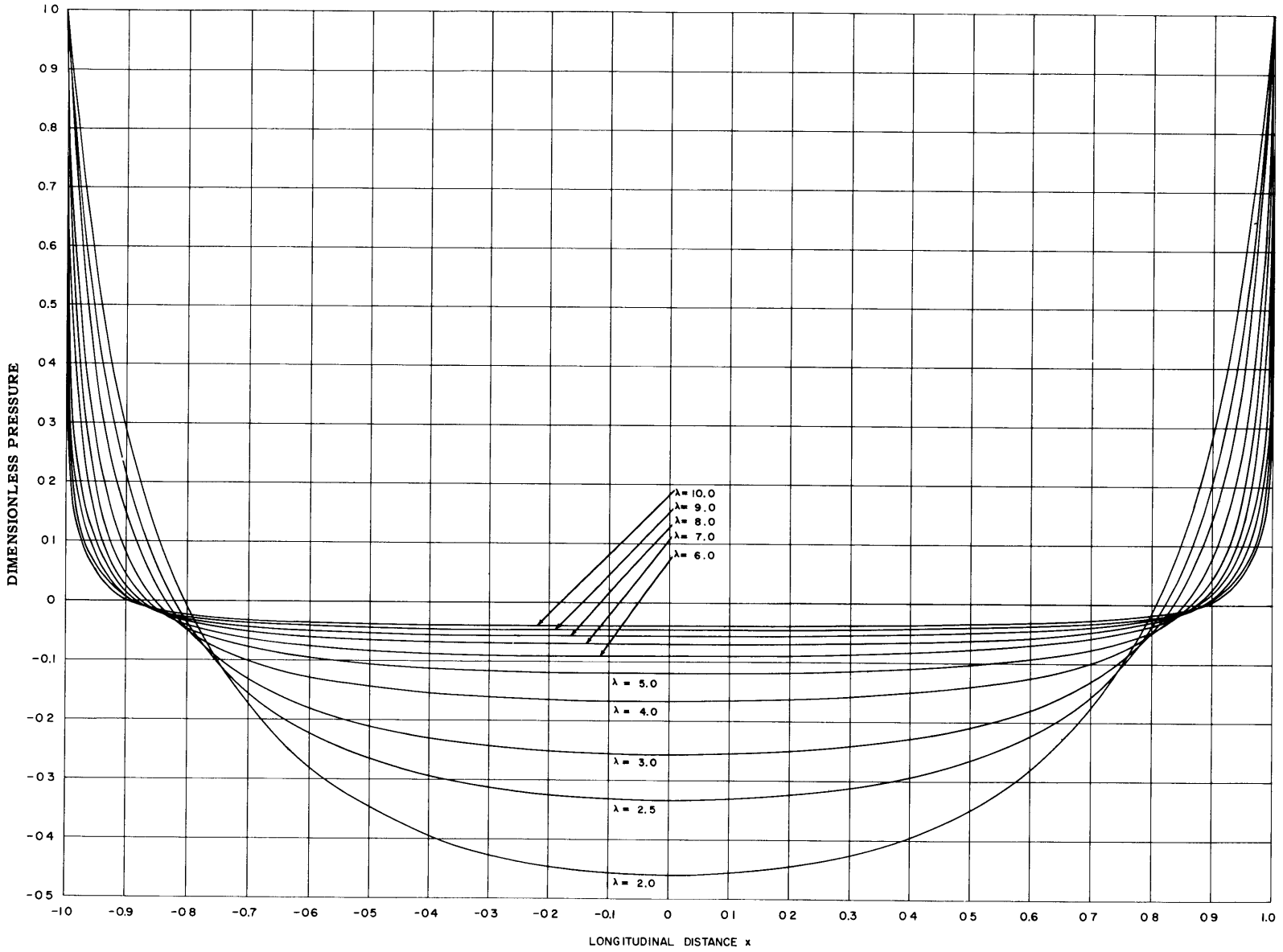

Figure 48 – Dimensionless Pressure Distributions of Prolate Spheroids

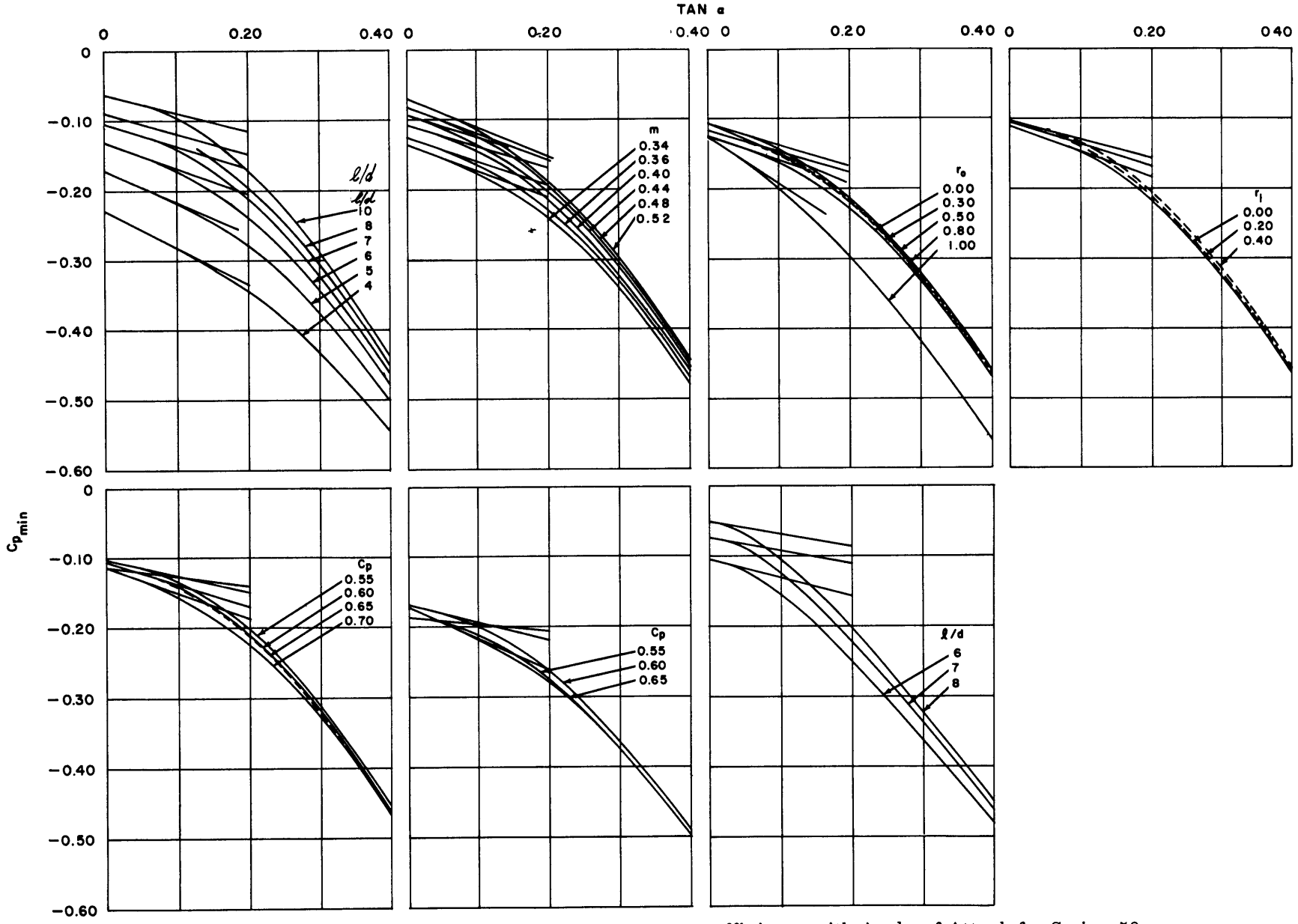

Figure 49 – Variation of Minimum Pressure Coefficients with Angle of Attack for Series 58

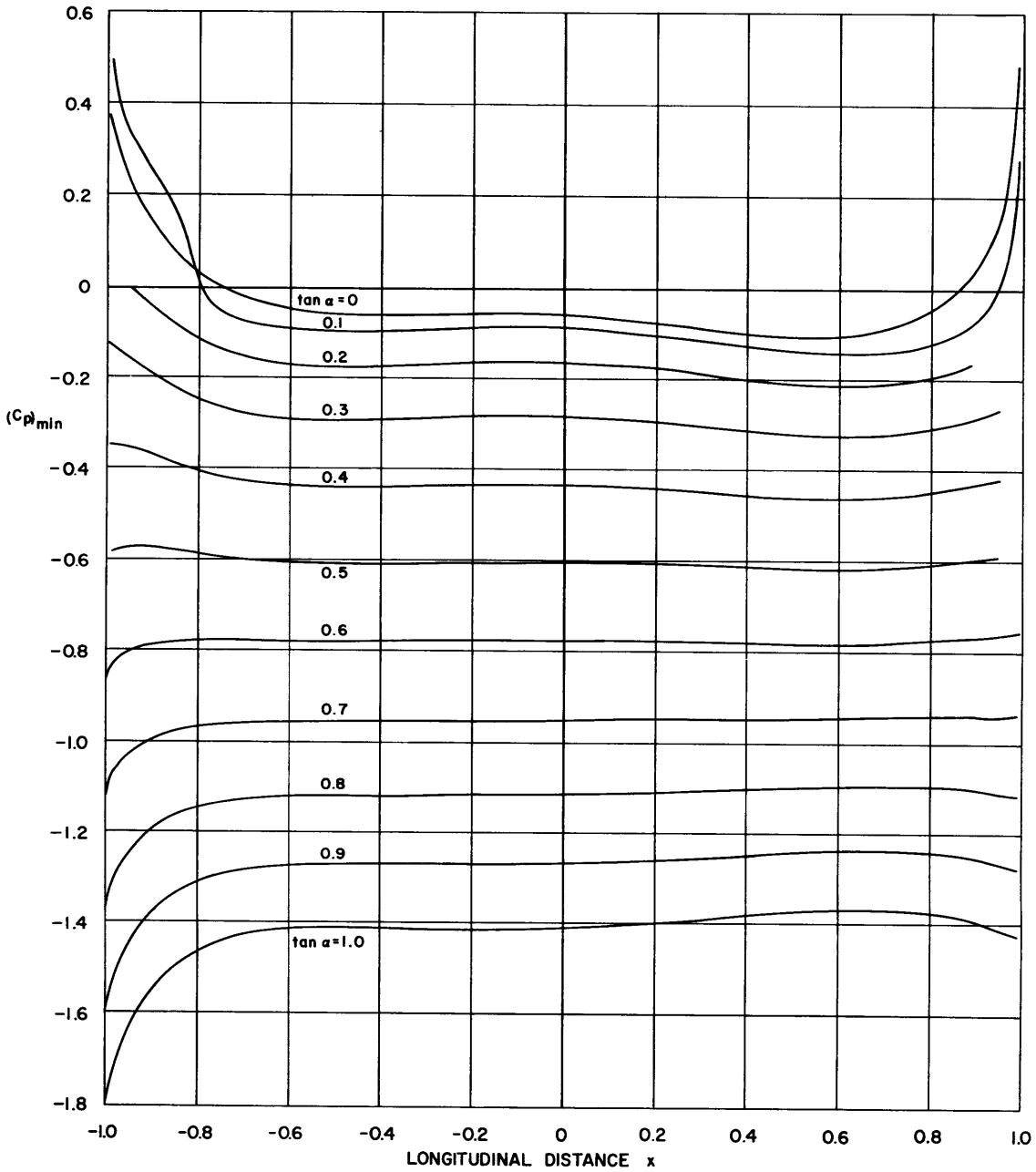

Figure 50 – Minimum Pressure Coefficients $(C_p)_{min}$ versus x for Body 4 at Various Angles of Attack

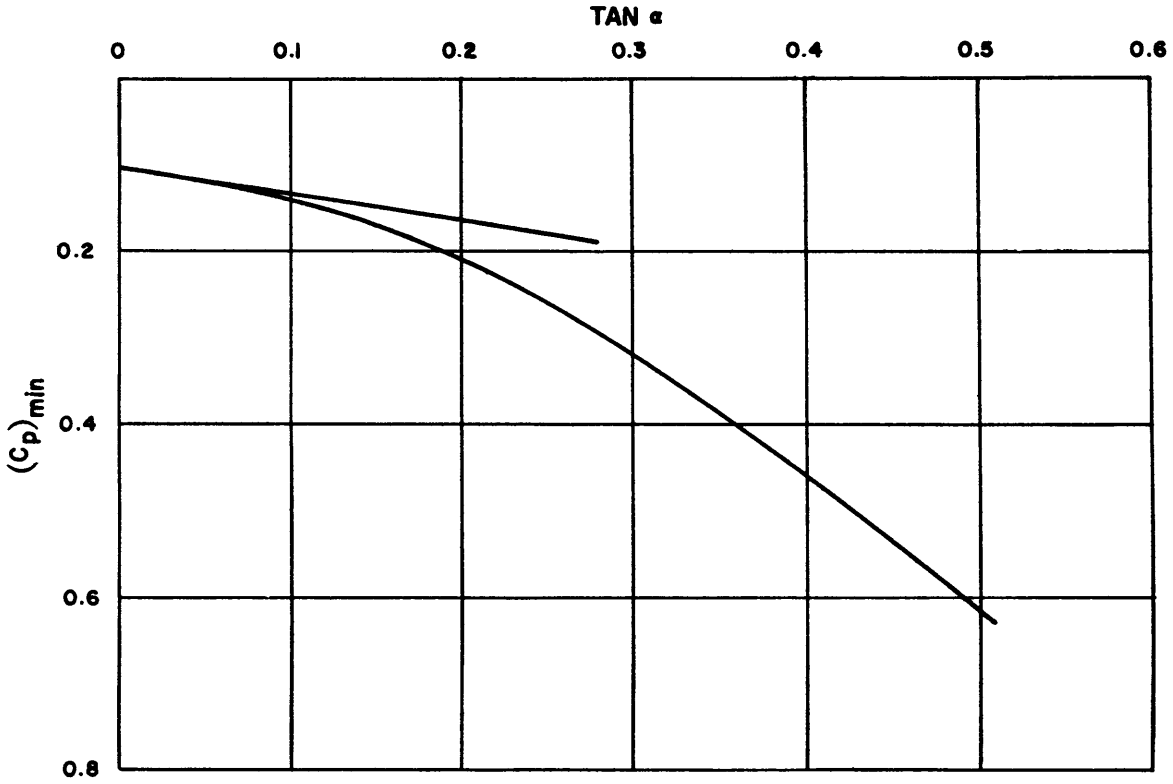

Figure 51 – Overall Minimum Pressure Coefficients over Forward Part of Body 4 at Various Angles of Attack

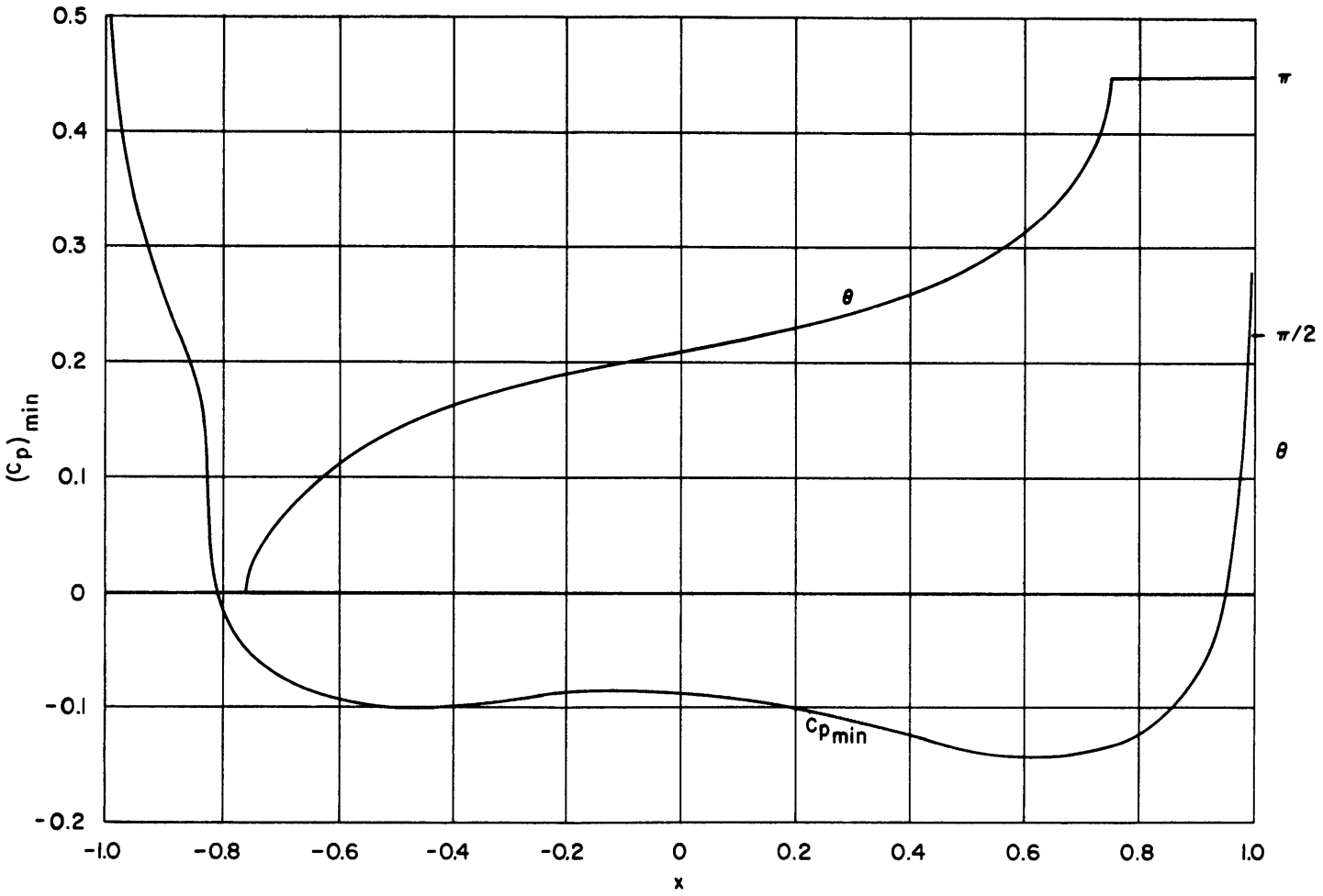

Figure 52 – Minimum Pressure Coefficients and Corresponding θ for Body 4 at a Fixed Angle of Attack, $\bar{\epsilon}$ = arctan 0.1

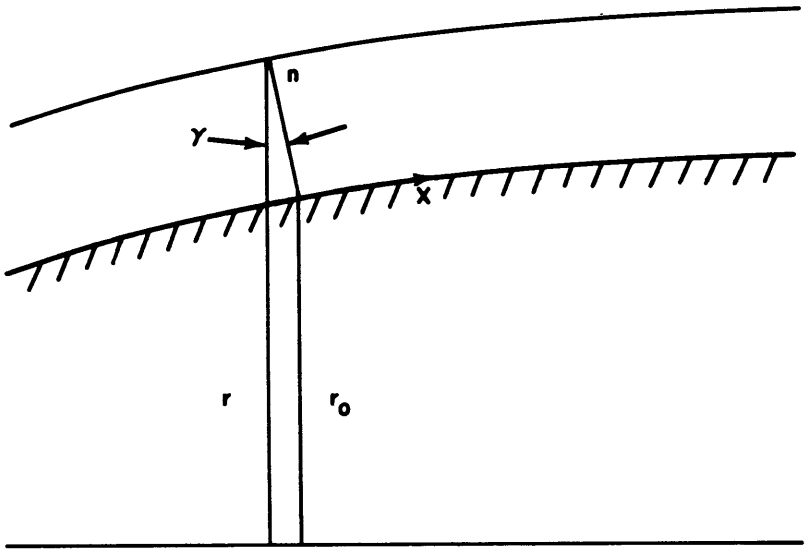

Figure 53 – System of Parallel Orthogonal Coordinates

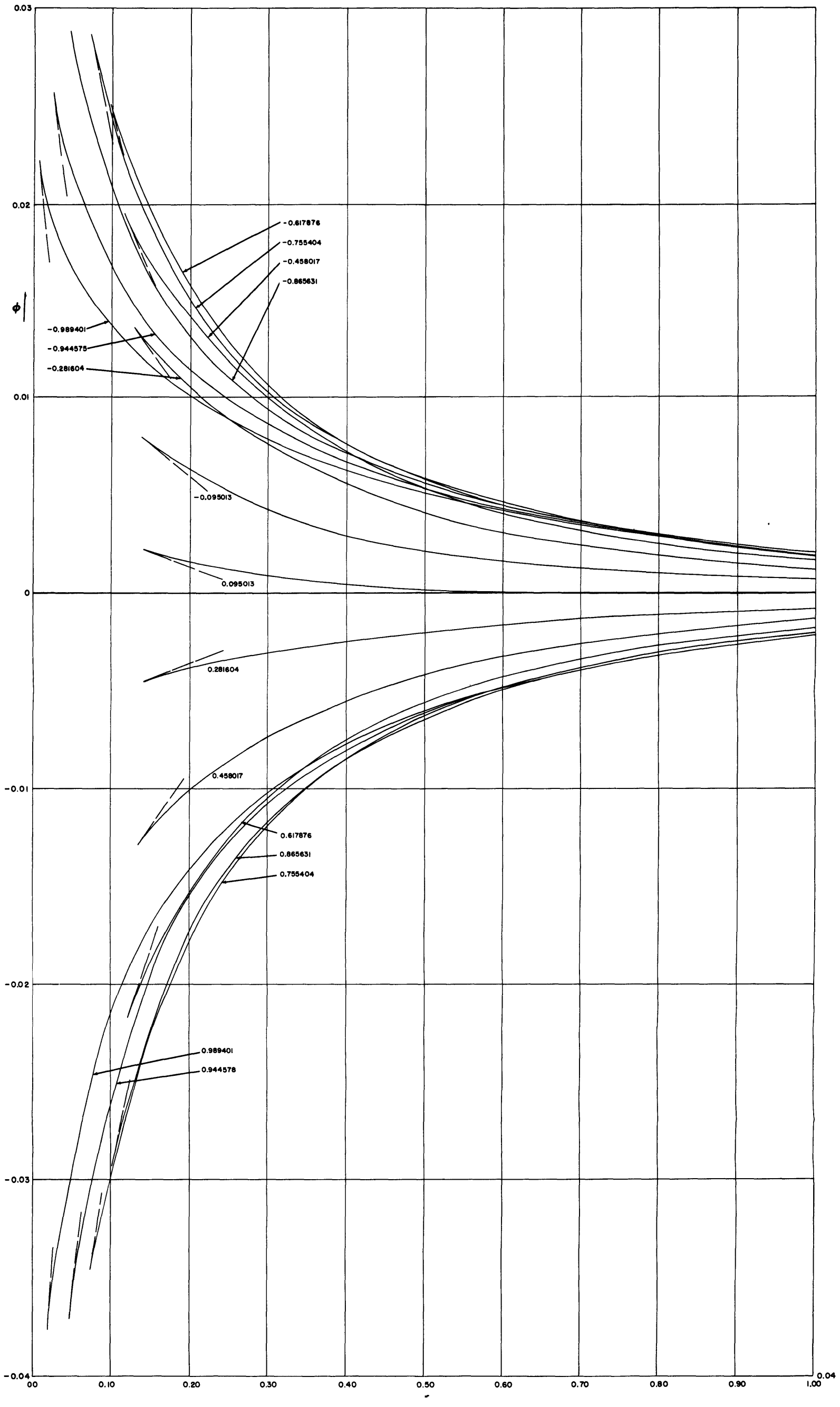
0.03
0.02
0.01
0
-0.01
-0.02
-0.03
-0.04
00
0.10
0.20
0.30
0.40
0.50
0.60
0.70
0.80
0.90
1.00
0.04
Φ
r
-0.617876
-0.755404
-0.458017
-0.865631
-0.989401
-0.944575
-0.281604
-0.095013
0.095013
0.281604
0.458017
0.617876
0.865631
0.755404
0.989401
0.944578

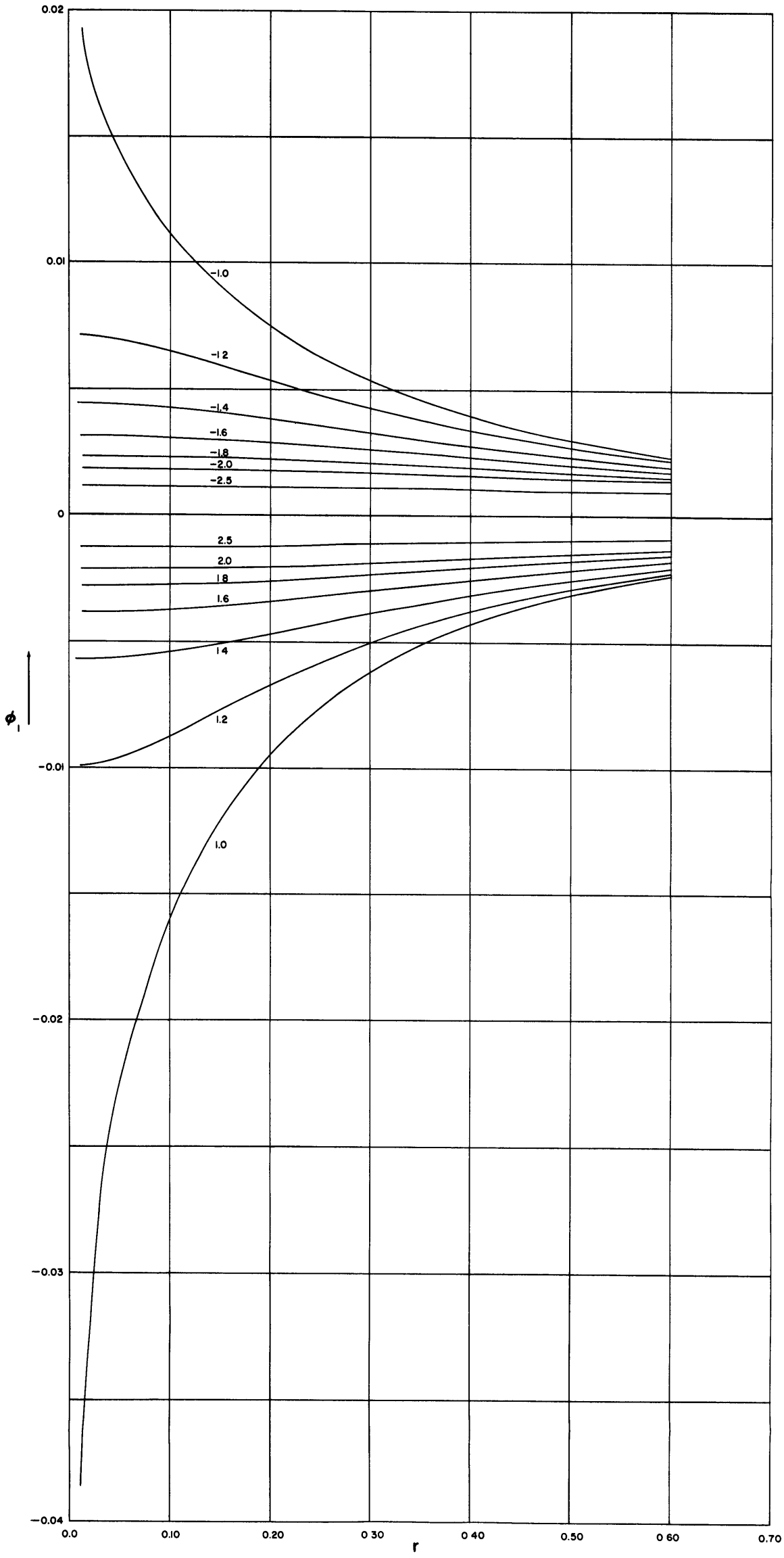
0.02
0.01
0
-0.01
-0.02
-0.03
-0.04
0.0
0.10
0.20
0 30
0 40
0.50
0 60
0.70
r
ϕ_1
-1.0
-1 2
-1.4
-1.6
-1.8
-2.0
-2.5
2.5
2.0
1 8
1.6
1 4
1.2
1.0

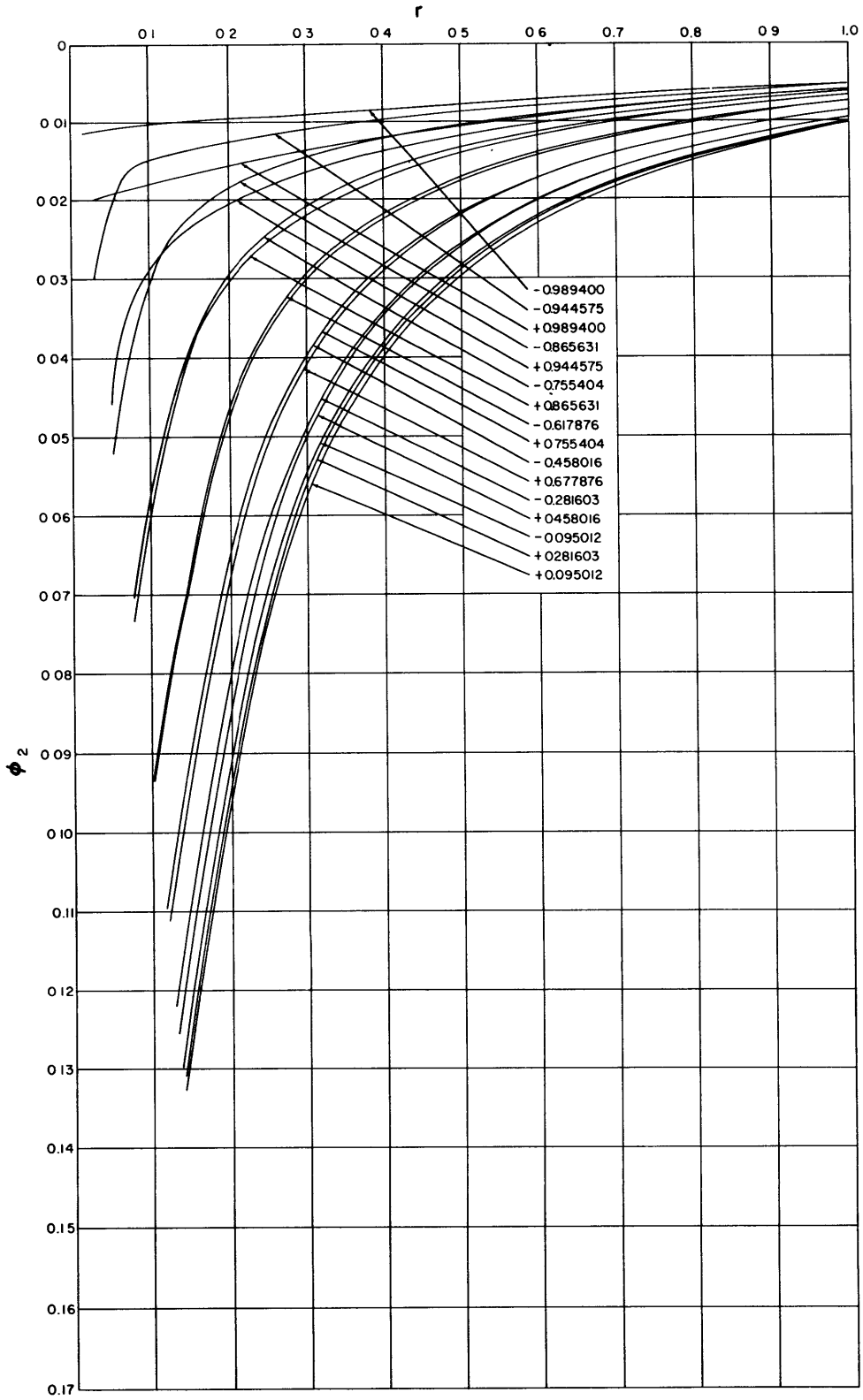

Figure 56 – Velocity Potential ϕ_2 versus r for Body 4, $|x| \leq 1$

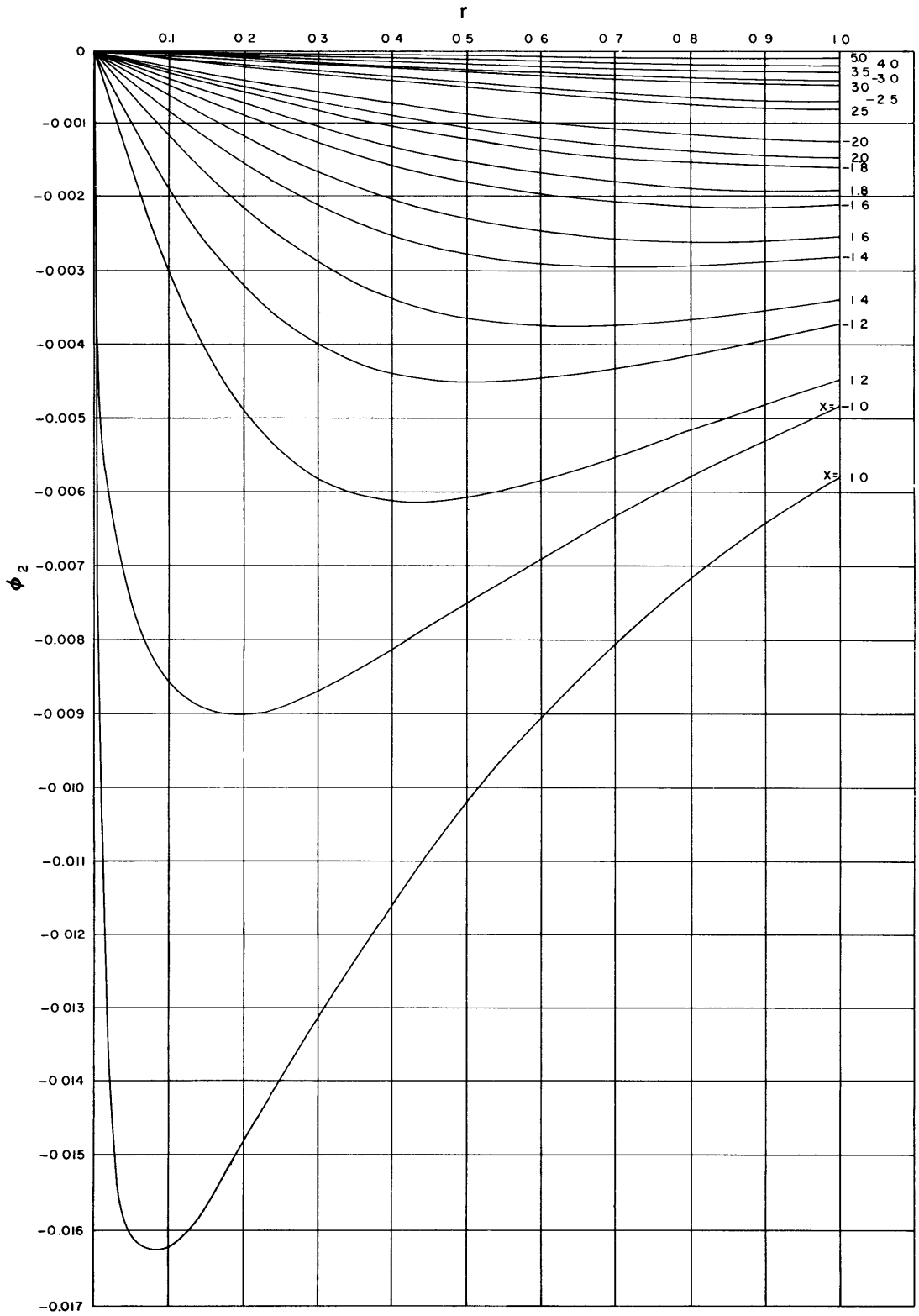

Figure 57 – Velocity Potential ϕ_2 versus r for Body 4, $|x| \geq 1$

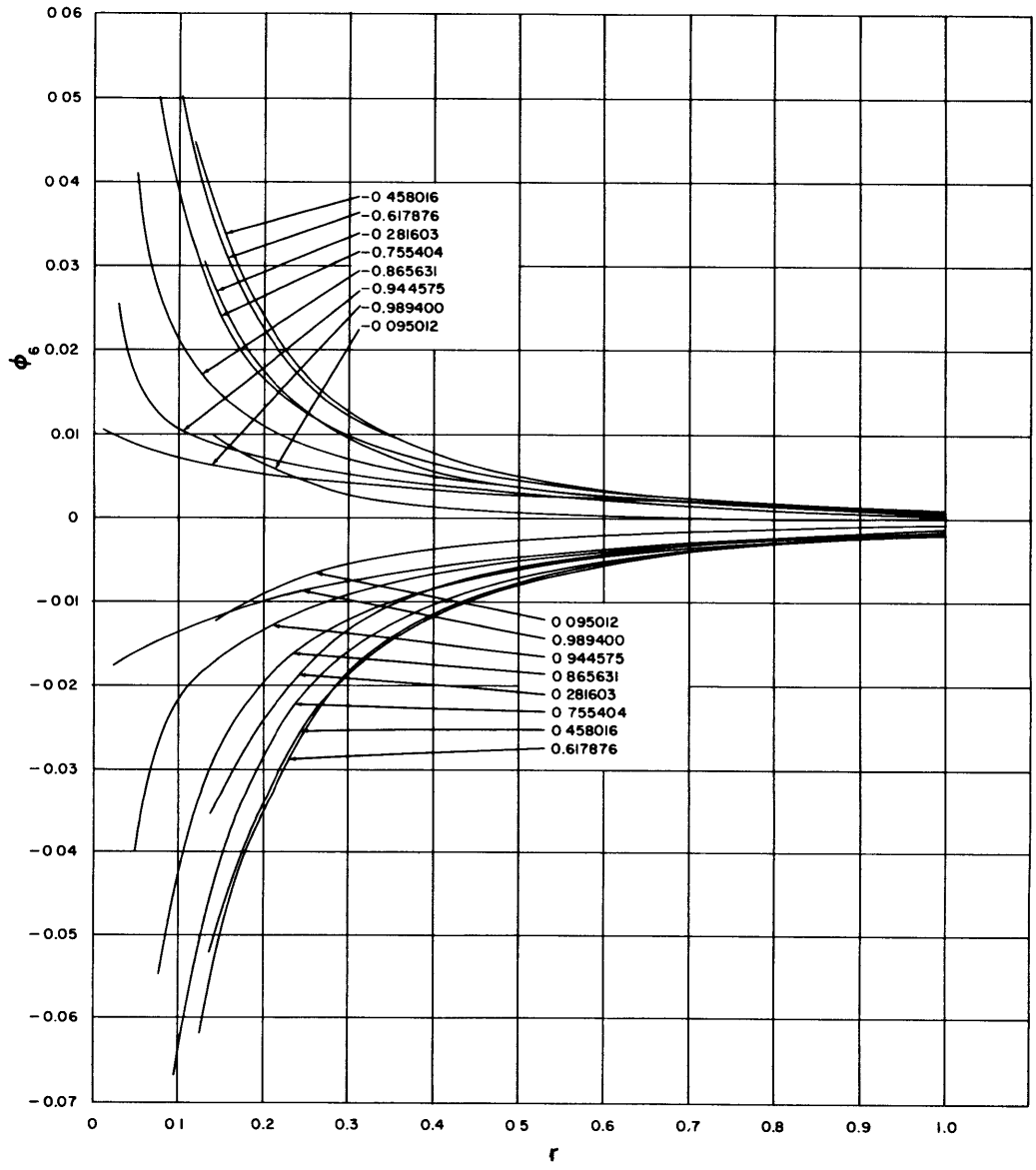

Figure 58 – Velocity Potential ϕ_6 versus r for Body 4, $|x| < 1$

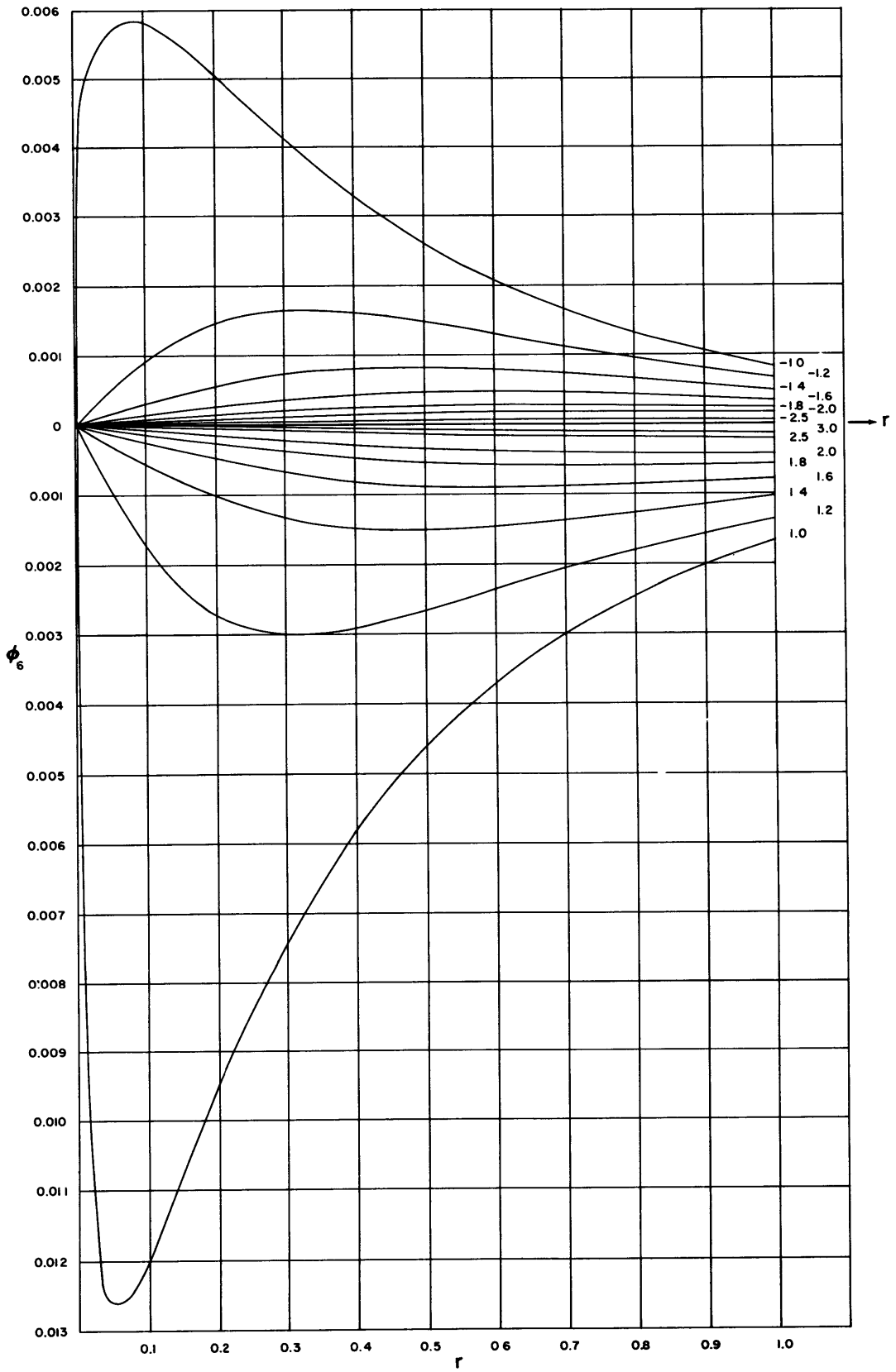

Figure 59 – Velocity Potential ϕ_6 versus r for Body 4, $|x| \geq 1$

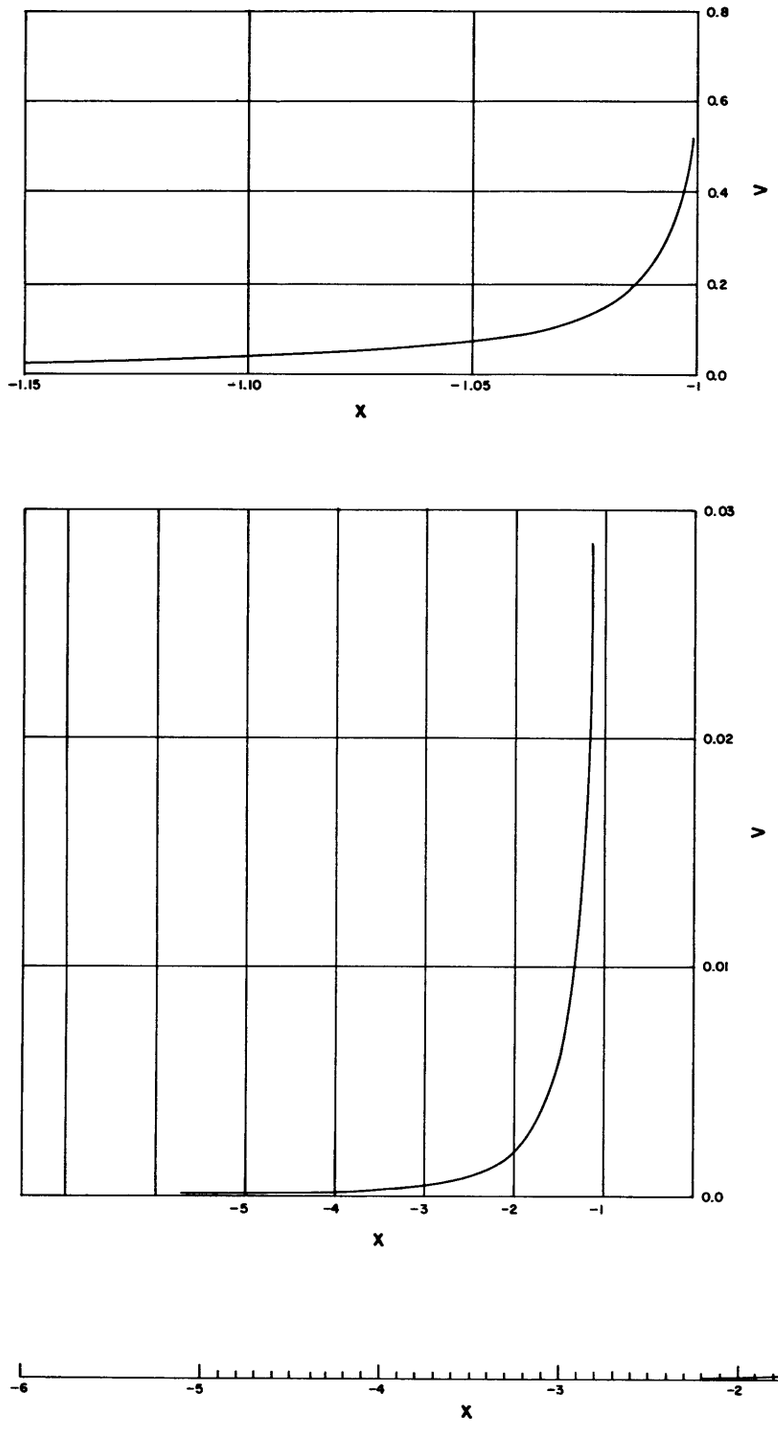

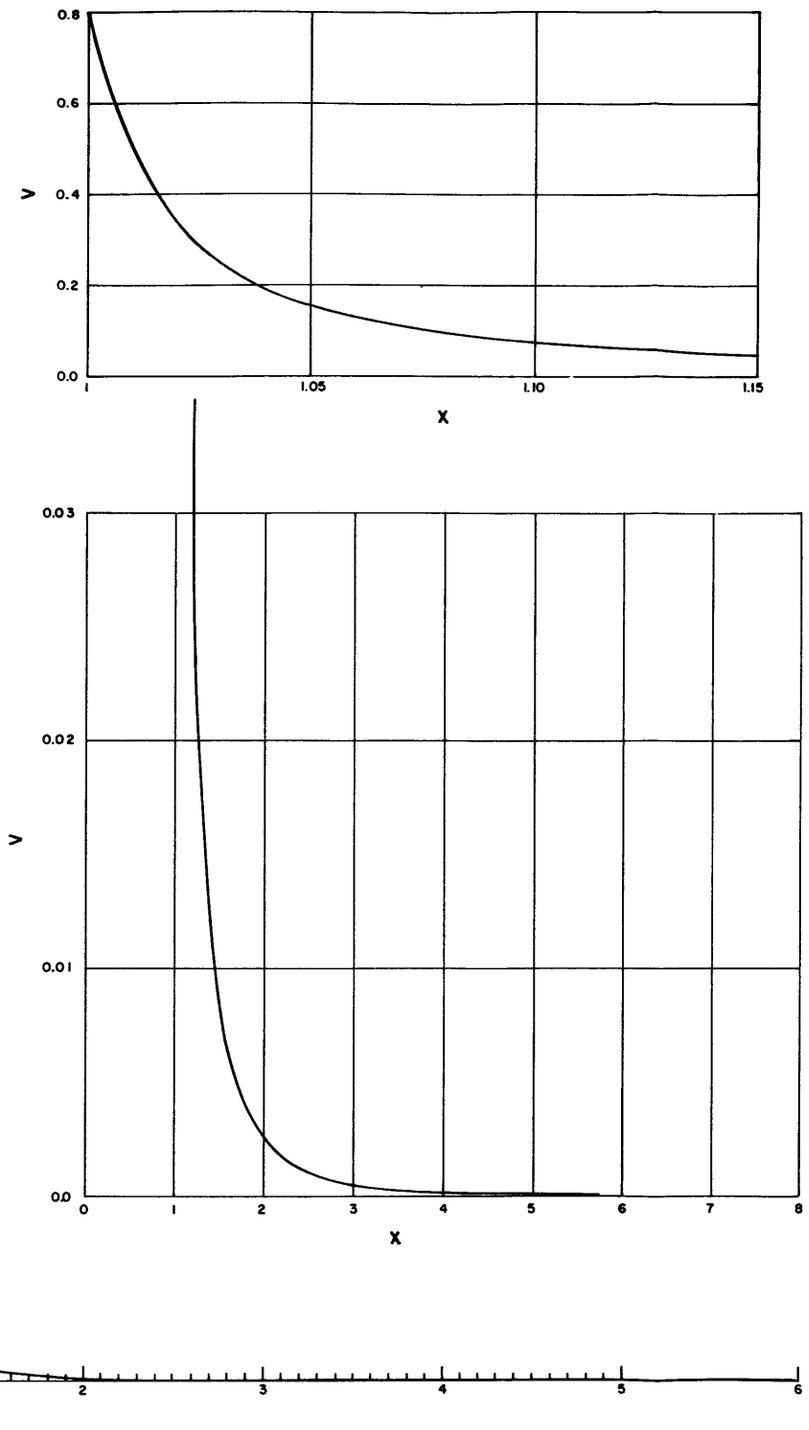

Figure 60 – Velocity along Axis for Body 4

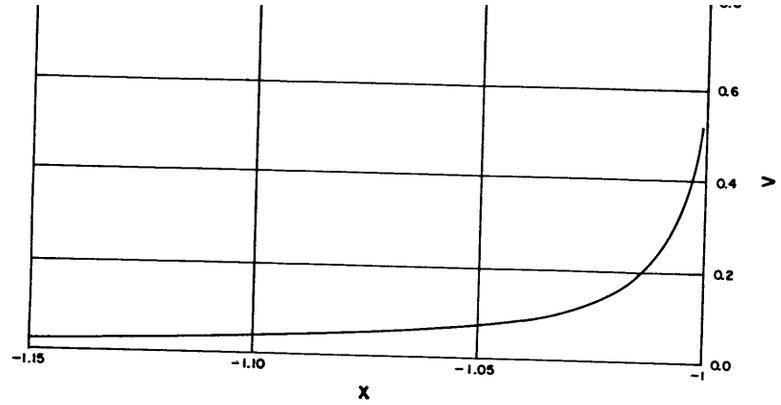

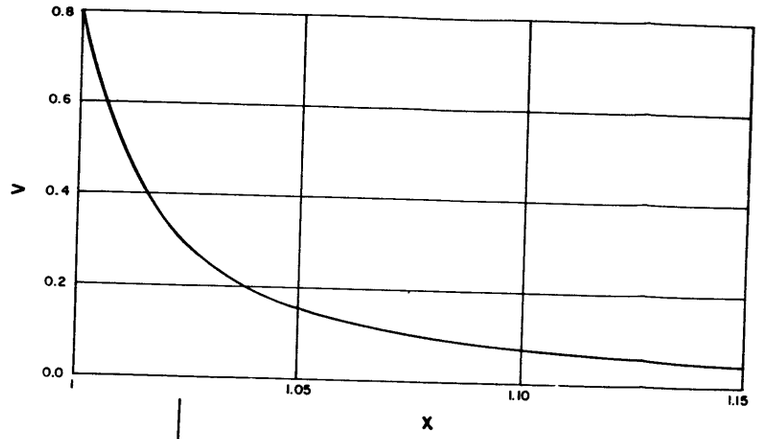

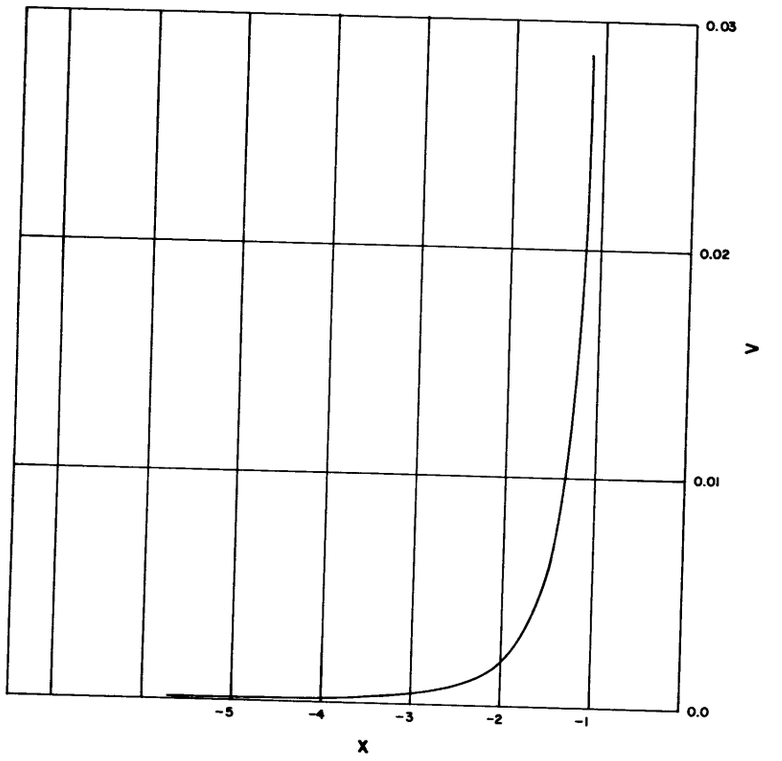

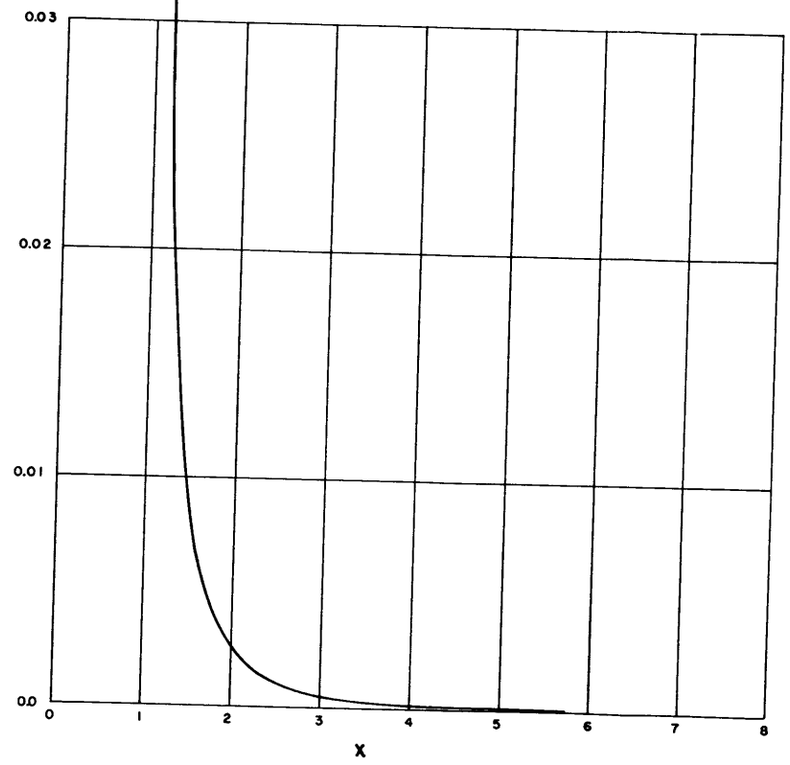

Figure 60 – Velocity along Axis for Body 4

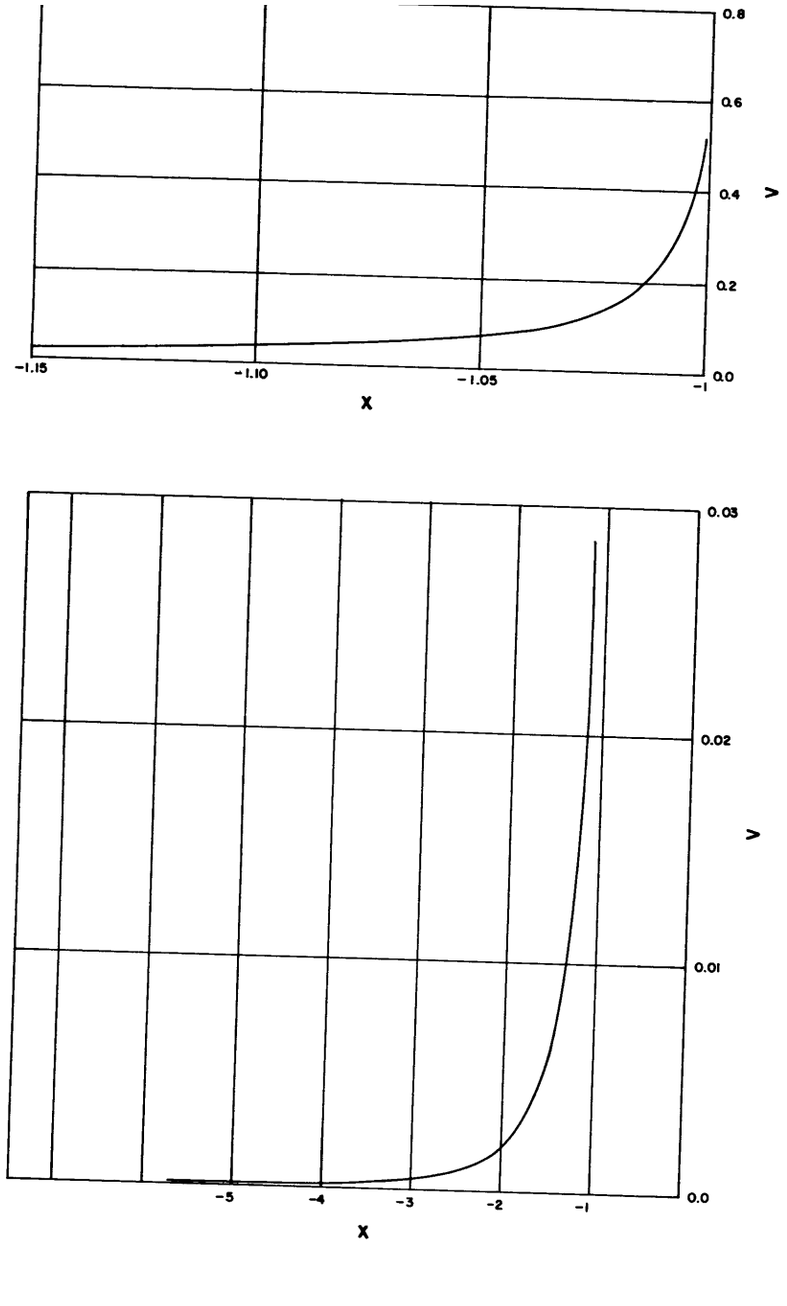

Figure 60 – Velocity along Axis for Body 4

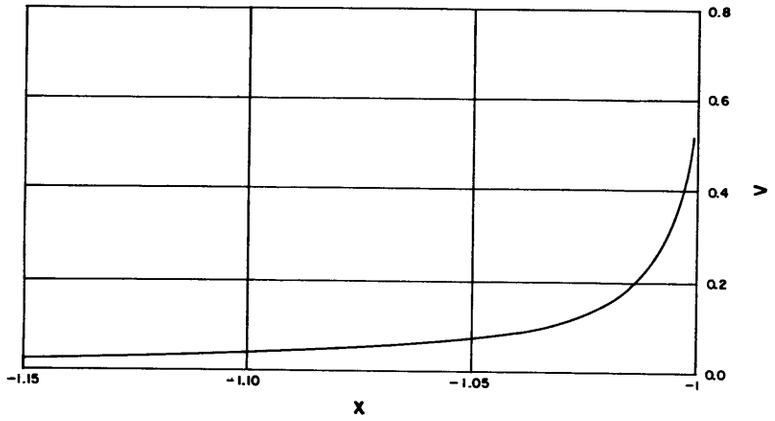

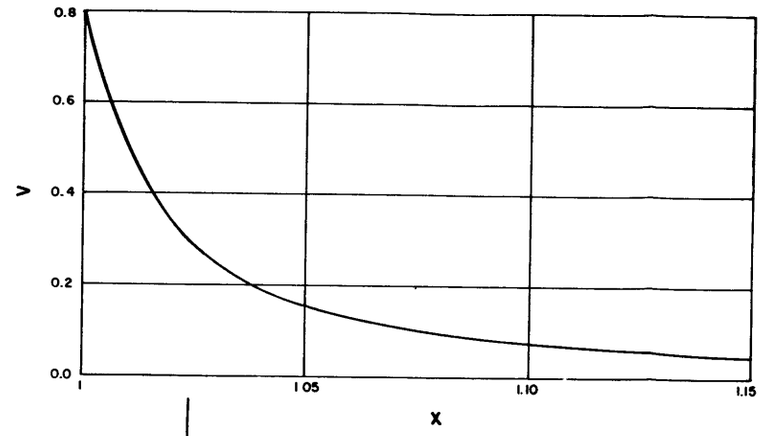

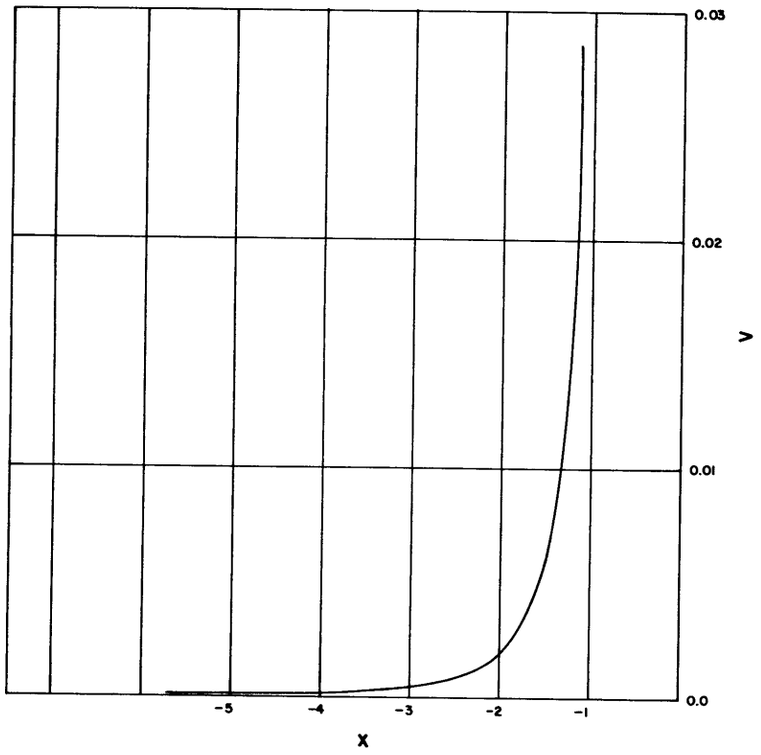

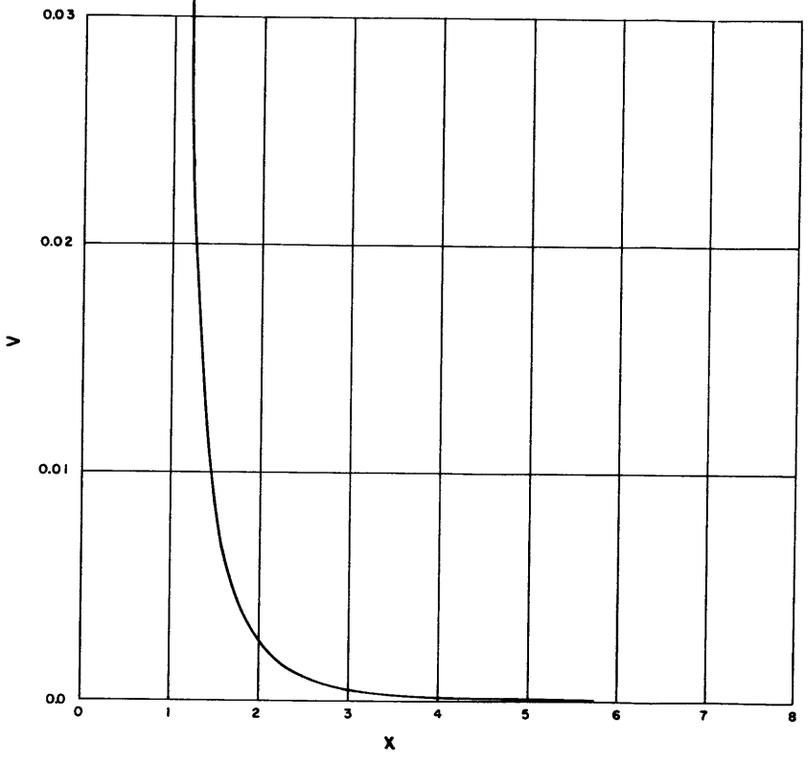

Figure 60 – Velocity along Axis for Body 4

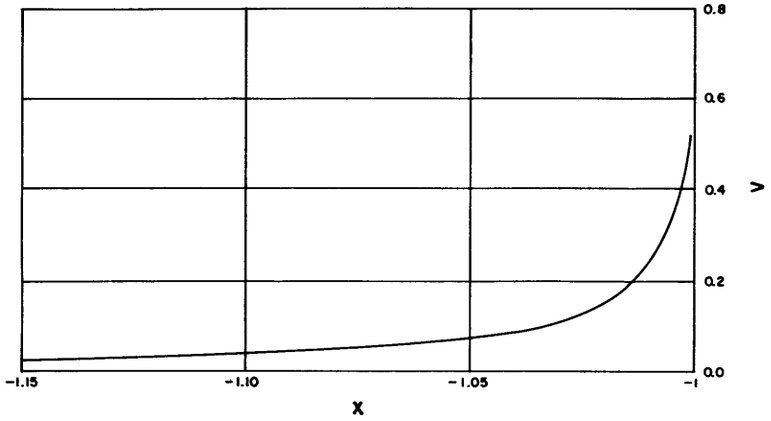

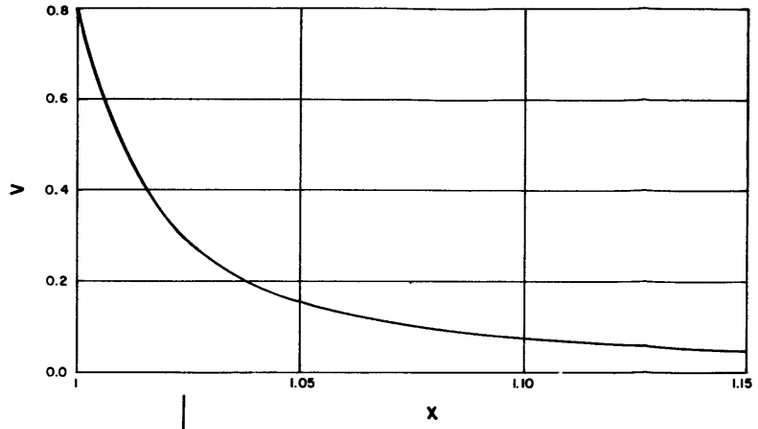

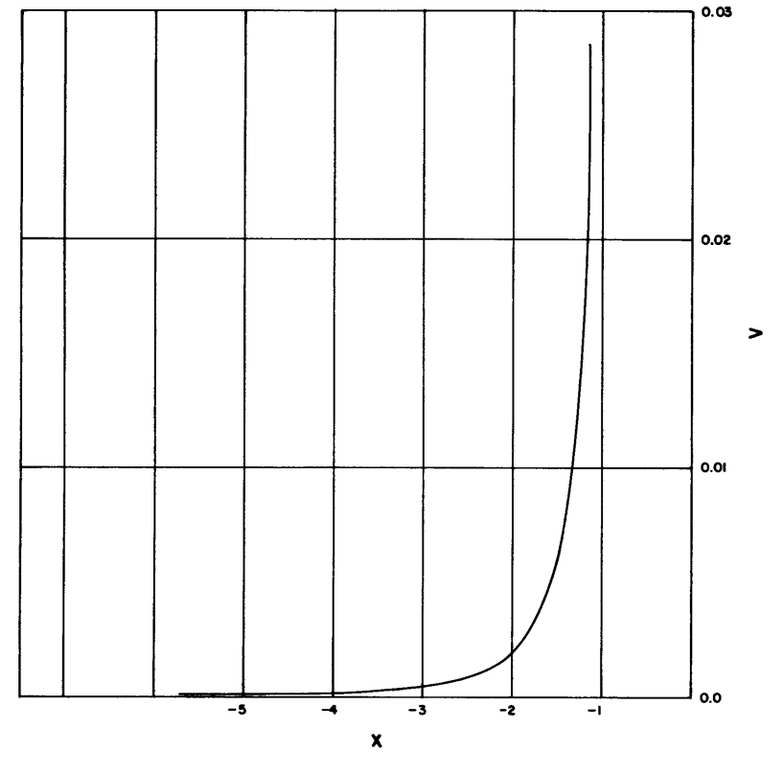

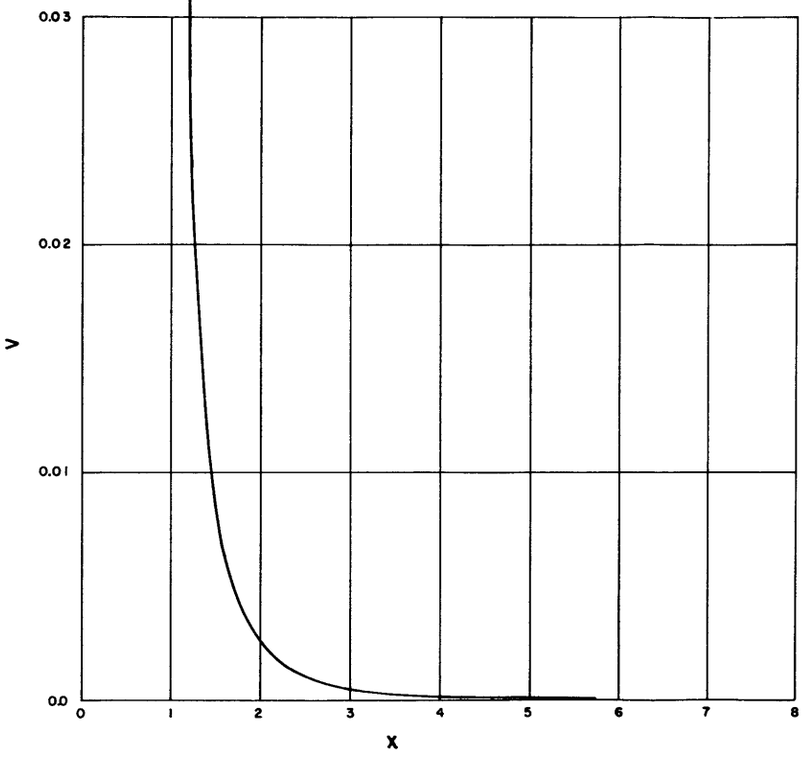

Figure 60 – Velocity along Axis for Body 4

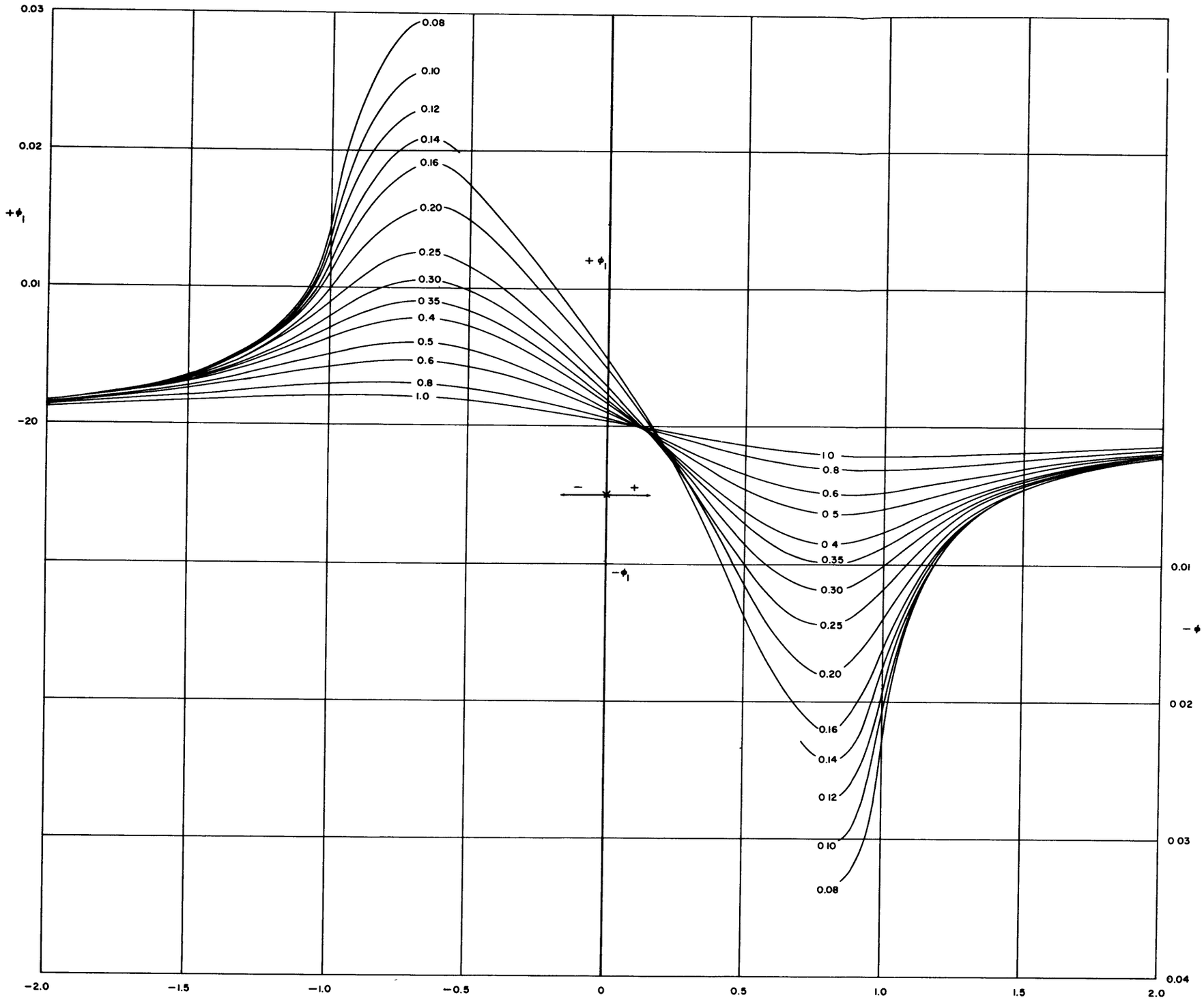

Figure 61 – Velocity Potential ϕ_1 versus x for Body 4

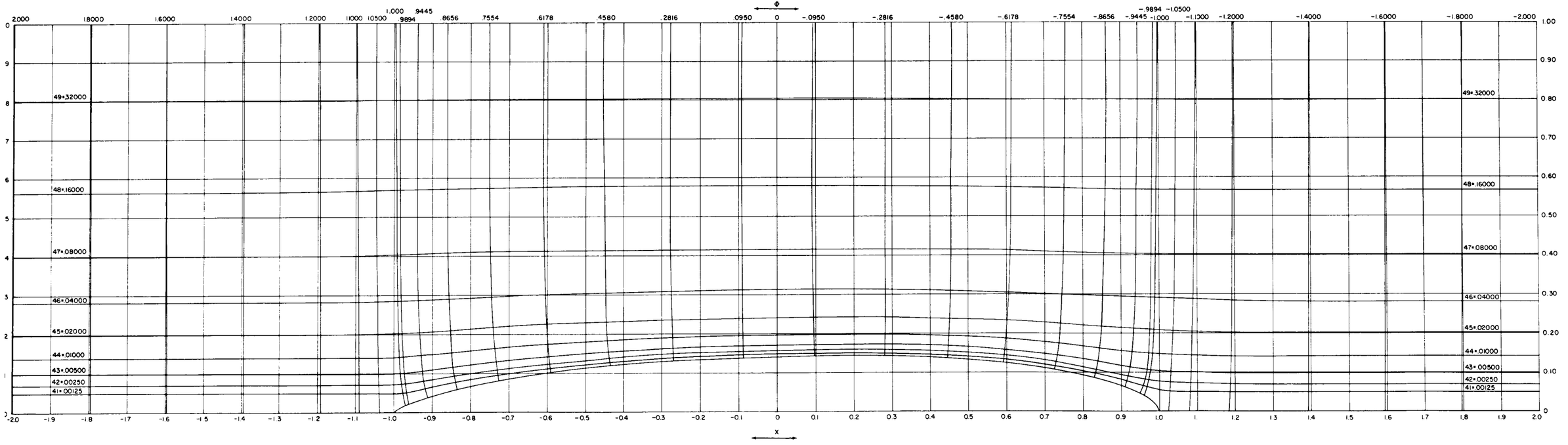

Figure 62 – Flow Pattern for Axial Flow, Body 4

TABLE 1

Characteristics of Series of Bodies

Body	Serial Number	Body Characteristics					
		ℓ/d	m	r_0	r_1	φ	V/ℓ^3
1	40 50 10 65 40	4	0.40	0.50	0.10	0.65	0.03191
2	40 50 10 65 50	5	0.40	0.50	0.10	0.65	0.02043
3	40 50 10 65 60	6	0.40	0.50	0.10	0.65	0.01418
4	40 50 10 65 70	7	0.40	0.50	0.10	0.65	0.01042
5	40 50 10 65 80	8	0.40	0.50	0.10	0.65	0.007977
6	40 50 10 65 100	10	0.40	0.50	0.10	0.65	0.005106
7	36 50 10 65 70	7	0.36	0.50	0.10	0.65	0.01042
8	44 50 10 65 70	7	0.44	0.50	0.10	0.65	0.01042
9	48 50 10 65 70	7	0.48	0.50	0.10	0.65	0.01042
10	52 50 10 65 70	7	0.52	0.50	0.10	0.65	0.01042
11	40 50 10 55 70	7	0.40	0.50	0.10	0.55	0.008816
12	40 50 10 60 70	7	0.40	0.50	0.10	0.60	0.009617
13	40 50 10 70 70	7	0.40	0.50	0.10	0.70	0.01122
14	40 00 10 65 70	7	0.40	0.00	0.10	0.65	0.01042
15	40 30 10 65 70	7	0.40	0.30	0.10	0.65	0.01042
16	40 70 10 65 70	7	0.40	0.70	0.10	0.65	0.01042
17	40 100 10 65 70	7	0.40	1.00	0.10	0.65	0.01042
18	40 50 00 65 70	7	0.40	0.50	0.00	0.65	0.01042
19	40 50 05 65 70	7	0.40	0.50	0.05	0.65	0.01042
20	40 50 15 65 70	7	0.40	0.50	0.15	0.65	0.01042
21	40 50 20 65 70	7	0.40	0.50	0.20	0.65	0.01042
22	40 50 10 60 50	5	0.40	0.50	0.10	0.60	0.01885
23	40 50 10 55 50	5	0.40	0.50	0.10	0.55	0.01728
24	34 50 10 65 70	7	0.34	0.50	0.10	0.65	0.01042
25	40 50 30 65 70	7	0.40	0.50	0.30	0.65	0.01042
26	40 50 40 65 70	7	0.40	0.50	0.40	0.65	0.01042
27	40 50 50 65 70	7	0.40	0.50	0.50	0.65	0.01042
28	36 50 00 55 60	6	0.36	0.50	0.00	0.55	0.01200
29	36 50 00 55 70	7	0.36	0.50	0.00	0.55	0.008816
30	36 50 00 55 80	8	0.36	0.50	0.00	0.55	0.006750

TABLE 2

Coordinates of Series of Bodies

Body	1	2	3	4	5	6
x	y	y	y	y	y	y
−0.989401	0.017358	0.013886	0.011572	0.009918	0.008678	0.006944
−0.944575	0.047848	0.038278	0.031898	0.027342	0.023924	0.019140
−0.865631	0.088506	0.070804	0.059004	0.050574	0.044252	0.035402
−0.755404	0.133120	0.106496	0.088746	0.076068	0.066560	0.053248
−0.617876	0.174012	0.139210	0.116008	0.099436	0.087006	0.069606
−0.458017	0.205932	0.164746	0.137288	0.117676	0.102966	0.082374
−0.281604	0.227740	0.182192	0.151826	0.130138	0.113870	0.091096
−0.095012	0.241378	0.193102	0.160918	0.137930	0.120688	0.096552
+0.095012	0.248752	0.199002	0.165834	0.142144	0.124376	0.099502
+0.281604	0.249110	0.199288	0.166074	0.142348	0.124556	0.099644
+0.458017	0.239118	0.191294	0.159412	0.136638	0.119558	0.095648
+0.617876	0.215946	0.172756	0.143964	0.123398	0.107972	0.086378
+0.755404	0.179770	0.143816	0.119846	0.102726	0.089886	0.071908
+0.865631	0.134350	0.107480	0.089566	0.076772	0.067176	0.053740
+0.944575	0.085156	0.068124	0.056770	0.048660	0.042578	0.034062
+0.989401	0.036596	0.029276	0.024396	0.020912	0.018298	0.014638

Body	7	8	9	10	11	12
x	y	y	y	y	y	y
−0.989401	0.009760	0.009926	0.009980	0.010048	0.009222	0.009570
−0.944575	0.027708	0.027302	0.027594	0.028186	0.020708	0.024250
−0.865631	0.051468	0.050628	0.051452	0.053016	0.032622	0.042556
−0.755404	0.077022	0.076516	0.078094	0.080726	0.047588	0.063446
−0.617876	0.099640	0.100642	0.103000	0.106372	0.067358	0.084924
−0.458017	0.116438	0.119782	0.122612	0.126046	0.090492	0.104968
−0.281604	0.127492	0.132746	0.135384	0.137986	0.113224	0.121978
−0.095012	0.134948	0.140084	0.141668	0.142634	0.131282	0.134648
+0.095012	0.140416	0.142818	0.142668	0.141678	0.141348	0.141748
+0.281604	0.142858	0.141068	0.139140	0.136540	0.141928	0.142136
+0.458017	0.137580	0.133858	0.130788	0.127478	0.133414	0.135034
+0.617876	0.126832	0.120140	0.116944	0.113892	0.117602	0.120536
+0.755404	0.105762	0.100052	0.097600	0.095448	0.096760	0.099788
+0.865631	0.078594	0.075224	0.073888	0.072776	0.072878	0.074854
+0.944575	0.049288	0.048142	0.047698	0.047354	0.047242	0.047962
+0.989401	0.020974	0.020862	0.020822	0.020790	0.020774	0.020846

Body	13	14	15	16	17	18
x	y	y	y	y	y	y
−0.989401	0.010270	0.010206	0.010028	0.009790	0.009608	0.004030
−0.944575	0.030118	0.029798	0.028346	0.026288	0.024632	0.020134
−0.865631	0.057486	0.056504	0.053016	0.048006	0.043852	0.045012
−0.755404	0.086872	0.084810	0.079678	0.072276	0.066184	0.073022
−0.617876	0.112082	0.108748	0.103258	0.095452	0.089452	0.089146
−0.458017	0.129136	0.124922	0.120628	0.114642	0.109948	0.118232
−0.281604	0.137812	0.133858	0.131638	0.128616	0.126300	0.130980
−0.095012	0.141132	0.138814	0.138278	0.137568	0.137028	0.138400
+0.095012	0.142548	0.142142	0.142148	0.142150	0.142158	0.142218
+0.281604	0.142548	0.142250	0.142308	0.142382	0.142438	0.142382
+0.458017	0.138222	0.134804	0.135906	0.137366	0.138450	0.136958
+0.617876	0.126192	0.116640	0.120740	0.125998	0.129798	0.123994
+0.755404	0.105582	0.088530	0.097302	0.107886	0.115190	0.103364
+0.865631	0.078642	0.055454	0.069040	0.083792	0.093338	0.077196
+0.944575	0.049356	0.025052	0.040888	0.055354	0.064094	0.048818
+0.989401	0.020982	0.005030	0.016510	0.024538	0.029142	0.020980

Body	19	20	21	22	23	24
x	y	y	y	y	y	y
−0.989401	0.007554	0.011804	0.013426	0.013398	0.012912	0.010068
−0.944575	0.024008	0.030302	0.033002	0.033950	0.028992	0.028220
−0.865631	0.047872	0.053138	0.055586	0.059578	0.045662	0.052488
−0.755404	0.074566	0.077544	0.078988	0.088824	0.066622	0.078292
−0.617876	0.099040	0.099816	0.100212	0.118894	0.094302	0.100542
−0.458017	0.117952	0.117392	0.117116	0.146954	0.126688	0.116318
−0.281604	0.130562	0.129706	0.129284	0.170768	0.158514	0.126152
−0.095012	0.138162	0.137690	0.137452	0.188506	0.183796	0.132984
+0.095012	0.142188	0.142112	0.142078	0.198446	0.197888	0.138950
+0.281604	0.142368	0.142324	0.142304	0.198990	0.198700	0.142706
+0.458017	0.136800	0.136478	0.136312	0.189048	0.186780	0.140352
+0.617876	0.123692	0.123092	0.122792	0.168750	0.164642	0.128682
+0.755404	0.103048	0.102412	0.102088	0.139702	0.135464	0.107482
+0.865631	0.076984	0.076558	0.076340	0.104796	0.102028	0.079662
+0.944575	0.048738	0.048582	0.048504	0.067148	0.066140	0.049678
+0.989401	0.020922	0.020904	0.020898	0.029184	0.029084	0.021016

Body	25	26	27	28	29	30
x	y	y	y	y	y	y
−0.989401	0.016168	0.018574	0.020642	0.002356	0.002020	0.001708
−0.944575	0.037818	0.042112	0.045982	0.013090	0.011220	0.009818
−0.865631	0.060162	0.064442	0.068434	0.030584	0.026216	0.022938
−0.755404	0.081802	0.084540	0.089172	0.052894	0.045320	0.039656
−0.617876	0.100982	0.101752	0.102508	0.077768	0.066658	0.058326
−0.458017	0.116552	0.115992	0.115420	0.103232	0.088484	0.077424
−0.281604	0.128418	0.127556	0.126686	0.127284	0.109102	0.093464
−0.095012	0.136972	0.136492	0.136010	0.147626	0.126538	0.110720
+0.095012	0.142008	0.141940	0.141868	0.161610	0.138522	0.121208
+0.281604	0.142264	0.142222	0.142184	0.166666	0.142858	0.125000
+0.458017	0.135990	0.135664	0.135338	0.161100	0.138086	0.120826
+0.617876	0.122184	0.121578	0.120962	0.144868	0.124172	0.108652
+0.755404	0.101456	0.100806	0.100160	0.119824	0.102706	0.089868
+0.865631	0.075916	0.075484	0.075058	0.089218	0.076472	0.066914
+0.944575	0.048336	0.048182	0.048032	0.056578	0.048496	0.042434
+0.989401	0.020882	0.020864	0.020852	0.024376	0.020894	0.018282

TABLE 3

Velocity Functions for Body 1

Serial 40 50 10 65 40

x	u_{1s}	$u_{1s} \sec \gamma$	$u_{2\theta}$	u_{2s}	$u_{R\theta}$	u_{Rs}
−0.989401	−0.609049	−0.825716	+2.219149	−1.451206	−1.026036	+0.634482
−0.944575	−0.779657	−0.901963	+2.087786	−0.955772	−0.860430	+0.309469
−0.865631	−0.902435	−0.994090	+1.968018	−0.748219	−0.686319	+0.155716
−0.755404	−0.989877	−1.049488	+1.902918	−0.591847	−0.546465	+0.054322
−0.617877	−1.043967	−1.075368	+1.874210	−0.429364	−0.424995	+0.031576
−0.458017	−1.066714	−1.079998	+1.867135	−0.292727	−0.307108	−0.095819
−0.281604	−1.068254	−1.072975	+1.870113	−0.179760	−0.183087	−0.142624
−0.095012	−1.066550	−1.068152	+1.870948	−0.098647	−0.050912	−0.168110
+0.095012	−1.075059	−1.075382	+1.861505	−0.021247	+0.082069	−0.171953
+0.281604	−1.093582	−1.093910	+1.843150	+0.068604	+0.204925	−0.152358
+0.458017	−1.108851	−1.113975	+1.824352	+0.198971	+0.311885	−0.109630
+0.617876	−1.102413	−1.124452	+1.813897	+0.360595	+0.405142	−0.045301
+0.755404	−1.060696	−1.118406.	+1.816001	+0.568192	+0.489781	+0.043589
+0.865631	−0.976704	−1.094960	+1.832558	+0.803326	+0.571036	+0.162772
+0.944575	−0.835662	−1.066848	+1.853034	+1.127243	+0.638863	+0.330808
+0.989401	−0.514195	−1.033765	+1.879365	+1.613427	+0.695013	+0.572863

TABLE 4

Velocity Functions for Body 2

Serial 40 50 10 65 50

−0.989401	−0.693824	−0.859970	+2.208179	−1.271534	−1.059765	+0.222782
−0.944575	−0.829860	−0.915253	+2.100598	−0.819547	−0.910309	+0.621708
−0.865631	−0.924704	−0.985825	+1.995376	−0.632919	−0.742777	+0.208271
−0.755404	−0.994367	−1.033109	+1.933556	−0.492662	−0.598979	+0.053007
−0.617877	−1.034777	−1.054819	+1.906000	−0.354129	−0.469451	−0.025334
−0.458017	−1.050042	−1,058404	+1.899616	−0.239715	−0.341100	−0.083816
−0.281604	−1.049874	−1.052822	+1.902873	−0.146764	−0.205266	−0.124565
−0.095012	−1.047885	−1.048934	+1.904355	−0.081594	−0.060645	−0.147233
+0.095012	−1.054100	−1.054311	+1.896442	−0.019548	+0.085359	−0.151478
+0.281604	−1.068336	−1.068550	+1.880241	+0.052929	+0.221910	−0.137112
+0.458017	−1.080726	−1.083978	+1.863584	+0.160612	+0.342952	−0.100817
+0.617876	−1.077891	−1.091646	+1.854582	+0.295193	+0.449625	−0.044712
+0.755404	−1.049705	−1.086538	+1.857734	+0.473967	+0.546442	+0.039091
+0.865631	−0.990132	−1.068449	+1.873362	+0.670405	+0.635841	+3.052987
+0.944575	−0.880785	−1.043337	+1.896461	+1.035209	+0.713480	+2.963808
+0.989401	−0.594104	−1.001992	+1.918769	+1.270114	+0.767778	+1.759574

TABLE 5

Velocity Functions for Body 3

Serial 40 50 10 65 60

x	u_{1s}	$u_{1s} \sec \gamma$	$u_{2\theta}$	u_{2s}	$u_{R\theta}$	u_{Rs}
−0.989401	−0.756190	−0.885884	+2.186607	−1.115770	−1.069159	+0.522290
−0.944575	−0.865273	−0.928006	+2.099338	−0.711523	−0.935525	+0.262886
−0.865631	−0.939344	−0.982886	+2.009561	−0.547370	−0.777492	+0.138603
−0.755404	−0.995440	−1.022538	+1.953262	−0.421598	−0.633569	+0.050436
−0.617876	−1.027683	−1.041536	+1.927251	−0.300865	−0.499397	−0.020887
−0.458017	−1.039098	−1.044844	+1.921195	−0.202512	−0.364188	−0.073741
−0.281604	−1.038296	−1.040477	+1.924409	−0.123787	−0.220377	−0.109800
−0.095012	−1.036318	−1.037044	+1.926225	−0.069443	−0.067270	−0.129896
+0.095012	−1.041109	−1.041213	+1.919520	−0.018060	+0.087676	−0.134312
+0.281604	−1.052535	−1.052640	+1.905179	+0.042698	+0.233748	−0.123023
+0.458017	−1.062894	−1.065131	+1.890340	+0.134212	+0.364677	−0.091920
+0.617876	−1.061759	−1.071186	+1.882587	+0.249759	+0.480896	−0.041991
+0.755404	−1.041155	−1.066648	+1.886254	+0.405253	+0.585974	+0.034813
+0.865631	−0.996085	−1.051388	+1.901632	+0.590536	+0.681566	+0.137676
+0.944575	−0.910103	−1.029644	+1.924505	+0.881196	+0.763467	+0.299902
+0.989401	−0.659951	−1.012195	+1.944082	+1.466032	+0.817412	+0.599632

TABLE 6

Velocity Functions for Body 4

Serial 40 50 10 65 70

−0.989401	−0.802757	−0.905944	+2.162974	−0.986020	−1.067642	+0.467759
−0.944575	−0.891168	−0.939060	+2.092207	−0.625736	−0.948020	+0.239010
−0.865631	−0.950084	−0.982608	+2.016390	−0.481237	−0.799733	+0.128500
−0.755404	−0.995753	−1.015763	+1.966251	−0.368480	−0.657465	+0.047555
−0.617876	−1.022267	−1.032384	+1.942165	−0.261444	−0.520570	−0.017609
−0.458017	−1.031410	−1.035552	+1.936380	−0.175108	−0.380599	−0.065548
−0.281604	−1.030455	−1.032003	+1.939376	−0.106841	−0.231116	−0.097774
−0.095012	−1.028634	−1.029148	+1.941301	−0.060370	−0.071946	−0.115752
+0.095012	−1.032451	−1.032554	+1.935565	−0.016721	+0.089423	−0.120129
+0.281604	−1.041902	−1.042006	+1.922804	+0.035525	+0.242394	−0.110902
+0.458017	−1.050723	−1.052301	+1.909532	+0.115056	+0.380528	−0.083742
+0.617876	−1.050431	−1.057303	+1.902814	+0.216330	+0.503687	−0.038878
+0.753404	−1.034517	−1.053265	+1.906774	+0.353488	+0.614664	+0.031301
+0.865631	−0.998836	−1.039913	+1.921728	+0.519389	+0.714524	+0.125378
+0.944575	−0.930049	−1.021246	+1.943452	+0.787342	+0.798621	+0.278708
+0.989401	−0.713412	−1.007359	+1.961040	+1.378098	+0.852650	+0.583479

TABLE 7

Velocity Functions for Body 5

Serial 40 50 10 65 80

x	u_{1s}	$u_{1s}\sec\gamma$	$u_{2\theta}$	u_{2s}	$u_{R\theta}$	u_{Rs}
−0.989401	−0.837916	−0.921495	+2.141072	−0.878848	−1.061938	+0.420193
−0.944575	−0.910644	−0.948390	+2.083108	−0.556945	−0.953864	+0.217759
−0.865631	−0.958342	−0.983621	+2.019175	−0.429538	−0.814566	+0.119357
−0.755404	−0.996021	−1.011394	+1.974950	−0.327268	−0.674673	+0.044727
−0.617876	−1.018180	−1.025874	+1.952967	−0.231180	−0.536201	−0.015103
−0.458017	−1.025791	−1.028980	+1.947490	−0.154144	−0.392775	−0.058871
−0.281604	−1.024870	−1.025998	+1.950211	−0.093869	−0.239069	−0.087938
−0.095012	−1.023247	−1.023656	+1.952124	−0.053340	−0.075386	−0.104154
+0.095012	−1.026384	−1.026487	+1.947161	−0.015531	+0.090766	−0.108386
+0.281604	−1.034339	−1.034442	+1.935782	+0.030229	+0.248928	−0.100649
+0.458017	−1.041943	−1.043195	+1.923872	+0.100577	+0.392515	−0.076544
+0.617876	−1.042081	−1.047317	+1.918012	+0.190720	+0.520885	−0.035881
+0.755404	−1.029280	−1.043576	+1.922113	+0.313301	+0.636214	+0.028444
+0.865631	−1.000195	−1.031761	+1.936406	+0.462662	+0.739010	+0.115947
+0.944575	−0.944098	−1.015705	+1.956721	+0.708888	+0.824322	+0.258015
+0.989401	−0.756800	−1.004246	+1.972593	+1.291354	+0.878333	+0.560228

TABLE 8

Velocity Functions for Body 6

Serial 40 50 10 65 100

−0.989401	−0.886355	−0.943935	+2.105206	−0.717231	−1.047522	+0.345583
−0.944575	−0.937277	−0.962297	+2.065331	−0.453868	−0.956866	+0.182813
−0.865631	−0.970101	−0.986577	+2.019202	−0.352174	−0.832124	+0.103222
−0.755404	−0.996706	−1.006570	+1.985040	−0.267389	−0.697390	+0.039650
−0.617876	−1.012728	−1.017612	+1.967106	−0.187785	−0.557581	−0.011565
−0.458017	−1.018284	−1.020324	+1.962370	−0.124276	−0.409561	−0.048762
−0.281604	−1.017597	−1.018310	+1.964525	−0.075362	−0.249996	−0.072992
−0.095012	−1.016356	−1.016559	+1.966253	−0.043199	−0.080118	−0.086457
+0.095012	−1.018603	−1.018603	+1.962451	−0.013538	+0.092596	−0.090333
+0.281604	−1.024466	−1.024466	+1.953330	+0.022999	+0.258009	−0.084584
+0.458017	−1.030226	−1.030948	+1.943699	+0.080176	+0.409301	−0.064940
+0.617876	−1.030685	−1.033994	+1.939149	+0.154176	+0.544971	−0.030726
+0.755404	−1.021787	−1.030858	+1.943133	+0.255172	+0.666127	+0.024140
+0.865631	−1.001281	−1.021611	+1.955766	+0.379268	+0.772425	+0.099188
+0.944575	−0.962092	−1.009434	+1.973140	+0.588489	+0.858607	+0.222239
+0.989401	−0.820905	−1.000982	+1.986183	+1.132853	+0.912178	+0.507260

TABLE 9

Velocity Functions for Body 7

Serial 36 50 10 65 70

x	u_{1s}	$u_{1s} \sec \gamma$	$u_{2\theta}$	u_{2s}	$u_{R\theta}$	u_{Rs}
−0.989401	−0.787390	−0.895677	+2.179136	−1.016071	−1.082376	+0.483414
−0.944575	−0.888674	−0.939104	+2.089820	−0.636354	−0.945736	+0.240948
−0.865631	−0.953142	−0.986792	+2.089820	−0.485701	−0.794138	+0.129137
−0.755404	−1.001336	−1.020938	+1.958989	−0.363470	−0.653427	+0.045934
−0.617876	−1.026444	−1.035556	+1.938610	−0.249452	−0.520015	−0.019585
−0.458017	−1.031284	−1.034698	+1.938575	−0.161485	−0.382857	−0.066766
−0.281604	−1.025561	−1.026793	+1.947146	−0.099256	−0.233499	−0.097816
−0.095012	−1.021674	−1.022287	+1.950952	−0.064710	−0.071641	−0.115390
+0.095012	−1.027857	−1.028166	+1.941439	−0.032088	+0.092328	−0.120601
+0.281604	−1.042813	−1.042813	+1.921612	+0.016552	+0.244764	−0.112619
+0.458017	−1.056889	−1.058053	+1.902111	+0.101332	+0.379384	−0.085781
+0.617876	−1.058624	−1.065342	+1.892310	+0.213680	+0.498427	−0.039867
+0.755404	−1.039862	−1.060110	+1.896880	+0.362841	+0.607237	+0.032256
+0.865631	−0.997526	−1.042455	+1.916126	+0.536126	+0.708710	+0.128694
+0.944575	−0.921005	−1.017011	+1.945252	+0.803568	+0.798581	+0.282159
+0.989401	−0.703560	−0.997533	+1.969644	+1.387376	+0.858910	+0.587817

TABLE 10

Velocity Functions for Body 8

Serial 44 50 10 65 70

−0.989401	−0.803288	−0.905827	+2.164212	−0.998729	−1.068008	+0.467250
−0.944575	−0.8894753	−0.937278	+2.095842	−0.627519	−0.950350	+0.240203
−0.865631	−0.947103	−0.980133	+2.020081	−0.486055	−0.801656	+0.130010
−0.755404	−0.993048	−1.013935	+1.968120	−0.3760730	−0.657640	+0.048951
−0.617876	−1.021582	−1.032632	+1.940993	−0.270249	−0.518940	−0.016771
−0.458017	−1.033718	−1.038391	+1.031787	−0.181480	−0.378299	−0.065581
−0.281604	−1.035155	−1.036710	+1.932428	−0.106650	−0.229987	−0.098450
−0.095012	−1.033430	−1.033740	+1.934865	−0.051559	−0.073194	−0.116237
+0.095012	−1.034507	−1.034507	+1.933045	−0.001572	+0.086690	−0.119584
+0.281604	−1.039628	−1.039940	+1.925808	+0.050996	+0.240780	−0.109307
+0.458017	−1.044874	−1.046864	+1.916994	+0.124482	+0.382151	−0.082024
+0.617876	−1.043850	−1.050574	+1.912036	+0.215902	+0.508630	+0.038227
+0.755404	−1.030798	−1.047985	+1.914667	+0.343298	+0.620945	+0.030140
+0.865631	−1.000857	−1.038556	+1.925341	+0.503356	+0.718845	+0.123501
+0.944575	−0.938199	−1.025354	+1.940778	+0.772253	+0.797901	+0.275120
+0.989401	−0.721810	−1.015490	+1.953060	+1.369349	+0.846917	+0.579169

TABLE 11

Velocity Functions for Body 9

Serial 48 50 10 65 70

x	u_{1s}	u_{1s} sec γ	$u_{2\theta}$	u_{2s}	$u_{R\theta}$	u_{Rs}
−0.989401	−0.798395	−0.901428	+2.171802	−0.991902	−1.073434	+0.471139
−0.944575	−0.884681	−0.929433	+2.100213	−0.638086	−0.952527	+0.243862
−0.865631	−0.944279	−0.978933	+2.020602	−0.496607	−0.800539	+0.132298
−0.755404	−0.992651	−1.014877	+1.965633	−0.385369	−0.654727	+0.050031
−0.617876	−1.023634	−1.035334	+1.936182	−0.276493	−0.515651	−0.016852
−0.458017	−1.037734	−1.042530	+1.925423	−0.182368	−0.375996	−0.066562
−0.281604	−1.039788	−1.041152	+1.925979	−0.100597	−0.229787	−0.099678
−0.095012	−1.036708	−1.036915	+1.930584	−0.039019	−0.075205	−0.116835
+0.095012	−1.034649	−1.034649	+1.933006	+0.013997	+0.083980	−0.118979
+0.281604	−1.036146	−1.036664	+1.930483	+0.064254	+0.239738	−0.107736
+0.458017	−1.039088	−1.041275	+1.924836	+0.130651	+0.384260	−0.080505
+0.617876	−1.038338	−1.044816	+1.920446	+0.212803	+0.513447	−0.037865
+0.755404	−1.028389	−1.044050	+1.920989	+0.332044	+0.626369	+0.028724
+0.865631	−1.003495	−1.038277	+1.927387	+0.488063	+0.722028	+0.120672
+0.944575	−0.945795	−1.029717	+1.937373	+0.758996	+0.796581	+0.271814
+0.989401	−0.729234	−1.023199	+1.945406	+1.361791	+0.841493	+0.575298

TABLE 12

Velocity Functions for Body 10

Serial 52 50 10 65 70

−0.989401	−0.788407	−0.893278	+2.185298	−1.007801	−1.083607	+0.478573
−0.944575	−0.876920	−0.929433	+2.105086	−0.657866	−0.954444	+0.250230
−0.865631	−0.941710	−0.979113	+2.017878	−0.512246	−0.796421	+0.135137
−0.755404	−0.994520	−1.018454	+1.959026	−0.395939	−0.648952	+0.507845
−0.617876	−1.028269	−1.040547	+1.928118	−0.280182	−0.510917	−0.017735
−0.458017	−1.043307	−1.047918	+1.917559	−0.178128	−0.373748	−0.068340
−0.281604	−1.044322	−1.045367	+1.920036	−0.089080	−0.230461	−0.101382
−0.095012	−1.038437	−1.038437	+1.928362	−0.022968	−0.077927	−0.117534
+0.095012	−1.032819	−1.032922	+1.935507	+0.029908	+0.081325	−0.118312
+0.281604	−1.031455	−1.032178	+1.936960	+0.075025	+0.239354	−0.106202
+0.458017	−1.033445	−1.035723	+1.933022	+0.133108	+0.386894	−0.079243
+0.617876	−1.034092	−1.040020	+1.927737	+0.206789	+0.518000	−0.037876
+0.755404	−1.027462	−1.041628	+1.925371	+0.319915	+0.630676	+0.027056
+0.865631	−1.006752	−1.039174	+1.927696	+0.474333	+0.723908	+0.118005
+0.944575	−0.952606	−1.033868	+1.933362	+0.747052	+0.794720	+0.268485
+0.989401	−0.735376	−1.029362	+1.938414	+1.354406	+0.836638	+0.571440

TABLE 13

Velocity Functions for Body 11

Serial 40 50 10 55 70

x	u_{1s}	$u_{1s}\sec\gamma$	$u_{2\theta}$	u_{2s}	$u_{R\theta}$	u_{Rs}
−0.989401	−0.916201	−0.997280	+2.010515	−0.797787	−0.949163	+0.369647
−0.944575	−0.970865	−0.986952	+2.027992	−0.371587	−0.918276	+0.149603
−0.865631	−0.966241	−0.975114	+2.046664	−0.279708	−0.848367	+0.081947
−0.755404	−0.962724	−0.971957	+2.047334	−0.279319	−0.727672	+0.046102
−0.617876	−0.971748	−0.982159	+2.023386	−0.277515	−0.567328	+0.005666
−0.458017	−0.992860	−1.002483	+1.985706	−0.255336	−0.392460	−0.038262
−0.281604	−1.018381	−1.025147	+1.949351	−0.202791	−0.221086	−0.077487
−0.095012	−1.040060	−1.043085	+1.922693	−0.132809	−0.058935	−0.104423
+0.095012	−1.053043	−1.053465	+1.907627	−0.046574	+0.094524	−0.114227
+0.281604	−1.055887	−1.056204	+1.903077	+0.042576	+0.241066	−0.106204
+0.458017	−1.049837	−1.052679	+1.906699	+0.136869	+0.381271	−0.078890
+0.617876	−1.037652	−1.045704	+1.915344	+0.227884	+0.513088	−0.035446
+0.755404	−1.021470	−1.038185	+1.925463	+0.340367	+0.631418	+0.030788
+0.865631	−0.998746	−1.032402	+1.933977	+0.484644	+0.729317	+0.121395
+0.944575	−0.948650	−1.029240	+1.939407	+0.749636	+0.800471	+0.271360
+0.989401	−0.735238	−1.028161	+1.941786	+1.356674	+0.840259	+0.574423

TABLE 14

Velocity Functions for Body 12

Serial 40 50 10 60 70

−0.989401	−0.855172	−0.947979	+2.093893	−0.898239	−1.014681	+0.422422
−0.944575	−0.927689	−0.959844	+2.068307	−0.518632	−0.938988	+0.203604
−0.865631	−0.957073	−0.977802	+2.033483	−0.401298	−0.823554	+0.112691
−0.755404	−0.980760	−0.995291	+2.001896	−0.328909	−0.688196	+0.046634
−0.617876	−0.999481	−1.009373	+1.977567	−0.262859	−0.541622	−0.009516
−0.458017	−1.013540	−1.019760	+1.959603	−0.207253	−0.387067	−0.054586
−0.281604	−1.024547	−1.028042	+1.945442	−0.150312	−0.227140	−0.088774
−0.095012	−1.034122	−1.035572	+1.933046	−0.095126	−0.065836	−0.110388
+0.095012	−1.042680	−1.042888	+1.921900	−0.031329	+0.091912	−0.117244
+0.281604	−1.048901	−1.049111	+1.913038	+0.039061	+0.241734	−0.108591
+0.458017	−1.050293	−1.052503	+1.908212	+0.125772	+0.380936	−0.081386
+0.617876	−1.044142	−1.051608	+1.908964	+0.221859	+0.508309	−0.037249
+0.755404	−1.028138	−1.045812	+1.915860	+0.347014	+0.622830	+0.031014
+0.865631	−0.998805	−1.036105	+1.927804	+0.502222	+0.721838	+0.123803
+0.944575	−0.939179	−1.025081	+1.941656	+0.768894	+0.799705	+0.275235
+0.989401	−0.724169	−1.017520	+1.951643	+1.374507	+0.846645	+0.610498

TABLE 15

Velocity Functions for Body 13

Serial 40 50 10 70 70

x	u_{1s}	u_{1s} sec γ	$u_{2\theta}$	u_{2s}	$u_{R\theta}$	u_{Rs}
−0.989401	−0.757442	−0.869922	+2.220059	−1.050800	−1.110183	+0.506645
−0.944575	−0.859931	−0.922970	+2.105667	−0.721724	−0.949725	+0.263488
−0.865631	−0.944691	−0.988998	+1.998251	−1.050800	−0.777168	+0.138436
−0.755404	−1.008438	−1.033977	+1.936912	−0.402224	−0.632045	+0.048769
−0.617876	−1.041692	−1.052426	+1.913413	−0.264581	−0.502862	−0.022574
−0.458017	−1.047506	−1.050447	+1.915611	−0.151550	−0.374066	−0.073442
−0.281604	−1.036259	−1.036674	+1.932047	−0.069946	−0.233791	−0.105164
−0.095012	−1.023500	−1.023602	+1.947870	−0.028207	−0.077416	−0.120620
+0.095012	−1.022371	−1.022371	+1.948664	−0.002631	+0.087038	−0.122903
+0.281604	−1.034904	−1.034904	+1.932381	+0.031921	+0.243038	−0.113138
+0.458017	−1.051120	−1.052277	+1.910686	+0.104734	+0.380057	−0.085981
+0.617876	−1.056535	−1.062912	+1.896886	+0.211195	+0.499212	−0.040349
+0.755404	−1.040595	−1.060316	+1.898187	+0.359838	+0.606901	+0.031621
+0.865631	−0.998871	−1.043643	+1.915736	+0.539426	+0.707361	+0.128312
+0.944575	−0.921234	−1.017600	+1.944844	+0.800108	+0.797255	+0.281651
+0.989401	−0.702958	−0.997245	+1.970000	+1.392665	+0.858293	+0.587435

TABLE 16

Velocity Functions for Body 14

Serial 40 00 10 65 70

−0.989401	−0.762631	−0.874978	+2.210664	−1.055618	−1.104641	+0.502608
−0.944575	−0.866547	−0.927780	+2.098910	−0.696199	−0.946936	+0.259498
−0.865631	−0.949630	−0.991574	+1.995937	−0.528775	−0.778354	+0.135529
−0.755404	−1.010279	−1.033639	+1.938569	−0.387389	−0.636002	+0.047313
−0.617876	−1.039409	−1.048954	+1.918799	−0.253480	−0.508178	−0.022860
−0.458017	−1.041697	−1.044412	+1.923630	−0.147689	−0.378755	−0.071937
−0.281604	−1.030442	−1.031060	+1.938876	−0.077616	−0.235877	−0.102907
−0.095012	−1.022964	−1.023169	+1.947210	−0.041634	−0.077421	−0.117890
+0.095012	−1.030087	−1.030190	+1.937328	−0.009676	+0.084815	−0.119782
+0.281604	−1.047966	−1.048071	+1.914968	+0.048383	+0.235042	−0.106431
+0.458017	−1.060668	−1.063539	+1.896471	+0.149681	+0.368492	−0.073473
+0.617876	−1.050772	−1.063857	+1.896338	+0.285607	+0.492801	−0.018941
+0.755404	−1.006703	−1.038802	+1.927468	+0.439755	+0.623205	+0.057358
+0.865631	−0.922015	−0.976297	+2.011819	+0.595899	+0.784774	+0.155708
+0.944575	−0.809129	−0.878724	+2.184784	+0.765717	+1.016815	+0.290498
+0.989401	−0.714273	−0.789427	+2.439219	+1.000972	+1.317283	+0.517452

TABLE 17

Velocity Functions for Body 15

Serial 40 30 10 65 70

x	u_{1s}	$u_{1s} \sec \gamma$	$u_{2\theta}$	u_{2s}	$u_{R\theta}$	u_{Rs}
−0.989401	−0.785944	−0.892915	+2.183264	−1.014888	−1.083510	+0.482432
−0.944575	−0.880951	−0.934300	+2.095539	−0.656165	−0.948026	+0.248070
−0.865631	−0.949854	−0.986144	+2.008080	−0.501188	−0.790963	+0.131693
−0.755404	−1.001797	−1.023182	+1.954641	−0.376208	−0.648482	+0.047321
−0.617876	−1.029339	−1.039212	+1.932444	−0.257764	−0.515443	−0.019907
−0.458017	−1.035588	−1.039121	+1.931251	−0.163644	−0.379912	−0.068297
−0.281604	−1.030433	−1.031568	+1.939307	−0.094828	−0.233093	−0.099881
−0.095012	−1.026346	−1.026756	+1.943751	−0.052856	−0.074149	−0.116654
+0.095012	−1.031521	−1.001621	+1.936302	−0.013830	+0.087591	−0.119972
+0.281604	−1.044340	−1.044444	+1.919739	+0.040510	+0.239491	−0.109190
+0.458017	−1.054663	−1.056777	+1.904613	+0.128676	+0.375909	−0.079773
+0.617876	−1.050426	−1.059431	+1.901138	+0.242260	+0.500042	−0.031768
+0.755404	−1.023756	−1.046892	+1.916088	+0.383554	+0.619254	+0.039597
+0.865631	−0.972824	−1.017066	+1.953210	+0.535847	+0.739845	+0.130865
+0.944575	−0.896756	−0.975265	+2.009388	+0.754547	+0.859416	+0.270658
+0.989401	−0.732226	−0.944564	+2.057918	+1.284385	+0.947841	+0.571080

TABLE 18

Velocity Functions for Body 16

Serial 40 70 10 65 70

−0.989401	−0.819672	−0.919224	+2.142155	−0.959453	−1.051365	+0.453140
−0.944575	−0.901939	−0.944438	+2.087796	−0.591261	−0.947259	+0.228923
−0.865631	−0.950363	−0.979150	+2.024881	−0.461776	−0.808832	+0.124918
−0.755404	−0.989377	−1.008025	+1.978685	−0.360617	−0.667056	+0.047990
−0.617876	−1.014863	−1.025321	+1.952461	−0.265935	−0.525934	−0.014952
−0.458017	−1.027141	−1.032095	+1.941531	−0.187377	−0.381191	−0.062520
−0.281604	−1.030500	−1.032462	+1.939256	−0.119293	−0.229031	−0.095568
−0.095012	−1.030933	−1.031552	+1.938751	−0.067954	−0.069717	−0.114813
+0.095012	−1.033375	−1.033478	+1.934780	−0.019644	+0.091243	−0.120281
+0.281604	−1.039453	−1.039556	+1.925788	+0.030644	+0.245255	−0.112561
+0.458017	−1.046809	−1.047961	+1.914116	+0.101800	+0.384939	−0.087520
+0.617876	−1.050578	−1.055645	+1.903566	+0.192276	+0.506622	−0.045120
+0.755404	−1.044963	−1.060123	+1.896887	+0.327792	+0.609366	+0.024922
+0.865631	−1.021639	−1.060781	+1.894696	+0.509032	+0.692490	+0.155454
+0.944575	−0.953946	−1.058763	+1.895684	+0.822962	+0.753984	+0.287585
+0.989401	−0.693080	−1.056524	+1.897410	+1.429206	+0.789550	+0.583246

TABLE 19

Velocity Functions for Body 17

Serial 40 100 10 65 70

x	u_{1s}	$u_{1s} \sec \gamma$	$u_{2\theta}$	u_{2s}	$u_{R\theta}$	u_{Rs}
−0.989401	−0.846943	−0.940525	+2.107730	−0.923863	−1.024162	+0.429279
−0.944575	−0.919176	−0.953304	+2.078877	−0.536987	−0.944539	+0.210461
−0.865631	−0.950920	−0.974004	+2.037902	−0.422252	−0.823155	+0.117970
−0.755404	−0.979100	−0.995829	+1.999182	−0.348642	−0.682811	+0.049110
−0.617876	−1.003060	−1.014216	+1.969120	−0.274655	−0.534460	−0.010089
−0.458017	−1.020513	−1.026879	+1.949285	−0.207572	−0.381846	−0.057387
−0.281604	−1.030633	−1.033527	+1.938664	−0.138801	−0.225668	−0.092049
−0.095012	−1.034410	−1.035341	+1.934729	−0.079512	−0.066330	−0.113337
+0.095012	−1.034744	−1.034848	+1.933520	−0.024056	+0.093962	−0.120503
+0.281604	−1.035751	−1.035854	+1.930125	+0.023476	+0.249480	−0.114956
+0.458017	−1.041036	−1.041765	+1.920384	+0.082633	+0.391185	−0.092838
+0.617876	−1.051018	−1.054075	+1.903309	+0.159066	+0.509964	−0.053222
+0.755404	−1.060141	−1.071282	+1.881670	+0.295590	+0.600827	+0.017980
+0.865631	−1.052119	−1.089714	+1.860055	+0.503159	+0.664118	+0.124765
+0.944575	−0.979328	−1.105087	+1.842750	+0.867264	+0.703837	+0.299736
+0.989401	−0.665263	−1.117337	+1.830717	+1.476237	+0.722766	+0.574323

TABLE 20

Velocity Functions for Body 18

Serial 40 50 00 65 70

−0.989401	−0.786602	−0.840387	+2.338346	−0.804183	−1.240141	+0.412102
−0.944575	−0.850145	−0.898768	+2.175358	−0.656744	−1.022470	+0.262801
−0.865631	−0.926699	−0.964508	+2.044950	−0.521667	−0.820618	+0.146450
−0.755404	−0.988218	−1.012207	+1.970844	−0.398487	−0.658105	+0.057336
−0.617876	−1.023210	−1.035218	+1.938080	−0.282105	−0.516059	−0.011719
−0.458017	−1.035131	−1.039810	+1.930518	−0.183420	−0.376711	−0.063409
−0.281604	−1.033302	−1.034750	+1.935271	−0.107413	−0.229424	−0.097162
−0.095012	−1.029132	−1.029543	+1.940294	−0.057284	−0.071703	−0.115929
+0.095012	−1.031270	−1.031373	+1.936728	−0.015240	+0.089592	−0.120275
+0.281604	−1.040758	−1.040862	+1.924062	+0.034521	+0.242879	−0.111282
+0.458017	−1.050883	−1.052357	+1.909451	+0.112457	+0.380683	−0.084096
+0.617876	−1.051842	−1.058617	+1.901292	+0.215052	+0.502890	−0.039234
+0.755404	−1.036006	−1.045889	+1.904629	+0.354487	+0.613033	+0.031469
+0.865631	−0.998993	−1.040834	+1.920151	+0.522857	+0.712960	+0.126538
+0.944575	−0.928129	−1.020482	+1.943591	+0.790870	+0.798371	+0.279524
+0.989401	−0.711110	−1.005102	+1.962869	+1.380285	+0.853950	+0.584203

TABLE 21

Velocity Functions for Body 19

Serial 40 50 05 65 70

x	u_{1s}	$u_{1s}\sec\gamma$	$u_{2\theta}$	u_{2s}	$u_{R\theta}$	u_{Rs}
−0.989401	−0.800445	−0.875760	+2.236467	−0.886436	−1.140301	+0.432583
−0.944575	−0.872721	−0.919816	+2.130284	−0.631250	−0.982375	+0.245272
−0.865631	−0.938937	−0.973799	+2.030318	−0.498960	−0.810060	+0.136108
−0.755404	−0.992054	−1.013955	+1.968669	−0.382976	−0.657929	+0.052186
−0.617876	−1.022736	−1.033798	+1.940190	−0.271727	−0.518358	−0.014690
−0.458017	−0.033272	−1.037734	+1.933457	−0.179246	−0.378659	−0.064499
−0.281604	−1.031886	−1.033332	+1.937316	−0.107131	−0.230268	−0.097463
−0.095012	−1.028884	−1.029296	+1.940799	−0.058822	−0.071824	−0.115846
+0.095012	−1.031856	−1.031959	+1.936153	−0.015985	+0.089506	−0.120196
+0.281604	−1.041332	−1.041436	+1.923433	+0.035033	+0.242636	−0.111100
+0.458017	−1.050804	−1.052383	+1.909492	+0.113744	+0.380609	−0.083916
+0.617876	−1.051133	−1.057904	+1.902055	+0.215695	+0.503289	−0.039059
+0.755404	−1.035265	−1.054026	+1.905698	+0.353985	+0.613845	+0.031392
+0.865631	−0.998919	−1.040324	+1.920937	+0.520794	+0.713741	+0.126305
+0.944575	−0.929072	−1.020858	+1.943538	+0.789150	+0.798511	+0.279092
+0.989401	−0.712292	−1.006204	+1.961920	+1.379074	+0.853269	+0.583851

TABLE 22

Velocity Functions for Body 20

Serial 40 50 15 65 70

−0.989401	−0.800576	−0.931660	+2.108104	−1.065875	−1.013287	+0.494621
−0.944575	−0.906924	−0.956772	+2.059705	−0.629360	−0.918458	+0.237737
−0.865631	−0.960352	−0.991075	+2.003214	−0.467847	−0.789769	+0.123090
−0.755404	−0.999350	−1.017565	+1.963612	−0.354676	−0.656740	+0.043242
−0.617876	−1.021821	−1.031101	+1.943992	−0.251395	−0.522659	−0.020390
−0.458017	−1.029542	−1.033469	+1.939285	−0.170938	−0.382525	−0.066606
−0.281604	−1.029020	−1.030566	+1.941438	−0.106594	−0.231962	−0.098062
−0.095012	−1.028378	−1.028892	+1.941803	−0.061911	−0.072063	−0.115668
+0.095012	−1.033046	−1.033149	+1.934973	−0.017470	+0.089341	−0.120048
+0.281604	−1.042477	−1.042582	+1.922169	+0.036029	+0.242151	−0.110716
+0.458017	−1.050638	−1.052322	+1.909572	+0.116355	+0.380450	−0.083557
+0.617876	−1.049724	−1.056698	+1.903581	+0.216980	+0.504090	−0.038707
+0.755404	−1.033753	−1.052380	+1.907870	+0.352975	+0.615497	+0.031224
+0.865631	−0.998764	−1.039405	+1.922520	+0.517622	+0.715310	+0.125997
+0.944575	−0.930977	−1.021480	+1.943413	+0.784933	+0.798775	+0.278133
+0.989401	−0.814615	−1.008346	+1.960075	+1.376825	+0.851952	+0.582944

TABLE 23

Velocity Functions for Body 21

Serial 40 50 20 65 70

x	u_{1s}	u_{1s} sec γ	$u_{2\theta}$	u_{2s}	$u_{R\theta}$	u_{Rs}
−0.989401	−0.796842	−0.954759	+2.064157	−1.128276	−0.969779	+0.513748
−0.944575	−0.920752	−0.973002	+2.031552	−0.636406	−0.892720	+0.238489
−0.865631	−0.969919	−0.999092	+1.990770	−0.456433	−0.780221	+0.118705
−0.755404	−1.002852	−1.019470	+1.960816	−0.341522	−0.655815	+0.039227
−0.617876	−1.021374	−1.029818	+1.945703	−0.241527	−0.524661	−0.023066
−0.458017	−1.027682	−1.031395	+1.942161	−0.166730	−0.384436	−0.067671
−0.281604	−1.027578	−1.029122	+1.943507	−0.106391	−0.232808	−0.098328
−0.095012	−1.028117	−1.028734	+1.942306	−0.063444	−0.072179	−0.115593
+0.095012	−1.033634	−1.033738	+1.934387	−0.018237	+0.089260	−0.119958
+0.281604	−1.043053	−1.043157	+1.921533	+0.036556	+0.241907	−0.110536
+0.458017	−1.050554	−1.052237	+1.909612	+0.117633	+0.380372	−0.083368
+0.617876	−1.049008	−1.056084	+1.904354	+0.217665	+0.504495	−0.038534
+0.755404	−1.033002	−1.051509	+1.908956	+0.352444	+0.616323	+0.031160
+0.865631	−0.998688	−1.038893	+1.923306	+0.515677	+0.716095	+0.125676
+0.944575	−0.931955	−1.021880	+1.943319	+0.783098	+0.798884	+0.277814
+0.989401	−0.715800	−1.009448	+1.959109	+1.375695	+0.851254	+0.582430

TABLE 24

Velocity Functions for Body 22

Serial 40 50 10 60 50

−0.989401	−0.764100	−0.919605	+2.129526	−1.173634	−1.004002	+0.534754
−0.944575	−0.880922	−0.939750	+2.087475	−0.698872	−0.914056	+0.258966
−0.865631	−0.931698	−0.970822	+2.032599	−0.539609	−0.783994	+0.136962
−0.755404	−0.970991	−0.998962	+1.986564	−0.442714	−0.642388	+0.052243
−0.617876	−1.000963	−1.020246	+1.953058	−0.354138	−0.497107	−0.018505
−0.458017	−1.023250	−1.035468	+1.928918	−0.279232	−0.349255	−0.074121
−0.281604	−1.040827	−1.047742	+1.909969	−0.201613	−0.200026	−0.115528
−0.095012	−1.056157	−1.059122	+1.893489	−0.126307	−0.052522	−0.140308
+0.095012	−1.069610	−1.070038	+1.878920	−0.039417	+0.089135	−0.146368
+0.281604	−1.079001	−1.079325	+1.867423	−0.055914	+0.221633	−0.133364
+0.458017	−1.080177	−1.084515	+1.860958	+0.172662	+0.343570	−0.098492
+0.617876	−1.068696	−1.083540	+1.861179	+0.300661	+0.455162	−0.044234
+0.755404	−1.040786	−1.075636	+1.868619	+0.464987	+0.556653	+0.038095
+0.865631	−0.990603	−1.061967	+1.882009	+0.662689	+0.646160	+0.148748
+0.944575	−0.892652	−1.046731	+1.897518	+0.976915	+0.718135	+0.319222
+0.989401	−0.606046	−1.033856	+1.910614	+1.541906	+0.764183	+0.600515

TABLE 25

Velocity Functions for Body 23

Serial 40 50 10 55 50

x	u_{1s}	$u_{1s}\sec\gamma$	$u_{2\theta}$	u_{2s}	$u_{R\theta}$	u_{Rs}
−0.989401	−0.851736	−0.994089	+2.021924	−1.049561	−0.923867	+0.471180
−0.944575	−0.946722	−0.977211	+2.046733	−0.520410	−0.898238	+0.203541
−0.865631	−0.941908	−0.958880	+2.069996	−0.393064	−0.830123	+0.109404
−0.755404	−0.939095	−0.956698	+2.061738	−0.381742	−0.702199	+0.053748
−0.617876	−0.957155	−0.977088	+2.017860	−0.370428	−0.532805	−0.002892
−0.458017	−0.992668	−1.011584	+1.961227	−0.337941	−0.356437	−0.057655
−0.281604	−1.032276	−1.045661	+1.912649	−0.268515	−0.192205	−0.103321
−0.095012	−1.065131	−1.071237	+1.879147	−0.175945	−0.043314	−0.132456
+0.095012	−1.085160	−1.086029	+1.860385	−0.060647	+0.093143	−0.140964
+0.281604	−1.089595	−1.090140	+1.854241	+0.058804	+0.221353	−0.129432
+0.458017	−1.079584	−1.085336	+1.857971	+0.185132	+0.344114	−0.096027
+0.617876	−1.059171	−1.075300	+1.868008	+0.306602	+0.460942	−0.043577
+0.755404	−1.031339	−1.064114	+1.880223	+0.455749	+0.567485	+0.037177
+0.865631	−0.990952	−1.055439	+1.890930	+0.641769	+0.656836	+0.147141
+0.944575	−0.905157	−1.059676	+1.898047	+0.958966	+0.722474	+0.319140
+0.989401	−0.618408	−1.048149	+1.901847	+1.534069	+0.760136	+0.599280

TABLE 26

Velocity Functions for Body 24

Serial 34 50 10 65 70

−0.989401	−0.791784	−0.897917	+2.173253	−1.003405	−1.076380	+0.474915
−0.944575	−0.885770	−0.938216	+2.088854	−0.648016	−0.944425	+0.245067
−0.865631	−0.954797	−0.989632	+2.003350	−0.489718	−0.789563	+0.128535
−0.755404	−1.005642	−1.025328	+1.952626	−0.362058	−0.649484	+0.044891
−0.617876	−1.030425	−1.038944	+1.934286	−0.241790	−0.518580	−0.021204
−0.458017	−1.032425	−1.035220	+1.938262	−0.150599	−0.383946	−0.068093
−0.281604	−1.022990	−1.023912	+1.951460	−0.090957	−0.235408	−0.098260
−0.095012	−1.016946	−1.017556	+1.957694	−0.064294	−0.072043	−0.115267
+0.095012	−1.024110	−1.024520	+1.946343	−0.040100	+0.093900	−0.120801
+0.281604	−1.042522	−1.042522	+1.921969	−0.004930	+0.246376	−0.113566
+0.458017	−1.060207	−1.061056	+1.898295	−0.092027	+0.379025	−0.086998
+0.617876	−1.063437	−1.070072	+1.886281	+0.210752	+0.495572	−0.040553
+0.755404	−1.043433	−1.064511	+1.890826	+0.367187	+0.602876	+0.032659
+0.865631	−0.997224	−1.044542	+1.912274	+0.545757	+0.704999	+0.130257
+0.944575	−0.915939	−1.014891	+1.945712	+0.813115	+0.798160	+0.283926
+0.989401	−0.697825	−0.991934	+1.974296	+1.392517	+0.862334	+0.590319

TABLE 27

Velocity Functions for Body 25

Serial 40 50 30 65 70

x	u_{1s}	$u_{1s} \sec \gamma$	$u_{2\theta}$	u_{2s}	$u_{R\theta}$	u_{Rs}
−0.989401	−0.784195	−0.992401	+1.999353	−1.220496	−0.905413	+0.538289
−0.944575	−0.944081	−1.002102	+1.985040	−0.655760	−0.849954	+0.242819
−0.865631	−0.987412	−1.014187	+1.967864	−0.439432	−0.762370	+0.112746
−0.755404	−1.009635	−1.023452	+1.954828	−0.317044	−0.653465	+0.032010
−0.617876	−1.020541	−1.027528	+1.948738	−0.222316	−0.528373	−0.028120
−0.458017	−1.023932	−1.027219	+1.947890	−0.158299	−0.388239	−0.069779
−0.281604	−1.024664	−1.026203	+1.947674	−0.106041	−0.234503	−0.098833
−0.095012	−1.027602	−1.028322	+1.943290	−0.066495	−0.072402	−0.115447
+0.095012	−1.034828	−1.034931	+1.933189	−0.019822	+0.089100	−0.119766
+0.281604	−1.044187	−1.044291	+1.920268	+0.037623	+0.241427	−0.110188
+0.458017	−1.050390	−1.052179	+1.909680	+0.120206	+0.380214	−0.082964
+0.617876	−1.047580	−1.054752	+1.905901	+0.219048	+0.505308	−0.038206
+0.755404	−1.031470	−1.049735	+1.911168	+0.351348	+0.618005	+0.031041
+0.865631	−0.998527	−1.037970	+1.924902	+0.512384	+0.717685	+0.125244
+0.944575	−0.933893	−1.022660	+1.943151	+0.779223	+0.799116	+0.277117
+0.989401	−0.718162	−1.011639	+1.957205	+1.373473	+0.849892	+0.581403

TABLE 28

Velocity Functions for Body 26

Serial 40 50 40 65 70

−0.989401	−0.773461	−1.026491	+1.948887	−1.280910	−0.855379	+0.550060
−0.944575	−0.963056	−1.027370	+1.947970	−0.677769	−0.815698	+0.249050
−0.865631	−1.003282	−1.028268	+1.947285	−0.426712	−0.746126	+0.108577
−0.755404	−1.016187	−1.027593	+1.948484	−0.294659	−0.650647	+0.025724
−0.617876	−1.019755	−1.025395	+1.951334	−0.203626	−0.531761	−0.032886
−0.458017	−1.020163	−1.023130	+1.953565	−0.149820	−0.392015	−0.071856
−0.281604	−1.021726	−1.023364	+1.951871	−0.105754	−0.236207	−0.099310
−0.095012	−1.027072	−1.027894	+1.944276	−0.069573	−0.072622	−0.115303
+0.095012	−1.036008	−1.036112	+1.931993	−0.021417	+0.088941	−0.119564
+0.281604	−1.045330	−1.045435	+1.918991	+0.038712	+0.240942	−0.109842
+0.458017	−1.050220	−1.052220	+1.909743	+0.122773	+0.380052	−0.082552
+0.617876	−1.046141	−1.053409	+1.907460	+0.220481	+0.506128	−0.037873
+0.755404	−1.029930	−1.048061	+1.913400	+0.350224	+0.619703	+0.030935
+0.865631	−0.998363	−1.036937	+1.926505	+0.508499	+0.719281	+0.124624
+0.944575	−0.935851	−1.023460	+1.942965	+0.775357	+0.799334	+0.276372
+0.989401	−0.720507	−1.013941	+1.955318	+1.371405	+0.848542	+0.580479

TABLE 29

Velocity Functions for Body 27

Serial 40 50 50 65 70

x	u_{1s}	$u_{1s}\sec\gamma$	$u_{2\theta}$	u_{2s}	$u_{R\theta}$	u_{Rs}
−0.989401	−0.758954	−1.053663	+1.911469	−1.327593	−0.817979	+0.557246
−0.944575	−0.978903	−1.049874	+1.917349	−0.699109	−0.787235	+0.254897
−0.865631	−1.017901	−1.041544	+1.928620	−0.417727	−0.731251	+0.106113
−0.755404	−1.022566	−1.031957	+1.941879	−0.274242	−0.647462	+0.020268
−0.617876	−1.019012	−1.023413	+1.953517	−0.185458	−0.534838	−0.037368
−0.458017	−1.016393	−1.018941	+1.959173	−0.141354	−0.395750	−0.073891
−0.281604	−1.018759	−1.020391	+1.956098	−0.105531	−0.237910	−0.099753
−0.095012	−1.026540	−1.027465	+1.945240	−0.072679	−0.072832	−0.115158
+0.095012	−1.037194	−1.037401	+1.930780	−0.023039	+0.088789	−0.119352
+0.281604	−1.046471	−1.046576	+1.917705	+0.039812	+0.240458	−0.109497
+0.458017	−1.050054	−1.052159	+1.909793	+0.125352	+0.379883	−0.082127
+0.617876	−1.044700	−1.052171	+1.909022	+0.221941	+0.506949	−0.037539
+0.755404	−1.029371	−1.046262	+1.915657	+0.349082	+0.621420	+0.030840
+0.865631	−0.998208	−1.036023	+1.928105	+0.505204	+0.720878	+0.124204
+0.944575	−0.937811	−1.024146	+1.942764	+0.771097	+0.799548	+0.275486
+0.989401	−0.722939	−1.016220	+1.953319	+1.369156	+0.847092	+0.579455

TABLE 30

Velocity Functions for Body 28

Serial 36 50 00 55 60

−0.989401	−0.875169	−0.904941	+2.203922	−0.557061	−1.130466	+0.028062
−0.944575	−0.901559	−0.925246	+2.149077	−0.471006	−1.014868	+0.199996
−0.865631	−0.927781	−0.948554	+2.092994	−0.419079	−0.867888	+0.132073
−0.755404	−0.953926	−0.971411	+2.045007	−0.368848	−0.708821	+0.066083
−0.617876	−0.976806	−0.990876	+2.007077	−0.319335	−0.544922	+0.006879
−0.458017	−0.996995	−1.007880	+1.975710	−0.272789	−0.378196	−0.045636
−0.281604	−1.016648	−1.024434	+1.947468	−0.220019	−0.211890	−0.087528
−0.095012	−1.036773	−1.041251	+1.921350	−0.159356	−0.051047	−0.116852
+0.095012	−1.055872	−1.057352	+1.898662	−0.081236	+0.099690	−0.128175
+0.281604	−1.070150	−1.070150	+1.881730	+0.012226	+0.237992	−0.120732
+0.458017	−1.074694	−1.076956	+1.872786	+0.127494	+0.364196	−0.090473
+0.617876	−1.065195	−1.075737	+1.873323	+0.254183	+0.480238	−0.040904
+0.755404	−1.039066	−1.065709	+1.883670	+0.408989	+0.587646	+0.035935
+0.865631	−0.993561	−1.048724	+1.902244	+0.589812	+0.685087	+0.138367
+0.944575	−0.910809	−1.028930	+1.924604	+0.877875	+0.766416	+0.300938
+0.989401	−0.662231	−1.014136	+1.942067	+1.464087	+0.818357	+0.600615

TABLE 31

Velocity Functions for Body 29

Serial 36 50 00 55 70

x	u_{1s}	$u_{1s} \sec \gamma$	$u_{2\theta}$	u_{2s}	$u_{R\theta}$	u_{Rs}
−0.989401	−0.904617	−0.927337	+2.153046	−0.471561	−1.095941	+0.236258
−0.944575	−0.924421	−0.942325	+2.115738	−0.403247	−1.000164	+0.173556
−0.865631	−0.943634	−0.959173	+2.076022	−0.361864	−0.869771	+0.117612
−0.755404	−0.963169	−0.976152	+2.040034	−0.320367	−0.720252	+0.060988
−0.617876	−0.980739	−0.991146	+2.010134	−0.278082	−0.559956	+0.008697
−0.458017	−0.996673	−1.004711	+1.984360	−0.238079	−0.392888	−0.038329
−0.281604	−1.012485	−1.018187	+1.960367	−0.192557	−0.223555	−0.076390
−0.095012	−1.028891	−1.032194	+1.937581	−0.139994	−0.057639	−0.103710
+0.095012	−1.044557	−1.045602	+1.917456	−0.072097	+0.099730	−0.115180
+0.281604	−1.056357	−1.056357	+1.902340	+0.009362	+0.245650	−0.109655
+0.458017	−1.060370	−1.062070	+1.894454	+0.110000	+0.379705	−0.082967
+0.617876	−1.053151	−1.060789	+1.895321	+0.221084	+0.502979	−0.037935
+0.755404	−1.032640	−1.052211	+1.905292	+0.357641	+0.616243	+0.032520
+0.865631	−0.996634	−1.037620	+1.922879	+0.519431	+0.717719	+0.127045
+0.944575	−0.930635	−1.020657	+1.943819	+0.784005	+0.801092	+0.279150
+0.989401	−0.715599	−1.009023	+1.959282	+1.375915	+0.853118	+0.583824

TABLE 32

Velocity Functions for Body 30

Serial 36 50 00 55 80

−0.989401	−0.925650	−0.943482	+2.118488	−0.408607	−1.072079	+0.203828
−0.944575	−0.940415	−0.954445	+2.091765	−0.355016	−0.988929	+0.160923
−0.865631	−0.955015	−0.967104	+2.062472	−0.318185	−0.869904	+0.105655
−0.755404	−0.970088	−0.980085	+2.034801	−0.282650	−0.727629	+0.056153
−0.617876	−0.983913	−0.991948	+2.010931	−0.246016	−0.570501	+0.009551
−0.458017	−0.996708	−1.002825	+1.989668	−0.211098	−0.403580	−0.032912
−0.281604	−1.009651	−1.014011	+1.969249	−0.171209	−0.232169	−0.067687
−0.095012	−1.023258	−1.025720	+1.949360	−0.124896	−0.062487	−0.093082
+0.095012	−1.036408	−1.037238	+1.931441	−0.064836	+0.099890	−0.104303
+0.281604	−1.046419	−1.046419	+1.917853	+0.007379	+0.251559	−0.100013
+0.458017	−1.049995	−1.051256	+1.910820	+0.096724	+0.391509	−0.076132
+0.617876	−1.044290	−1.050066	+1.911863	+0.195623	+0.520156	−0.035000
+0.755404	−1.027605	−1.042513	+1.921352	+0.317582	+0.637681	+0.029701
+0.865631	−0.998254	−1.029871	+1.937847	+0.463573	+0.741919	+0.116948
+0.944575	−0.944613	−1.015276	+1.957179	+0.705835	+0.826396	+0.258167
+0.989401	−0.758852	−1.005768	+1.970985	+1.128919	+0.878457	+0.560208

TABLE 33

Values of C_D and $\bar{\epsilon}$ for Bodies of Series 58

Body	C_D	$\bar{\epsilon}$
1	0.00160	0.0004
2	0.00042	0.0001
3	0.00588	0.0014
4	0.00148	0.0004
5	0.00169	0.0004
6	0.00197	0.0005
7	0.00054	0.0001
8	0.00236	0.0006
9	0.00164	0.0004
10	0.00141	0.0004
11	0.00410	0.0010
12	0.00140	0.0004
13	0.00225	0.0006
14	0.00238	0.0006
15	0.00531	0.0013
16	0.00741	0.0018
17	0.00059	0.0001
18	0.00232	0.0006
19	0.00286	0.0007
20	0.00062	0.0002
21	0.00011	0.00003
22	0.00084	0.0002
23	0.00022	0.00005
24	0.00227	0.0006
25	0.00222	0.0005
26	0.00021	0.00005
27	0.00408	0.00102
28	0.00069	0.00017
29	0.00180	0.0045
30	0.00026	0.00006

TABLE 34

Values of $(C_p)_{min}$ and $\left(\frac{\partial C_p}{\partial \alpha}\right)_{\alpha=0}$ for Bodies of Series 58

Body	x_{min}	$(C_p)_{min}$	$\left(\frac{\partial C_p}{\partial \alpha}\right)_{\alpha=0}$
1	0.4970	−0.2285	−0.5246
2	0.5190	−0.1710	−0.4600
3	0.5280	−0.1300	−0.3664
4	0.5290	−0.1045	−0.3220
5	0.5400	−0.0875	−0.2912
6	0.5640	−0.0625	−0.2692
7	0.5650	−0.0123	−0.3406
8	0.5140	−0.0094	−0.3126
9	0.5570	−0.0080	−0.3744
10	0.5900	−0.0700	−0.4106
11	0.2540	−0.1150	−0.1087
12	0.4250	−0.1050	−0.2288
13	0.5870	−0.1150	−0.3904
14	0.4730	−0.1235	−0.3574
15	0.4850	−0.1150	−0.3114
16	0.6330	−0.1050	−0.4338
17	0.7700	−0.1240	−0.6678
18	0.5660	−0.1072	−0.3812
19	0.5560	−0.1064	−0.3776
20	0.5260	−0.1050	−0.3312
21	0.5120	−0.1043	−0.3120
22	0.3860	−0.1670	−0.2636
23	0.3420	−0.1890	−0.0872
24	0.5820	−0.1340	−0.3784
25	0.4850	−0.1035	−0.2720
26	0.4670	−0.1029	−0.2672
27	0.4420	−0.1026	−0.2500
28	0.4400	−0.1050	−0.2522
29	0.4220	−0.0750	−0.1824
30	0.4400	−0.0520	−0.1726

APPENDIX A

EVALUATION OF AUXILIARY INTEGRAL*

The integral to be evaluated is

$$I(x,r) = \int_{-1}^{1} \frac{2k_E r_{0E} r'_{0E} K(k_E)}{\sqrt{r r_{0E}}}\, d\xi \qquad [88]$$

For a point on the x-axis outside the body, it is seen from the equation following Equation [42] in Reference 7 that the integral reduces to

$$I(x,0) = 2\pi \int_{-1}^{1} \frac{r_0 r'_0}{\sqrt{(x-\xi)^2 + r_0^2}}\, d\xi \qquad [89]$$

Let e denote the eccentricity of the ellipse. Its equation is then

$$\xi^2 + \frac{r_0^2}{1-e^2} = 1 \qquad [90]$$

and hence we have

$$r_0 r'_0 = -\xi(1-e^2) \qquad [91]$$

Also we find, with the aid of [90],

$$(x-\xi)^2 + r_0^2 = \left(e\xi - \frac{x}{e}\right)^2 + (1-e^2)\left(1 - \frac{x^2}{e^2}\right) \qquad [92]$$

Substituting [91] and [92] into [89] and integrating, we obtain

$$I(x,0) = -\frac{2\pi(1-e^2)}{e}\left[-\frac{2}{e} + \frac{x}{e^2}\,\ell n\,\frac{x+e}{x-e}\right], \quad x > 1 \qquad [93]$$

or since, from [70], $\mu = 1$ and $\zeta = x/e$ when $r = 0$ and $x > 1$,

$$I(x,0) = -\frac{2\pi(1-e^2)}{e}\left[-\frac{2}{e} + \frac{\zeta}{e}\,\ell n\,\frac{\zeta+1}{\zeta-1}\right] = -\frac{4(1-e^2)}{e^2}\, Q_1(\zeta) \qquad [94]$$

where $Q_1(\zeta)$ is the associated Legendre function of degree 1 and order 0.

We now recall, from Equation [22] of Reference 7, that the integral [88] is also a harmonic function which may be expanded in terms of ellipsoidal harmonics. The form of Equation [94] immediately suggests the generalization

---

*Equation [69]

$$I(x,r) = -\frac{4\pi(1-e^2)}{e^2} P_1(\mu)\, Q_1(\zeta) \qquad [95]$$

a harmonic function which reduces to [94] when $\mu = 1$. Since there is a unique harmonic function which satisfies this condition, Equation [95] must give the value of the integral [88]. Equation [69] can now be obtained by substituting $P_1(\mu) = \mu$ and the value of e^2 given in Equation [71].

APPENDIX B

PROGRAM 1

VELOCITY POTENTIALS IN FLOW FIELD

```
      DIMENSION A(16),X(35),Y(35),W1(16), SUM(33),YA(16),YB(16),W2(16),
     1YC(16),W6(16),XB(16),T(16),G(16),R(16),P(16),Z(16),ZA(16),GY(16),
     2CK(16),CE(16),BE(16),CKP(16),EL(16),ELE(16),YE(16),YEP(16),ZE(16),
     3PE(16),CKE(16)
    1 READ INPUT TAPE 3,90, A,X,Y,YB,YA,YC
   90 FORMAT(8F9.6)
      S = 0.0
      S1 = 0.0
      DO 9 I = 1,16
      S = S + A(I)*Y(2*I+1)
      III = 17 - I
      S1 = S1 + A(III) *Y(2*I+1)
      W2 (I) = YB(I)*(1.0-YA(I))
    9 W6(I)=-YB(I)*YC(I)
      Y(1) = S1
      Y(35) = S
   12 DO 26 I = 4,32,2
      K3M = I-3
      K1M = I-1
      K3P = I+3
      K1P = I + 1
   13 A1 = X(I) - X(K3M)
   14 A1 = X(I) - X(K1M)
      A3 = X(I) - X(K1P)
      A4 = X(I) - X(K3P)
      P1 = (X(K3M) - X(K1M))*(X(K3M) - X(K1P))*(X(K3M)-X(K3P))
      P2 = (X(K1M) - X(K3M))*(X(K1M)-- X(K1P))*(X(K1M)-X(K3P))
      P3 = (X(K1P) - X(K3M))*(X(K1P) - X(K1M))*(X(K1P)-X(K3P))
      P4 = (X(K3P) - X(K3M))*(X(K3P) - X(K1M))*(X(K3P)-X(K1P))
      Q1=(A2*A3*A4*Y(K3M))/P1
      Q2=(A1*A3*A4*Y(K1M))/P2
```

```
      Q3=(A1*A2*A4*Y(K1P))/P3
      Q4=(A1*A2*A3*Y(K3P))/P4

   26 Y(I)=Q1+Q2+Q3+Q4
      SUM(3) = (Y(1) + Y(3))*(X(2)+1.0)
      W1(1) = SUM(3)
      SUM (I +2) = 0.0
      DO 33 I = 3, 31, 2
      SUM (I+2) = (Y(I) + 4.0 *Y(I+1) + Y(I+2))*(X(I+1)-X(I))/3.0
      M = (I-1)/2

   33 W1(M+1) = W1(M) + SUM(I+2)
      WRITE OUTPUT TAPE 2, 86, (W1(I), I = 1, 16), (W2(I),I = 1, 16),(W6(I),
      1I = 1, 16)

   86 FORMAT(9H1 RESULTS/6H W1 = F13.9/5F20.9/5F20.9/5F20.9/6H W2 = F13.9/5F20.9/
      15F20.9/5F20.9/6H W 6 = F13.9/5F20.9/5F20.9/5F20.9)
      READ INPUT TAPE 3, 91,XB,T,R

   91 FORMAT(8F9.6)

    2 READ INPUT TAPE 3, 99,XX,YY

   99 FORMAT (8F9.6)
      PI = 12.566371
      E = 0.000001
      IF(ABSF(XX)-1.0)400,96,96
  400 DO 498 I = 1,16
      IF(XX-XB(I))498,500,498

  500 YU=YB(I)
      GO TO 499

  498 CONTINUE

  499 B1=1.0-XX**2
      BU=(YU**2)/B1
      EC=1.0-BU
      DO 74 I=1,16
      YE(I)=YU* SQRTF((1.0-XB(I)**2)/B1)
      YEP(I)= -(BU*XB(I))/YE(I)
      ZE(I)=(XX-XB(I))**2+(YY+YE(I))**2
      PE(I)=2.0*SQRTF(YY*YE(I)/ZE(I))
      C=PE(I)**2
```

```
      CC=1.0-C
      IF(PE(I)-0.9)71,70,70

   70 PP=SQRTF(CC)
      AL=LOGEF(4.0/PP)
      BL1=(AL-1.0)*CC/4.0
      BL2=0.140625*(AL-1.16666667)*CC**2
      BL3=0.09765625*(AL-1.23333333)*CC**3
      CKE(I)=AL+BL1+BL2+BL3
      GO TO 74

   71 SU=1.0
      D=1.0
      DO 72 M1=1,50
      Q=2*M1
      D=D*(((Q-1.0)/Q/*PE(I))**2
      SU=SU+D
      V=D*C/CC
      IF(V-E)73,72,72

   72 CONTINUE

   73 CKE(I)=SU*PI/8. 0

   74 CONTINUE

   96 DO 44 I=1,16
      AE = (XX-XB(I))**2
      B = (YY+YB(I))**2
      Z(I) = AE+ B
      P(I)=2.0*SQRTF((YY*YB(I))/Z(I))
      C = P(I)**2
      CC=1.0-C
      IF(P(I)-0.9)98,97,97

   97 PP=SQRTF(CC)
      AL=LOGEF(4.0/PP)
      BL1=(AL-1.0)*CC/4.0
      BL2=0.140625*(AL-1.16666667) *CC**2
      BL3=0.09765625*(AL-1.23333333)*C**3
      CK(I)=AL+BL1+BL2+BL3
```

```
      BL1=(AL-0.5)*CC/2.0
      BL2=0.1875*(AL-1.08333333)*CC**2
      BL3=0.1171875*(AL-1.2)*CC**3
      CE(I)=1.0+BL1+BL2+BL3
      GO TO 44

   98 SU=1.0
      D=1.0
      DO 19 M=1,50
      Q=2*M
      D=D*(((Q-1.0)/Q)*P(I))**2
      SU=SU+D
      V=D*C/CC
      IF(V-F)20,19,19

   19 CONTINUE

   20 CK(I)=SU*PI/8.0
      D=(P(I)/2.0)**2
      SU=1.0-D
      DO 30 N=2,50
      Q=2*N
      PA=(Q-1.0)*(Q-3.0)*(P(I)/Q)**2
      D=D*PA
      SU=SU-D
      V=(D*C)/CC
      IF(V-E)31,30,30

   30 CONTINUE

   31 CE(I)=SU*PI/8.0

   44 CONTINUE

   45 DO 47 I=1,16
      AE=(XX-XB(I))
      C=P(I)**2
      QA=AE**2+YY**2-YB(I)**2-2.0*YB(I)*T(I)*AE
```

```
      AM=(C*CE(I))/(2.0*(1.0-C)*YY*YB(I))
      AN=-2.0*CK(I)+AM*QA
      AP=SQRTF(Z(I))
      IF(ABSF(XX)-1.0) 102,101,101

  101 AO=4.0*YB(I)*T(I)*CK(I)
      ZA(I)=(AO+W1(I)*AN)/AP
      GO TO 47

  102 DO 104J=1,16
      IF(XB(J)-XX)104,103,104

  103 W11=W1(J)
      GO QO 105

  104 CONTINUE

  105 CY=(W1(I)-W11)*AN
      EG=4.0*YE(I)*YEP(I)*CKE(I)
      EE=EG/SQRTF(ZE(I))
      AO=4.0*YB(I)*CK(I)
      ZA(I)=(AO+CY)/AP-EE

   47 CONTINUE
      S1=0.0
      DO 48 I=1,16

   48 S1=S1+ZA(I)*R(I)
      IF(ABSF(XX)-1.0) 49,50,50

   49 AA1=XX**2
      AA2=YY**2
      AA=((EC+AA1+AA2)/2.0)
      BB=EC*AA1
      BG=SQRTF(AA**2-BB)
      BG1=AA+BG
      BG2=SQRTF(1.0/BG1)
      PL1=XX*BG2
      RO=AA1/(EC*KPL1**2))
      RE=SQRTF(RO)
      QL1=((LOGEF((RE+1.0)/(RE-1.0))*RE/2.0)-1.0)
      ADD=((1.0-EC)*PL1*QL1)/EC
      S1=S1-PI*ADD
```

```
50 PH1=S1/PI
   DO 78 I=1,16
   C=P(I)**2
   BE(I)=(CE(I)-CK(I)*(1.0-C))/C
   CKP(I)=(BE(I)*P(I))/(1.0-C)
   AE=2.0/C
   B = (1.0 - AE)*CK(I)+AE*CE(I)
   C2=YY*YB(I)
   C1=SQRTF(C2)
   G(I) = -2.0 *P(I)*B/C1
   A1 = YY + YB(I)
   A2 = SQRTF(Z(I))
   A3 = (2.0 *YB(I)*A1)/A2**3
   A4 = A2/(2.0*C2)
   B5 = CK(I)*(A3-A4)
   A3 = (2.0*YB(I)*(A1 + YY))/Z(I)
   A4 = (4.0*YY*A1*YB(I)**2)/Z(I)**2
   B2 = CKP(I)*(1.0-A3 + A4)/C1
   B3 = A2*CE(I)/(2.0*C2)
   GL = (2.0/YB(I))*(B5 + B2 + B3)
   D1 = CK(I)/A2
   D2 = (CKP(I)*(1.0-2.0*C2/Z(I)))/C1
   GX = -(4.0*(XX-XB(I))*(D1-D2))/Z(I)
   GY(I) = G1 - T(I)*GX
   EL(I) = (-G(I) + W2(I)*GY(I)) *YB(I)
   EM = (XB(I) + YB(I)*T(I))*G(I)

78 ELE(I) = (-EM+W6(I)*GY(I))*YB(I)
   S1 = 0.0
   S2 = 0.0
   DO 79 I = 1,16
   S1 = S1 + EL(I)*R(I)

79 S2 = S2 + ELE(I)*R(I)
   PH2 = S1/PI
   PH6 = S2/PI
   WRITE OUTPUT TAPE 2, 89, XX, YY, PH1, PH2, PH6

89 FORMAT(6H XX = F9.6,6H YY = F9.6/7H PH1 = F13.9,12H PH2 = F13.9,12H
   1PH6 = F13.9/)
   GO TO 2
   END FILE 2
```

PROGRAM 2

VELOCITIES ON THE X-AXIS

```
      DIMENSION U(16), XB(16), YB2(16), R(16), B(16)
    1 READ INPUT TAPE 3, 11, U, XB, YB2, R
   11 FORMAT (8F10.6)
      DO 20 KXQ=1,24
      S=0.0
      READ INPUT TAPE 3, 13, XX
   13 FORMAT (F10.2)
      DO 10 I = 1, 16
      RS = (XX-XB(I))**2+YB2(I)
      RC =RS**1.5
      B(I)=(U(I)*YB2(I))/RC
   10 S=S+B(I)*R(I)
      A1 = -0.5*S
      WRITE OUTPUT TAPE 2, 15,XX, A1
   15 FORMAT (6HXX = F10.2, 6H A1 = F10.7/)
   20 CONTINUE
      END FILE 2
      PAUSE
      END
```

APPENDIX C

STREAM FUNCTION IN NEIGHBORHOOD OF STAGNATION POINT

Take the origin 0 of a cylindrical coordinate system (x,r,θ) at the stagnation point of a body of revolution in an axisymmetric flow with the x-axis the axis of symmetry. Then we have

$$\frac{\partial \psi}{\partial r} = ru \qquad [96]$$

where u, v are the velocity components in the x, r directions, and

$$\psi = \int_0^r rudr \qquad [97]$$

For small values of r we have, from its Taylor expansion,

$$u(x,r) = u_0 + r\left(\frac{\partial u}{\partial r}\right)_0 + \frac{r^2}{2}\left(\frac{\partial^2 u}{\partial r^2}\right)_0$$

in which the zero subscripts denote that the quantity is evaluated at the point $(x,0)$. But, by symmetry,

$$\left(\frac{\partial u}{\partial r}\right)_0 = 0 \qquad [98]$$

Hence, substituting this into [97] and integrating gives

$$\psi\,(x,r) = \frac{r^2}{2}u_0 + \frac{r^4}{8}\left(\frac{\partial^2 u}{\partial r^2}\right)_0 \qquad [99]$$

To evaluate the second derivative, we apply the equation of continuity

$$\frac{\partial u}{\partial x} + \frac{\partial v}{\partial r} + \frac{v}{r} = 0 \qquad [100]$$

and the irrotational condition

$$\frac{\partial u}{\partial r} = \frac{\partial v}{\partial x} \qquad [101]$$

From [101] we have

$$\frac{\partial^2 u}{\partial r^2} = \frac{\partial^2 v}{\partial x \partial r}$$

and hence from [100]

$$\frac{\partial^2 u}{\partial r^2} = -\frac{\partial}{\partial x}\left(\frac{\partial u}{\partial x} + \frac{v}{r}\right) = \frac{\partial^2 u}{\partial x^2} - \frac{1}{r}\frac{\partial v}{\partial x}$$

or, again applying [101],

$$\frac{\partial^2 u}{\partial r^2} = -\frac{\partial^2 u}{\partial x^2} - \frac{1}{r}\frac{\partial u}{\partial r} \qquad [102]$$

Hence, by [98], we have

$$\left(\frac{\partial^2 u}{\partial r^2}\right)_0 = -\left(\frac{\partial^2 u}{\partial x^2}\right)_0$$

whence [99] becomes

$$\psi(x,r) = \frac{r^2 u_0}{2} - \frac{r^4}{8}\left(\frac{\partial^2 u}{\partial x^2}\right)_0$$

the desired result.

REFERENCES

1. Landweber, L. and Gertler, M., "Mathematical Formulation of Bodies of Revolution," David Taylor Model Basin Report 719 (Sep 1950).

2. Landweber, L. and Winzer, A., "A Comparison of the Added Masses of Streamlined Bodies and Prolate Spheroids," Schiffstechnik, Issue 16 (1956).

3. Landweber, L., "Potential Flow about Bodies of Revolution and Symmetric Two-Dimensional Forms," State University of Iowa, Final Report, Contract Nonr-2451(00), (Dec 1959).

4. Kellogg, O.D., "Foundations of Potential Theory," Murray Printing Company, New York (1929).

5. Lamb, H., "Hydrodynamics," Sixth Edition, Cambridge University Press (1932) p. 20.

6. Breslin, J.P. and Landweber, L., "A Manual for Calculation of Inception of Cavitation on Two- and Three-Dimensional Forms," Davidson Laboratory Report R-847 (Jun 1961).

7. Landweber, L. and Todd, M.A., "Determination of the Motion of a Body from Measurements of Flow Ahead of the Body," David Taylor Model Basin Report 987 (Apr 1956).

8. "Advanced Mechanics of Fluids," Edited by H. Rouse, Wiley and Sons, New York (1959) pp. 319, 415.

INITIAL DISTRIBUTION

Copies	
20	DDC
3	CHONR 2 Code 438 1 Code 411
1	ONR, Boston
1	ONR, Chicago
1	ONR, New York
1	ONR, Pasadena
1	ONR, San Francisco
3	ONR, London
25	ONR, London Attn: Dr. F.H. Todd
1	NAVFACENGCOM Attn: Code 0321
1	DIR, SPO Attn: Dr. John Craven, Code NSP-001
1	NAVAIRDEVCEN
1	NASL
1	CDR, NCCCLC
1	DIR, NRL
1	NAVUWRES
1	NAVOCEANO
1	NMDL
1	NWL
1	NAVCIVENGRLAB
1	CDR, NWC
1	NAVSHIPYD BSN
1	NAVSHIPYD CHASN
1	NAVSHIPYD LBEACH
1	NAVSHIPYD NORVA
1	NAVSHIPYD PEARL
1	NAVSHIPYD PHILA
1	NAVSHIPYD PTSMH
1	NAVSHIPYD BREM

Copies	
1	NAVSHIPYD SFRANBAY VJO
1	AFFDL (FDDS - Mr. J. Olsen) Wright-Patterson AFB, Ohio 45433
1	NASA Scientific and Technical Info Facility P.O. Box 33 College Park, Md. 20740
1	AFORSR (SREM) 1400 Wilson Blvd Arlington, Va. 22209
1	Library of Congress Science & Technology Div Washington, D.C. 20540
1	U.S. Coast Guard Washington, D.C. 20226 Attn: Division of Merchant Marine Safety
1	DIR, BuStand, Wash., D.C. 20234 Attn: Dr. G.B. Schubauer, Chief, Fluid Mechanics Br
1	Dir of Research, National Aeronautics & Space Adm 600 Independence Ave S.W. Washington, D.C. 20546
1	Dir, Waterways Experiment Station Box 631, Vicksburg, Miss. 39180 Attn: Research Center Lib
1	Comm, Naval Ordnance Systems Comm Dept of the Navy Washington, D.C. 20360 Attn: Code ORD-035
1	Univ of Bridgeport Bridgeport, Connecticut 06602 Attn: Prof. Earl Uram Mechanical Engr Dept
1	Brown University Providence. R.I. 02912 Attn: Div of Applied Math
4	Naval Architecture Dept College of Eng, Univ of Calif Berkeley, Calif 94720 1 Attn: Librarian 1 Prof. J.R. Paulling 1 Prof. J.V. Wehausen 1 Dr. H.A. Schade

Copies	
2	CIT, Pasadena, Calif 91109 1 Attn: Dr. A.J. Acosta 1 Dr. T.Y. Wu
1	Univ of Connecticut Box U-37 Storrs, Connecticut 06268 Attn: Prof V. Scottron Hydraulic Research Lab
1	Cornell Univ Graduate School of Aerospace Engr. Ithaca, New York 14850 Attn: Prof. W.R. Sears
1	Harvard University 2 Divinity Avenue Cambridge, Mass. 02138 Attn: Prof. G. Birkhoff Dept of Mathematics
1	Univ of Illinois College of Engineering Urbana, Illinois 61801 Attn: Dr. J.M. Robertson Theoretical & Applied Mechanics Dept
1	The University of Iowa Iowa City, Iowa 52240 Attn: Dr. Hunter Rouse
2	The State Univ of Iowa Iowa Inst of Hydraulic Resh Iowa City, Iowa 52240 1 Attn: Dr. L. Landweber 1 Dr. J. Kennedy
1	The JHU Mechanics Dept Baltimore, Md. 21218 Attn: Prof. O.M. Phillips
1	Kansas State Univ Eng Experiment Station Seaton Hall Manhattan, Kansas 66502 Attn: Prof. D.A. Nesmith
1	Univ of Kansas Lawrence, Kansas 66044 Attn: Chm. Civil Eng Dept
1	Lehigh Univ Bethlehem, Pa. 18015 Attn: Fritz Lab Library

Copies	
1	MIT, Hydrodynamics Lab Cambridge, Mass. 02139 Attn: Prof. A.T. Ippen
6	MIT, Dept of Naval Arch & Marine Engineering Cambridge, Mass. 02139 1 Attn: Dr. A.H. Keil, Rm 5-226 1 Prof. P. Mandel, Rm 5-325 1 Prof. J.R. Kerwin, Rm 5-23 1 Prof. P. Leehey, Rm 5-222 1 Prof M. Abkowitz 1 Prof. F.M. Lewis
1	USMA, Attn: Capt. L.S. McCready, Head Dept of Eng
3	Univ of Michigan Dept of Naval Architecture & Marine Engineering Ann Arbor, Michigan 48104 1 Attn: Dr. T.F. Ogilvie 1 Dr. F. Michelsen 1 Prof H. Benford
5	St. Anthony Falls Hydraulic Lab Univ of Minnesota 1 Attn: Dir 1 Dr. C.S. Song 1 Mr. J.M. Killen 1 Mr. F. Schiebe 1 Mr. J.M. Wetzel
2	USNA 1 Attn: Library 1 Prof. Bruce Johnson
2	USNAVPGSCOL, Monterey 1 Attn: Library 1 Prof. J. Miller
1	New York University University Heights Bronx, New York 10453 Attn: Prof. W.J. Pierson, Jr.
2	NYU, Courant Inst of Mathe- matical Sciences 251 Mercier Street New York, New York 10012 1 Attn: Prof. A.S. Peters 1 Prof. J.J. Stoker
1	Univ of Notre Dame Notre Dame, Indiana 46556 Attn: Dr. A.F. Strandhagen

Copies

2 ORL, Penn State Univ
Univ Park, Pa. 16801
1 Attn: Dir
1 Dr. G. Wislicenus

1 Princeton Univ
Aerodynamics Lab, Dept of
Aerospace & Mech Sciences
The James Forrestal Res Cen
Princeton, N.J. 08540
Attn: Prof. G.L. Mellor

2 Scripps Inst of Oceanography
Univ of Calif
La Jolla, Calif 92038
1 Attn: J. Pollock
1 M. Silverman

3 Stanford University
Stanford, Calif 94305
1 Attn: Prof. H. Ashley
Dept of Aeronautics and
Astronautics
1 Prof. R.L. Street
Dept of Civil Engineering
1 Prof. B. Perry
Dept of Civil Engineering

3 Davidson Laboratory
SIT
Hoboken, N.J. 07030
Attn: Dr. J. Breslin

1 Univ of Texas
Defense Research Lab
P.O. Box 8029
Austin, Texas 78712
Attn: Director

1 Univ of Washington
Applied Physics Laboratory
1013 N. E. 40th St
Seattle, Wash. 98105
Attn: Director

2 Webb Inst of Naval Arch
Crescent Beach Road
Glen Cove, L.I., N.Y. 11542
1 Attn: Prof. E.V. Lewis
1 Prof. L.W. Ward

1 Worcester Polytechnic Inst
Alden Research Labs
Worcester, Mass 01609
Attn: Director

Copies

1 Aerojet-General Corp
1100 W. Hollyvale St
Azusa, Calif 91702
Attn: Mr. J. Levy
Bldg 160, Dept. 4223

1 Bethlehem Steel Corp
Central Technical Div
Sparrows Point Yard
Sparrows Point, Md. 21219
Attn: Mr. A.D. Haff
Technical Manager

1 Bethlehem Steel Corp
25 Broadway
New York, N.Y. 10004
Attn: Mr. H. de Luce

1 Bolt Beranek and Newman, Inc.
1501 Wilson Blvd
Arlington, Va. 22209
Attn: Dr. F.J. Jackson

1 Cornell Aeronautical Lab
Applied Mechanics Dept
P.O. Box 235
Buffalo, New York 14221
Attn: Dr. I.C. Statler

1 Douglas Aircraft Co.
Aircraft Div
Long Beach, Calif 90801
Attn: A.M.O. Smith
Aerodynamics Research Group

1 Electric Boat Division
General Dynamics Corp
Groton, Connecticut 06340
Attn: Mr. V.T. Boatwright, Jr.

1 Esso International
15 West 51st Street
New York, N.Y. 10019
Attn: Mr. R.J. Taylor,
Manager R&D, Tanker Dept

1 General Applied Sciences
Labs Inc., Merrick &
Stewart Avenues
Westbury, L.I., N.Y. 11590
Attn: Dr. F. Lane

1 Gibbs & Cox, Inc.
Attn: Technical Info Con Sec

1 Grumann Aircraft Eng Corp.
Bethpage, L.I., N.Y. 11714
Attn: Mr. W.P. Carl

Copies

1 Hudson Laboratories
145 Palisade Street
Dobbs Ferry, N.Y. 10522
Attn: Library

2 Hydronautics, Inc.
Pindell School Rd
Howard County
Laurel, Md. 20810
1 Attn: Mr. P. Eisenberg
1 Mr. M.P. Tulin

1 Lockheed Missiles & Space Co.
P.O. Box 504
Sunnyvale, Calif. 94088
Attn: Dr. J.W. Cuthbert,
Facility 1, Dept. 57-01,
Bldg. 150

1 National Science Foundation
Engineering Division
1800 G Street, N.W.
Washington, D.C 20550
Attn: Director

1 Newport News Shipbldg & DD Co.
4101 Washington Ave
Newport News, Va. 23607
Attn: Technical Lib Dept.

1 Oceanics, Incorporated
Technical Industrial Park
Plainview, L.I., N.Y. 11803
Attn: Dr. Paul Kaplan

1 Robert Taggart, Inc.
3930 Walnut Street
Fairfax, Va. 22030
Attn: Mr. R. Taggart

1 Sperry Gyroscope Co.
Great Neck, L.I., N.Y. 11020
Attn: Mr. D. Price G-2

1 Sperry-Piedmont Co.
Charlottesville, Va. 22901
Attn: Mr. T. Noble

1 Society of Naval Architects &
Marine Engineers
74 Trinity Place
New York, N.Y. 10006

2 SWRI, San Antonio, Texas 78206
1 Attn: Dr. H.N. Abramson
1 Attn: Applied Mechanics
Review

Copies

1 Sun Shipbuilding & Dry Dock Co.
Chester, Pa. 18013
Attn: Mr. F.L. Pavlik
Chief Naval Architect

1 Therm, Inc.

1 Tracor Inc.
6500 Tracor Lane
Austin, Texas 78721

1 Tracor Inc.
627 Loftstrand Lane
Rockville, Md. 20850

1 TRG/A Division of Control
Data Corp.
535 Broad Hollow Road
(Route 110)
Melville, L.I., N.Y. 11746
Attn: Dr. Jack Kotik

1 WHOI, Attn: Reference Rm

1 Measurement Analysis Corp.
10960 Santa Monica Blvd
Los Angeles, Calif. 90025
Attn: Dr. P.H. White

1 Colorado State Univ
Dept of Civil Engineering
Fort Collins, Colorado 80521
Attn: Prof. M. Albertson,
Head Fluid Mechanics Resear

1 Pierce Hall
Harvard University
Cambridge, Mass. 02138
Attn: Prof. G.F. Carrier

UNCLASSIFIED

Security Classification

DOCUMENT CONTROL DATA - R & D

(Security classification of title, body of abstract and indexing annotation must be entered when the overall report is classified)

1 ORIGINATING ACTIVITY (Corporate author)	2a. REPORT SECURITY CLASSIFICATION
Naval Ship Research and Development Center Washington, D.C. 20007	Unclassified
	2b. GROUP

3 REPORT TITLE

POTENTIAL FLOW ABOUT SERIES 58 BODIES IN GENERAL TRANSLATIONAL AND ROTATIONAL MOTION

4 DESCRIPTIVE NOTES *(Type of report and inclusive dates)*

5 AUTHOR(S) *(First name, middle initial, last name)*

L. Landweber and Matilde Macagno

6 REPORT DATE	7a. TOTAL NO OF PAGES	7b. NO. OF REFS
June 1967	127	8

8a. CONTRACT OR GRANT NO	9a. ORIGINATOR'S REPORT NUMBER(S)
N600(167)55727(x)	
b. PROJECT NO.	2505
c.	9b. OTHER REPORT NO(S) *(Any other numbers that may be assigned this report)*
d.	

10 DISTRIBUTION STATEMENT

Each transmittal of this document outside the agencies of the U.S. Government must have prior approval of Commanding Officer and Director, Naval Ship Research and Development Center.

11. SUPPLEMENTARY NOTES	12. SPONSORING MILITARY ACTIVITY
	Naval Ship Research and Development Center Washington, D.C. 20007

13 ABSTRACT

The potential-flow pressure and velocity distributions for a family of bodies of revolution, Series 58, were computed for various modes of motion. The results of these computations are presented, and their application of the determination of the flow field and minimum-pressure coefficients for arbitrary motion of the bodies are discussed.

The calculations were performed with the original UNIVAC installation at the David Taylor Model Basin and were checked with IBM 650 and 7070 installations at the State University of Iowa.

DD FORM 1 NOV 65 1473 (PAGE 1)

S/N 0101-807-6801

Security Classification

14 KEY WORDS	LINK A		LINK B		LINK C	
	ROLE	WT	ROLE	WT	ROLE	WT
Bodies of Revolution						
Series 58						
Resistance – Mathematical analysis						
Velocity – Mathematical computations						
Angle of attack – Mathematical computations						
Potential flow – Mathematical computations						
Digital computer						

Naval Ship Research and Development Center. Report 2505.
POTENTIAL FLOW ABOUT SERIES 58 BODIES IN GENERAL TRANSLATIONAL AND ROTATIONAL MOTION by L. Landweber and Matilde Macagno, Iowa Institute of Hydraulic Research, State University of Iowa. June 1967. vii, 120p. tables, illus., refs.
UNCLASSIFIED

The potential-flow pressure and velocity distributions for a family of bodies of revolution, Series 58, were computed for various modes of motion. The results of these computations are presented, and their application of the determination of the flow field and minimum-pressure coefficients for arbitrary motion of the bodies are discussed.
The calculations were performed with the original UNIVAC installation at the David Taylor Model Basin and were checked with IBM 650 and 7070 installations at the State University of Iowa.

1. Bodies of revolution--Model Series 58
2. Bodies of revolution--Resistance--Mathematical analysis
3. Velocity--Mathematical computations
4. Angle of attack--Mathematical computations
5. Potential flow--Mathematical computations
6. Digital computer (UNIVAC) Application
I. Iowa Institute of Hydraulic Research
II. Landweber, L.
III. Macagno, Matilde
IV. Contract N600(167) 55727(x)

Naval Ship Research and Development Center. Report 2505.
POTENTIAL FLOW ABOUT SERIES 58 BODIES IN GENERAL TRANSLATIONAL AND ROTATIONAL MOTION by L. Landweber and Matilde Macagno, Iowa Institute of Hydraulic Research, State University of Iowa. June 1967. vii, 120p. tables, illus., refs.
UNCLASSIFIED

The potential-flow pressure and velocity distributions for a family of bodies of revolution, Series 58, were computed for various modes of motion. The results of these computations are presented, and their application of the determination of the flow field and minimum-pressure coefficients for arbitrary motion of the bodies are discussed.
The calculations were performed with the original UNIVAC installation at the David Taylor Model Basin and were checked with IBM 650 and 7070 installations at the State University of Iowa.

1. Bodies of revolution--Model Series 58
2. Bodies of revolution--Resistance--Mathematical analysis
3. Velocity--Mathematical computations
4. Angle of attack--Mathematical computations
5. Potential flow--Mathematical computations
6. Digital computer (UNIVAC) Application
I. Iowa Institute of Hydraulic Research
II. Landweber, L.
III. Macagno, Matilde
IV. Contract N600(167) 55727(x)

Naval Ship Research and Development Center. Report 2505.
POTENTIAL FLOW ABOUT SERIES 58 BODIES IN GENERAL TRANSLATIONAL AND ROTATIONAL MOTION by L. Landweber and Matilde Macagno, Iowa Institute of Hydraulic Research, State University of Iowa. June 1967. vii, 120p. tables, illus., refs.
UNCLASSIFIED

The potential-flow pressure and velocity distributions for a family of bodies of revolution, Series 58, were computed for various modes of motion. The results of these computations are presented, and their application of the determination of the flow field and minimum-pressure coefficients for arbitrary motion of the bodies are discussed.
The calculations were performed with the original UNIVAC installation at the David Taylor Model Basin and were checked with IBM 650 and 7070 installations at the State University of Iowa.

1. Bodies of revolution--Model Series 58
2. Bodies of revolution--Resistance--Mathematical analysis
3. Velocity--Mathematical computations
4. Angle of attack--Mathematical computations
5. Potential flow--Mathematical computations
6. Digital computer (UNIVAC) Application
I. Iowa Institute of Hydraulic Research
II. Landweber, L.
III. Macagno, Matilde
IV. Contract N600(167) 55727(x)

Naval Ship Research and Development Center. Report 2505.
POTENTIAL FLOW ABOUT SERIES 58 BODIES IN GENERAL TRANSLATIONAL AND ROTATIONAL MOTION by L. Landweber and Matilde Macagno, Iowa Institute of Hydraulic Research, State University of Iowa. June 1967. vii, 120p. tables, illus., refs.
UNCLASSIFIED

The potential-flow pressure and velocity distributions for a family of bodies of revolution, Series 58, were computed for various modes of motion. The results of these computations are presented, and their application of the determination of the flow field and minimum-pressure coefficients for arbitrary motion of the bodies are discussed.
The calculations were performed with the original UNIVAC installation at the David Taylor Model Basin and were checked with IBM 650 and 7070 installations at the State University of Iowa.

1. Bodies of revolution--Model Series 58
2. Bodies of revolution--Resistance--Mathematical analysis
3. Velocity--Mathematical computations
4. Angle of attack--Mathematical computations
5. Potential flow--Mathematical computations
6. Digital computer (UNIVAC) Application
I. Iowa Institute of Hydraulic Research
II. Landweber, L.
III. Macagno, Matilde
IV. Contract N600(167) 55727(x)